Theodor Boveri Institut Würzburg

Impact of the Tumor Suppressor Arf on Miz1 and Sumoylation of Myc and Miz1

Wirkung des Tumorsuppressors Arf auf Miz1 und Sumoylierung von Myc und Miz1

Doctoral thesis

for a doctoral degree

at the Graduate School of Life Sciences,

Julius-Maximilians-Universität Würzburg, Section Biomedicine

submitted by

Anne Dwertmann

from Lingen

Würzburg 2012

Members of the Thesis Committee:

Chairperson:	Prof. Dr. Manfred Gessler
Primary Supervisor:	Prof. Dr. Martin Eilers
Seond Supervisor:	Prof. Dr. Manfred Schartl
Third Supervisor:	Prof. Dr. Stefan Gaubatz

Submitted on:

Date of Public Defense:

Date of Receipt of Certificates:

Substantial parts of this thesis were published in the following article:

Herkert, B., Dwertmann, A., Herold, S., Abed, M., Naud, J.F., Finkernagel, F., Harms, G.S., Orian, A., Wanzel, M., and Eilers, M. (2010). The Arf tumor suppressor protein inhibits Miz1 to suppress cell adhesion and induce apoptosis. *J Cell Biol 188*, 905-918.

Contents

List of Figures

List of Tables

Abstract

Upon oncogenic stress, the tumor suppressor Arf can induce irreversible cell cycle arrest or apoptosis, depending on the oncogenic insult. In this study, it could be shown that Arf interacts with Myc and the Myc-associated zinc finger protein Miz1 to facilitate repression of genes involved in cell adhesion. Formation of a DNA-binding Arf/Myc/Miz1 complex disrupts interaction of Miz1 with its coactivator nucleophosmin and induces local heterochromatinisation, causing cells to lose attachment and undergo anoikis. The assembly of the complex relies on Myc, which might explain why high Myc levels trigger apoptosis and not cell cycle arrest in the Arf response. This mechanism could play an important role in eliminating cells harboring an oncogenic mutation.

Arf furthermore induces sumoylation of Miz1 at a specific lysine by repressing the desumoylating enzyme Senp3. A sumoylation-deficient mutant of Miz1 however does not show phenotypic differences under the chosen experimental conditions. Myc can also be modified by Sumo by multisumoylation at many different lysines, which is unaffected by Arf. The exact mechanism and effect of this modification however stays unsolved.

Zusammenfassung

Der Tumorsuppressor Arf wird durch onkogenen Stress induziert und kann entweder einen irreversiblen Zellzyklusarrest oder Apoptose auslösen. In dieser Arbeit konnte gezeigt werden, dass Arf mit Myc und dem Myc-interagierenden Zinkfingerprotein Miz1 assoziiert und dadurch Gene der Zelladhäsion reprimiert. Die Ausbildung eines DNA-bindenden Arf/Myc/Miz1 Komplexes verhindert eine Interaktion von Miz1 mit seinem Koaktivator Nucleophosmin und führt zur lokalen Ausbildung von Heterochromatin, was zum Ablösen der Zellen und schließlich zur Anoikis führt. Die Komplexbildung setzt die Beteiligung von Myc voraus, was erklären könnte warum hohe Mengen an Myc über Arf Apoptose und nicht Zellzyklusarrest auslösen. Dieser Mechanismus könnte eine wichtige Rolle bei der Eliminierung von Zellen mit einer onkogenen Mutation spielen.

Arf induziert darüber hinaus die Sumoylierung von Miz1 an einem bestimmten Lysin indem es das desumoylierende Enzyme Senp3 inhibiert. Eine Mutante von Miz1 die nicht mehr sumoyliert werden kann zeigt jedoch in den durchgeführten Untersuchungen keinen anderen Phänotyp als Wildtyp Miz1. Myc kann ebenfalls an vielen verschiedenen Lysinen mit Sumo modifiziert werden, wobei Arf jedoch keine Rolle spielt. Der genaue Mechanismus und Effekt dieser Modifikation konnte jedoch nicht geklärt werden.

Chapter 1.

Introduction

Cancer is the leading cause of death in economically developed countries. About 12.7 million cases of cancer and 7.6 million cancer-related deaths have occured in 2008 [Ferlay et al., 2010]. In a medical sense cancer is a broad group of diseases all involving unrestrained cell growth, and this is facilitated by accumulation of mutations. In order to transform a normal cell into a cancer cell, the genes which regulate cell growth and differentiation must be altered. According to their function, the genes involved in these processes are categorized into proto-oncogenes and tumor suppressors. The latter inhibit for example cell division and induce apoptosis. The most prominent member of this group is p53, the "guardian of the genome" which is stabilized by another tumor suppressor called Arf. Proto-oncogenes in contrast promote cell growth and cell division and can become oncogenes if expressed at inappropriately high levels or upon aquiring novel properties. The genes of the *MYC* family belong to some of the most potent and frequently deregulated oncogenes [Croce, 2008].

Posttranslational modifications (PTMs) play a central role in the development of cancer. Phosphorylation, ubiquitination and sumoylation for example have all been linked to certain aspects of tumorigenesis. PTMs are vital to processes such as alterations in gene expression, modulation of cellular signaling pathways and regulation of cell division or death which all are critical processes during neoplastic transformation. They are highly suitable to be used as cancer biomarkers or therapeutic targets. There are numerous clinical trials currently underway that are based on pharmacologically impeding tumor growth by interrupting a specific PTM. It is thus of great importance in terms of application to cancer detection and treatment to discover new posttranslational modifications on specific targets [Krueger and Srivastava, 2006].

1.1. Sumoylation

The Sumo protein was initially identified as a posttranslational modifier protein in the mid-1990s, when Sumo was found to covalently attach to RanGAP1 [Matunis et al., 1996; Mahajan et al., 1997]. Sumo stands for "small ubiquitin-like modifier" and is conjugated to different target proteins to alter their function [Hay, 2005]. Due to its structural and sequence similarities to ubiquitin, it is classified as a member of the ubiquitin-like proteins [Kerscher et al., 2006]. Several hundred Sumo targets are known and the sumoylation of a protein can have various different outcomes [Geiss-Friedlander and Melchior, 2007]. Sumoylation is essential for the viability of many different organisms, such as *Caenorhabditis elegans* [Jones et al., 2002], *Drosophila melanogaster* [Apionishev et al., 2001] and *Mus musculus* [Nacerddine et al., 2005].

1.1.1. The Sumo family

Sumo proteins are around 10 kDa in size and their overall structure closely resembles that of ubiquitin, even though they share only 18 % sequence identity [Geiss-Friedlander and Melchior, 2007; Bayer et al., 1998]. Lower eukaryotes have only one single *sumo* gene, whereas plants and vertebrates express several *sumo* paralogues. Four Sumo proteins have been described in mammals: Sumo1, Sumo2, Sumo3 and Sumo4. Sumo2 and Sumo3 are 98 % similar in sequence and lack a clearly distinguishable functional difference; Sumo1 shares only about 50 % sequence identity with Sumo2/3 [Wimmer et al., 2012]. Sumo4 shows a restricted pattern of expression in contrast to the other Sumo isoforms and its functionality is still under debate [Wei et al., 2008; Owerbach et al., 2005]. With Sumo1 and Sumo2/3 being as different as ubiquitin and NEDD8, it is not surprising that proteins are selectively modified by the different Sumo isoforms and that these modifications can have different consequences [Hay, 2007]. Nevertheless, they also share a substantial overlapping set of target proteins [Vertegaal et al., 2006].

1.1.2. Mechanism of Sumo conjugation

A three-step enzymatic pathway attaches Sumo to specific targets, ultimately forming an isopeptide bond between the C-terminal carboxyl group of Sumo and the ϵ-amino group of a lysine side chain in the target protein [Johnson, 2004]. All Sumo proteins are translated as immature precursors and need to be processed by specific isopeptidases to expose a C-terminal diglycine motif. The heterodimeric E1 enzyme containing the SAE1 and SAE2 subunits adenylates the C-terminal glycine. Next, the Sumo adenylate is transferred to a

cysteine in the E1 activating enzyme generating a thioester bond. Sumo is then passed on to a cysteine in the E2 conjugating enzyme Ubc9. The E2 enzyme can directly transfer Sumo to an acceptor lysine in the target protein forming an isopeptide bond, but E3 protein ligases often facilitate this process. They recruit a Sumo-loaded E2 enzyme and the substrate into a complex and stimulate the E2 to discharge Sumo onto the target [Gareau and Lima, 2010]. In contrast to ubiquitination, sumoylation only knows Ubc9 as an E2 enzyme. Deletion of Ubc9 in mice results in early embryonic lethality with severe abnormalities in nuclear structure and chromosome segregation, illustrating the importance of an intact sumoylation pathway in mammals [Nacerddine et al., 2005].

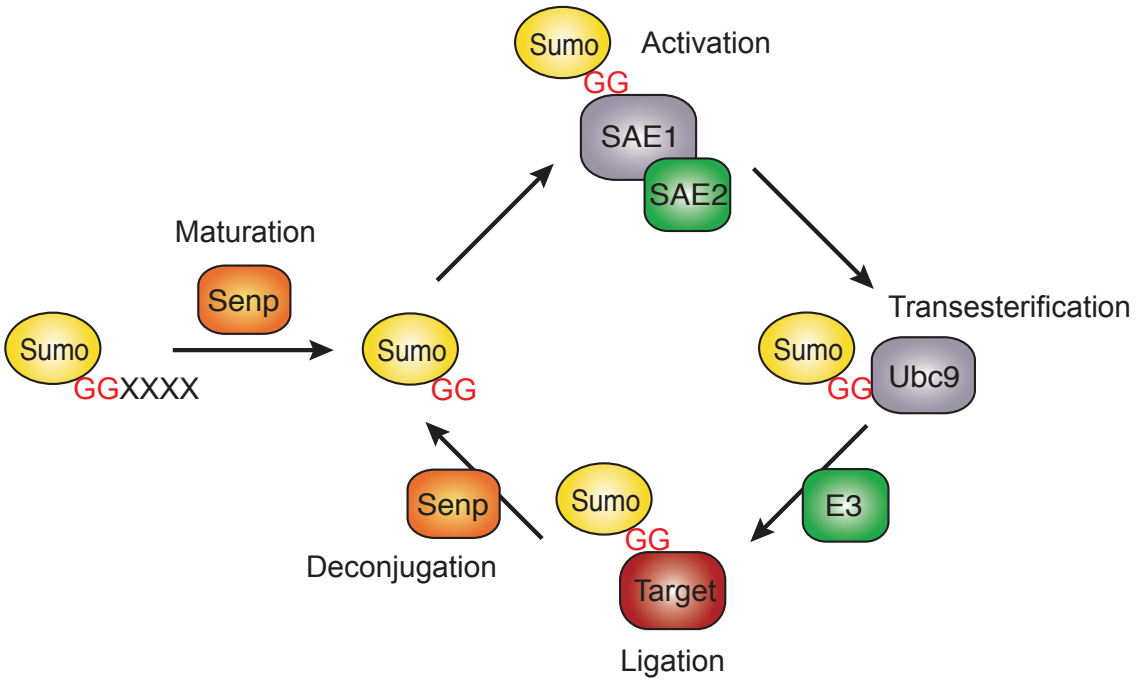

Figure 1.1.:
The Sumo conjugation pathway

The Sumo precursor is processed by a Sumo specific protease (Senp) to expose the C-terminal diglycine that is activated and conjugated to the E1 enzyme SAE1/SAE2. Sumo is transferred to the E2 enzyme in a transesterification reaction, then discharged to a lysine in the target protein, often with the help of an E3 enzyme. Sumoylation is a reversible process as Sumo can be deconjugated from the target protein by the same proteases that also induce the maturation of Sumo. (adapted after Geiss-Friedlander and Melchior [2007] and Hay [2005])

1.1.3. Transferral of Sumo to a substrate

Many but not all proteins are sumoylated within a tetrapeptide Sumo consensus motif [Hietakangas et al., 2006]. This motif is composed of Ψ-K-X-E/D, in which Ψ is a hydrophobic residue, K is the lysine conjugated to Sumo, X is any amino acid which is followed by an aspartic or glutamic acid (E/D). Most target lysines are modified by a single copy of Sumo, however a consensus motif in Sumo2/3 which is absent in Sumo1 allows the formation of poly-Sumo chains [Tatham et al., 2001]. The sumoylation consensus motif directly interacts with Ubc9 and is sufficient for catalytic specificity of Ubc9 *in vitro*. However, with some exceptions like the sumoylation of RanGAP1, Sumo modification needs additional components next to the E1 and E2 enzymes to be efficient [Bernier-Villamor et al., 2002; Lin et al., 2002].

Several proteins have been identified which can induce sumoylation by acting as Sumo E3 ligases. The biggest group of these are characterized by a SP-RING motif which resembles the RING-domain of certain E3 ubiquitin ligases. The SP-RING directly attaches to Ubc9 and a Sumo-interacting-motif in the E3 ligase binds to Sumo, thereby creating a platform for sumoylation [Hochstrasser, 2001]. Examples for SP-RING Sumo E3 ligases are the PIAS family members, which have been shown to induce sumoylation of p53 [Kahyo et al., 2001], Sp3 [Sapetschnig et al., 2002] and Mdm2 [Melchior and Hengst, 2000]. The nuclear pore protein RanBP2 can induce sumoylation of RanGAP1, a GTPase activating protein important for nuclear transport of proteins [Saitoh et al., 1997]. The Polycomb group protein PC2 has been shown to sumoylate a transcriptional co-repressor called CtBP and induce its localization into PcG bodies in the nucleus [Rytinki et al., 2009]. Other proteins can induce sumoylation without interacting with Ubc9. The tumor suppressor Arf can promote sumoylation of proteins to which it binds, for example nucleophosmin [Haindl et al., 2008], Hdm2 [Xirodimas et al., 2002], the Werner helicase [Woods et al., 2004] and the transcription factors E2F-1 and HIF-1α [Rizos et al., 2005]. It has been shown that Arf induces sumoylation of nucleophosmin by decreasing the stability of a Sumo deconjugating enzyme, Senp3, which in absence of Arf constantly removes Sumo from NPM. Mechanistically, Arf promotes phosphorylation and subsequent ubiquitination of Senp3 which is then targeted for degradation by the proteasome [Haindl et al., 2008].

A large fraction of Sumo2/3 is constantly present as a free, non-conjugated pool, which can be readily conjugated to proteins in response to stress stimuli such as heat shock, oxidative stress and ethanol exposure. In contrast to that, the majority of Sumo1 exists

in a conjugated rather than in a free form [Saitoh and Hinchey, 2000]. Even though there are clear distinctions between Sumo1 and Sumo2/3 regarding their availability, target specificity and their ability to form poly-Sumo chains, Sumo2/3 appear to be able to substitute for Sumo1 in knockout mice. In contrast to Ubc9 knockout animals, Sumo1 null mice are phenotypically normal [Zhang et al., 2008].

1.1.4. Removing Sumo from a substrate

Sumoylation is a highly dynamic process that can constantly be reversed by a group of Sumo-specific proteases (Senps). It is the Senps that induce maturation of the Sumo precursor proteins. They cut away a C-terminal amino acid extension to reveal the diglycine motif needed for Sumo conjugation to a target. To balance the cellular abundance of a particular sumoylated protein, Senps catalyze the removal of Sumo by cleaving the amide bond between Sumo's C-terminus and the lysine in the sumoylated target. Humans have six Senps which differ in localization and target specificity [Kim and Baek, 2009; Gareau and Lima, 2010]. Senps are critical regulators of sumoylation and essential in mammals. Proviral mutation of Senp1 in a mouse model increases steady-state levels of the sumoylated form of several proteins and prevents proper embryonic development [Yamaguchi et al., 2005].

1.1.5. Molecular consequences of sumoylation

Sumoylation can have different functional consequences for a target protein which are impossible to predict. Modification by Sumo may influence the localization, activity or stability of a modified protein. At the molecular level, sumoylation can have three general consequences [Geiss-Friedlander and Melchior, 2007]. Sumoylation can interfere with the binding to another protein meaning that interaction can occur only in absence of modification with Sumo. For instance, the Sumo acceptor site of the transcriptional repressor protein ZNF76 overlaps with its binding site for the TATA-binding protein TBP [Zheng and Yang, 2004]. Sumoylation can also provide a new binding interface for a partner protein. For instance, the acetyltransferase p300 can only interact with HDAC6 when sumoylated [Girdwood et al., 2003]. Finally sumoylation can induce a conformational change in the modified target, which so far has only been shown for the thymine DNA glycosylase [Hardeland et al., 2002].

1.1.6. Sumo and transcription factors

Although both Sumo1 and Sumo2/3 modulate many different cellular processes, a multitude of their target proteins have been shown to be involved in transcriptional regulation [Vertegaal et al., 2006]. Sumoylation can both activate and repress transcription. In most cases, however, it leads to repression, with various models explaining how this is achieved [Girdwood et al., 2004]. To illustrate these mechanisms, several examples of how Sumo modification increases or represses transcriptional activation will be discussed here.

Examples of how sumoylation can activate transcription

The transcription factor Oct4 is a master regulator in the fate of stem cells and can also have dramatic effects in oncogenesis, which is why it is tightly regulated. When Oct4 gets sumoylated by Sumo1 a fraction of this protein colocalizes with Sumo1 in nuclear aggregates. Sumoylation increases the overall stability, DNA binding capacity and transactivation potential of Oct4 [Wei et al., 2007]. Another example for compartimentalization and subsequent change in activity upon sumoylation has been shown for the heat shock factors HSF1 and HSF2. These are normally retained inactive in a complex with heat shock proteins. Upon heat stress they are released and can be sumoylated, which recruits the HSFs into nuclear stress granules and increases their DNA binding and transactivation capacity [Goodson et al., 2001; Hong et al., 2001].

Examples for transcriptional repression upon sumoylation

The Sp3 protein has been described either as an activator or repressor of transcription, depending on the promoter context [Suske, 1999]. It was found that repression by Sp3 occurs upon sumoylation mediated by the E3 ligase PIAS1. This goes along with relocalization of Sp3 from a diffuse nuclear distribution to distinct nuclear dots and the nuclear periphery [Sapetschnig et al., 2002]. Gene repression at sumoylated Sp3 binding sites occurs because of local heterochromatinisation with a H3K9$^{\mathrm{triMe}}$ and H4K20$^{\mathrm{triMe}}$ signature [Stielow et al., 2008].

Sumoylation also affects chromatin remodeling via the acetyltransferase p300, which acts as a coactivator for several transcription factors such as Miz1 [Staller et al., 2001]. Sumoylation of p300 at two sites creates a new binding interface for the histone deacetylase

HDAC6, which silences transcription. Interestingly, another HDAC, SIRT1, increases the repressive effect by deacetylating the exact same lysines in p300 which are then free to be sumoylated [Girdwood et al., 2003].

Another way of how sumoylation acts on transcription factors is by preventing other post-translational modifications. This is the case for NF-κB, an important regulator of the immune response. It is normally retained inactive by the inhibitory protein IκB in the cytosol. Upon stimuli such as cytokine release, the Iκb kinase phosphorylates IκB which is subsequently ubiquitinated and degraded and NF-κb is free to enter the nucleus and activate transcription. Sumoylated Iκb is resistant to degradation, as Sumo blocks the exact same lysine that is targeted for ubiquitination [Hay et al., 1999].

1.1.7. Non-covalent interactions with Sumo

In general, sumoylation alters the inter- and/or intramolecular interactions of a substrate and hence its localization, activity or stability. Non-covalent interaction with Sumo is needed to mediate these effects [Wimmer et al., 2012]. In contrast to ubiquitin, which can be bound by a large number of different recognition domains, Sumo is exclusively recognized by a short conserved motif called SIM (Sumo interacting motif), first described by Minty et al. [2000]. SIMs can be classified into three major types: SIMa, SIMr and SIMb. SIMa contains four consecutive hydrophobic amino acids, often in a V/I-X-V/I-V/I motif, which is followed by a cluster of acidic residues. SIMr resembles SIMa but has a reversed orientation, the four hydrophobic positions are preceded by an acidic stretch. SIMb is better conserved and mostly follows the consensus sequence V-I-D-L-T and can be for example found in PIAS E3 ligases [Miteva et al., 2010].

SIMs allow the recruitment of effector proteins to sumoylated targets, thus providing a unique interaction platform [Wimmer et al., 2012]. The Sumo interacting motif is also needed for E3 ligases like PIAS proteins to bring together Ubc9 and the sumoylation target [Hochstrasser, 2001]. In the case of the ubiquitin protease USP25, a SIM is needed to enable sumoylation of USP25 itself. Sumo-loaded Ubc9 is recruited to USP25 via an internal SIM, which enables E3-independent conjugation of Sumo to lysine residues in USP25. This mechanism is even more remarkable considering that the target lysines in USP25 are non-consensus sumoylation sites [Mohideen and Lima, 2008].

The Sumo interacting motif also allows for a crosstalk between the ubiquitination and sumoylation pathways. In humans, the RING ubiquitin ligase RNF4 was identified as a SUMO-targeted ubiquitin ligase (STUbL). RNF4 binds with four SIMs to polysumoylated PML and subsequently mediates its ubiquitination and degradation via the proteasome. This explains why patients with acute promyelocytic leukemia (APL) can be very effectively treated with arsenic trioxide. These patients express a PML-RARα fusion protein which blocks hematopoietic differentiation [Grignani et al., 1998]. Arsenic treatment induces polysumoylation of PML, also in its fused form, which is subsequently recognized and targeted to degradation by RNF4 [Tatham et al., 2008].

PML is also essential for the assembly and stability of PML bodies, which are nuclear sumoylation hot spots. These nuclear bodies have been described as an intrinsic antiviral defense mechanism, especially against DNA viruses. Immediate early proteins encoded by the herpes simplex and cytomegalovirus genomes can induce dispersal of PML bodies, these viral proteins contain Sumo interacting motifs. There are several more examples how pathogens take advantage of the Sumo machinery, mostly by inhibiting its function and therefore relieving a transcriptionally repressive environment that is induced by sumoylation [Wimmer et al., 2012].

1.1.8. The Sumo Enigma

A characteristic feature of sumoylation is that the biological consequences of Sumo conjugation do not appear proportionate to the small fraction of substrate that is modified, which often is only a few percent of a given protein [Hay, 2005; Johnson, 2004]. Even though sumoylation is a labile, short-lived modification it allows global, long-lasting control of proteins [Wimmer et al., 2012]. One model explains this by assuming that upon Sumo conjugation the target protein is immediately recruited into a repressive complex. Shortly after the recruitment, Sumo could be deconjugated again while retaining the target protein in the complex. This concept is supported by the rapid Sumo deconjugation observed after expression of the adenoviral Gam-1 protein, which blocks the Sumo E1 enzyme [Boggio et al., 2004]. This means that there must be constant deconjugation of Sumo modification going on in the cell. Another model suggests that a Sumo-modified transcription factor could recruit chromatin-remodelling enzymes and thus create a permanent repressive or activating environment without the need of constant sumoylation. In both models, Sumo is required only for initiation but not for maintenance of the effect.

Reactivation of a sumoylated protein targeted for repression could be triggered by disassembly of the complex, probably induced by other posttranslational modifications such as acetylation or phosphorylation. This has been shown for example for ELK-1. The MAP kinase-induced phosphorylation of ELK-1 results in loss of sumoylation and escape of the transcription factor from the repressive complex [Yang et al., 2003].

In general, sumoylation often recruits factors required for assembly or disassembly of macromolecular complexes. Once incorporated into such a complex, the Sumo target protein may rapidly lose its modification again. Thus, otherwise identical unmodified proteins may have different properties depending on their history of modification by Sumo [Hay, 2005].

1.2. The transcription factor Miz1

Miz1 is a zinc finger protein that was identified in a yeast two-hybrid screen as an interactor of Myc and was therefore called *MYC interacting zinc-finger-protein 1* [Schneider et al., 1997]. In mice Miz1 is ubiquitously expressed and essential for survival, as Miz1 homozygous knockout animals are severely retarded in early embryonic development and not viable [Adhikary et al., 2003]. In humans, high Miz1 levels are associated with favorable disease outcome for example in neuroblastoma, which points to a role of Miz1 as a tumor suppressor in this type of cancer [Ikegaki et al., 2007].

1.2.1. Miz1 protein structure

Miz1 is a member of the BTB/POZ (*poxvirus and zinc-finger/ bric-à-brac, tramtrack, broad complex*) zinc finger transcription factors. The N-terminal BTB/POZ domain acts as a hydrophobic interaction surface for di- and tetramerization of Miz1 itself and binding to other proteins for example of the POZ family [Stead et al., 2007]. In contrast to other POZ proteins Miz1 is expressed in a soluble form residing predominantly in the nucleoplasm, however it can also be found in the cytoplasm where it can interact with microtubuli [Ziegelbauer et al., 2001]. The C-terminal DNA binding domain of Miz1 consists of 12 consecutive Cys_2His_2 zinc fingers, separated from an isolated 13th zinc finger by an alpha-helical buffer region of 80 amino acids. The buffer region and a stretch of residues N-terminal to the first 12 zinc fingers mediate the binding to important Miz1 interaction partners such as c-Myc and p300 [Peukert et al., 1997; Staller et al., 2001].

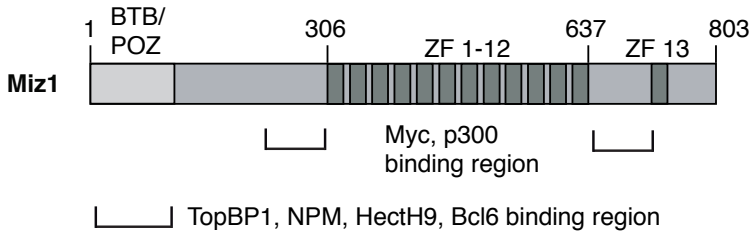

Figure 1.2.:
Schematic diagram of the Miz1 protein
Human Miz1 consists of 803 amino acids and contains an amino-terminal BTB/POZ domain and 13 zinc fingers (ZF). The binding sites for several protein interactors are indicated by the brackets.

1.2.2. Transcriptional regulation by Miz1

ChIP-seq analysis revealed that Myc is bound to an estimated number of 30.000 sites in the human genome, whereas Miz1 binds strongly to about 800 sites. There are about 500 joint Miz1/Myc binding sites, the remaining 300 Miz1 only sites are mostly far away from promoters. This indicates an important role of Myc in the transcriptional activity of Miz1 and probably vice versa, which appears to be dose-dependent but has not been completely elucidated yet [Walz and Wolf, 2012]. Miz1 binds close to the transcriptional start site of RNA polymerase II dependent target genes such as *CDKN2B*, *CDKN1A* or *p57Kip2*, which encode the p15ink4b, p21Cip1 and p57Kip2 cell cycle inhibitors [Seoane et al., 2001, 2002; Adhikary et al., 2003]. Miz1 binding to DNA is followed by recruitment of coactivators such as nucleophosmin or the histone acetyltransferase p300 to activate transcription [Wanzel et al., 2008; Staller et al., 2001].

Miz1 activity can be modified in various ways. TopBP1 for example can act as a negative regulator of Miz1 by retaining it in an inactive complex. DNA damage signaling disrupts this complex by recruiting TopBP1 to the damage sites, which frees Miz1 to activate transcription of the cell cycle inhibitor p21 [Herold et al., 2002]. In B cells, Miz1 heterodimerizes with Bcl6 to repress transcription of the Miz1 target *CDKN1A*. This counteracts a p53-induced cell cycle arrest, which is activated in response to class switch recombination events in mature B cells [Phan et al., 2005].

Two more major mechanisms of Miz1 regulation will be explained here in more detail, the L23-nucleophosmin regulatory circuit and the Myc-mediated repression.

Regulation of Miz1 transactivation by L23 and nucleophosmin

Nucleophosmin (NPM) is a critical regulator of ribosome biogenesis. It acts as a nucleolar endoribonuclease by inducing maturation of 47S rRNA and it directs the nuclear export of both ribosomal subunits [Savkur and Olson, 1998; Maggi et al., 2008]. It also functions as a chaperone for the highly basic Arf protein in the nucleolus [Colombo et al., 2005]. In the nucleoplasm, it is an essential coactivator of Miz1. NPM binds to the POZ domain of Miz1 which enables expression of the cell cycle inhibitors p15ink4b and p21Cip1. The ribosomal protein L23 inhibits Miz1-dependent transactivation by retaining nucleophosmin in the nucleolus. High levels of L23 therefore inhibit G1 arrest induced by Miz1. Interestingly, the L23 protein is encoded by a direct target gene of Myc, providing a feedback mechanism

that links Myc-induced translation of ribosomal proteins to Miz1-dependent cell cycle arrest [Wanzel et al., 2008].

Repression of Miz1 transactivation by Myc

Miz1-dependent gene expression can be inhibited by direct binding of Myc. This is mediated by interaction of the helix-loop-helix domain of Myc with two regions in Miz1 flanking the twelve core zinc fingers (see Fig. 1.2). Miz1 binds to and therefore recruits the Myc/Max heterodimer to the promotors of p21Cip1 and p15ink4B, which induces transcriptional repression [Herold et al., 2002; Peukert et al., 1997; Staller et al., 2001]. A point mutant of Myc, Myc V394D disrupts the binding and therefore lacks the repressive effect on Miz1 [Herold et al., 2002]. Mechanistically, the association of Myc to Miz1 blocks binding of coactivators such as the histone acetyltransferase p300 and nucleophosmin to Miz1 [Wanzel et al., 2008].

Miz1 repression by Myc is important for the resistance of Myc-transformed cells to the antiproliferative effects of TGF-β. Smad proteins activated upon TGF-β signaling bind to the promotor region of *CDKN2B*, where they interact with Miz1 and activate transcription [Seoane et al., 2001]. Myc can repress this by inducing a repressive Sp1/Smad/Myc complex and by blocking recruitment of coactivators to Miz1 as described above [Feng et al., 2002]. However, elevated levels of TGF-β can decrease Myc expression by direct binding of the cytokine to a TGF-β- responsive element within the Myc promotor [Chen et al., 2002; Gomis et al., 2006]. T-cell lymphomas that express high levels of TGF-β are addicted to Myc, because it is needed to constantly inhibit expression of cell cycle inhibitors via Miz1 [van Riggelen et al., 2010].

Myc-mediated repression of Miz1 in keratinocytes

A connection between the TGF-β signaling pathway and Myc-mediated repression of Miz1 could be confirmed in keratinocytes. Using the Myc V394D (Myc VD) mutant deficient in Miz1 binding, it could be shown that Miz1 is required as a mediator for the repressive effects of Myc in response to TGF-β. Microarray analysis revealed that in keratinocytes Myc wild type but not Myc VD inhibits genes involved in cell-cell and cell-matrix adhesion, which induces premature terminal differentiation and finally loss of epidermal stem cells in the skin [Gebhardt et al., 2006]. Thus, interaction between Myc and Miz1 must be tightly controlled during skin differentiation. High Myc expression in basal epidermal

layers induces loss of adhesion and exit of cells from the stem cell compartment induced by Miz1 [Gebhardt et al., 2006; Frye et al., 2003].

1.2.3. Transcription-independent functions of Miz1

Miz1 was initially described as a transcription factor, but it also exerts transcription-independent functions, two examples of which will be described here.

The ubiquitin ligase HectH9 (also called Arf-BP1 or Mule) was found to interact with the POZ domain of Miz1 in a yeast two-hybrid screen. HectH9 catalyzes attachment of K63-linked polyubiquitin chains to the Miz1 interacting protein c-Myc, which enhances its transcriptional activity. Miz1 antagonizes binding and activation of c-Myc by HectH9 because it competes with Myc for binding to the ubiquitin ligase [Adhikary et al., 2005].

Miz1 also acts as a signal- and pathway-specific modulator or regulator (SMOR) in the pleiotropic TNF-α/JNK1 pathway. Miz1 prevents TNF-α- induced JNK1 activation and induction of apoptosis by inhibiting ubiquitination of TRAF2 with K63-linked chains. The regulation by Miz1 is highly specific, as it does not affect JNK activation by other factors than TNF-α and has no influence on other branches of TNF-α signalling. Interestingly, Miz1 itself is rapidly degraded in the proteasome upon TNF-α stimulation, suggesting that it is part of a network that regulates the kinetics of JNK-induced activation and cell death [Liu et al., 2009].

1.3. The oncogenic transcription factor Myc

C-Myc was identified as the cellular homologue of the transforming viral oncogene *v-myc* which induces myelocytomatosis in chicken [Sheiness and Bishop, 1979; Vennstrom et al., 1982]. The Myc oncoprotein family comprises also N- and L-Myc [Sugiyama et al., 1989]. Myc is evolutionary highly conserved, it is expressed in all vertebrates and can even be found in *Drosophila melanogaster* [Gallant et al., 1996]. It is indispensable for embryonic development: homozygous deletion of c-Myc is embryonic lethal between day 8.5 and 9.5 [Davis et al., 1993], N-Myc-deficient mice die around day 11.5 [Sawai et al., 1993].

Elevated levels of active c-Myc can be observed in about 70 % of all human tumors with different causative mechanisms. Increased Myc protein levels in more than 80 % of human colon carcinomas for example are based on mutation of the *APC* gene which induces accumulation of β-catenin and thus results in increased *MYC* expression [He et al., 1998]. Amplification of the *MYC* gene leads to development of solid tumors such as mamma carcinomas [Park et al., 2005], small cell lung carcinomas [Yamada et al., 2000] or nodular malignant melanomas [Treszl et al., 2004]. In leukemias and lymphomas overexpression of Myc is often caused by translocations [Vita and Henriksson, 2006]. For instance, in 80 % of Burkitt's Lymphoma the t(8;14)(q24;q32) chromosomal translocation places the *MYC* coding region under the control of immunoglobulin gene enhancer elements [Dalla-Favera et al., 1982].

1.3.1. Structural and functional domains of the Myc protein

Myc proteins contain a C-terminal basic helix-loop-helix/leucine zipper domain (bHLH/LZ). This domain mediates sequence-specific DNA binding and heterodimerisation with another bHLH/LZ protein, Max (Myc-associated factor-X) [Blackwood and Eisenman, 1991]. The same region also allows for interaction with cofactors such as p300, Miz1 and CBP [Peukert et al., 1997; Vervoorts et al., 2003]. The amino terminal domain of Myc contains additional conserved elements, the so called Myc boxes I-IV. These mediate important functions such as Myc-induced apoptosis [Evan et al., 1992], transformation [Stone et al., 1987] and inhibition of differentiation [Freytag et al., 1990]. More precisely, Myc box I is essential for the transformation of primary rat fibroblasts by Myc and Ras [Stone et al., 1987]. Furthermore it plays an important role in Myc stability as it contains the phosphorylation sites threonine 58 and serine 62, which mediate binding of the ubiquitin ligase Fbw7 and thus enable proteasomal degradation of Myc [Sears et al., 2000; Welcker et al.,

2004b; Yada et al., 2004]. Myc box II serves as a binding platform for several interaction partners such as TRRAP (transactivation/transformation-associated protein) [McMahon et al., 1998], TIP48/49 (TBP interacting protein) [Wood et al., 2000] and Skp2 (S-phase kinase-associated protein 2) [Kim et al., 2003; von der Lehr et al., 2003] and is needed for transformation as well as transcriptional activation and repression by Myc. Myc boxes III and IV are crucial in modulating Myc-induced transformation and apoptosis [Herbst et al., 2005; Cowling et al., 2006].

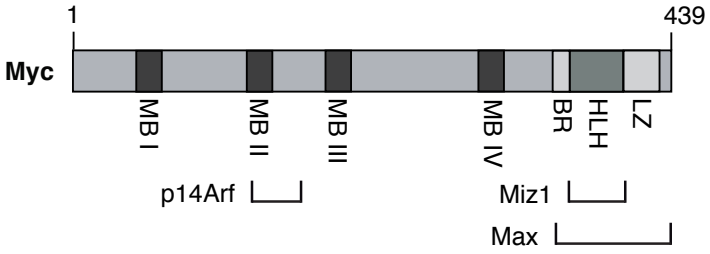

Figure 1.3.:
Schematic diagram of the Myc protein
Human c-Myc consist of 439 amino acids and contains several conserved regions: Myc boxes I-IV (MB I, II, III, IV), a basic region (BR), a helix-loop-helix motif (HLH) and a leucine zipper (LZ). The binding sites for several protein interactors are indicated by the brackets.

1.3.2. Transcriptional regulation by Myc

C-Myc has been shown to be a weak but expansive transcription factor that activates or represses transcription of about 10 % of the human genome. Myc has a broad range of target genes which however are typically regulated by less than twofold. It influences many different cellular processes such as proliferation and differentiation, ribosome biogenesis and protein synthesis, metabolism and genomic stability, cell adhesion, angiogenesis and apoptosis [Cole and Cowling, 2008].

Activation by Myc

For transcription of RNA polymerase I- and II-dependent target genes, the Myc/Max heterodimer binds to promoter sequences called E-boxes, which can be canonical (CACGTG) or non-canonical (such as CACGTT or CACATG) [Blackwell et al., 1990, 1993]. For *Drosophila melanogaster* also a Max-independent activation of RNA polymerase III-transcribed target genes has been described [Gallant and Steiger, 2009]. Transcriptional

activation by Myc involves recruitment of different coactivators such as the histone acetyltransferases CBP, GCN5, Tip60 and the ATPases Tip48/Tip49 [Adhikary and Eilers, 2005; Cole and Nikiforov, 2006], resulting in an open chromatin structure and therefore enabling transcription of target genes [Lee and Workman, 2007]. Additionally, Myc induces transcriptional activation by binding to the mediator complex and to the transcription elongation factor P-TEFb, thus enabling recruitment of RNA polymerase II to the promoter and allowing entry into the elongation phase [Bouchard et al., 2004; Eberhardy and Farnham, 2001].

Repression by Myc

Transcriptional repression by Myc is less well understood but essential for Myc-induced apoptosis and transformation [Patel and McMahon, 2006, 2007; Staller et al., 2001; Wu et al., 1999]. Transformation occurs because Myc represses a variety of genes from cell adhesion, cell-cell communication and inhibition of cell cycle progression [Frye et al., 2003; Gebhardt et al., 2006; Knoepfler et al., 2002; Wilson et al., 2004]. In general, Myc appears to repress genes by binding to their core promoter region. One mechanism of transcriptional repression is based on association of Myc to a transcriptional activator which is thus transformed to a repressor. This applies for example for Miz1 [Schneider et al., 1997] and Sp1 [Gartel et al., 2001], where Myc acts by displacing activating cofactors and by recruiting repressive cofactors [Lüscher and Vervoorts, 2012]. Earlier studies suggested this to be independent of Myc binding to the DNA, more recent studies provide evidence that repression requires Max and E-boxes [Mao et al., 2003; Herkert and Eilers, 2010]. Next to Miz1 and Sp1, other interaction partners of Myc have been identified which are blocked in their transactivation function by Myc, such as FoxO3a [Chandramohan et al., 2008], YY-1 [Shrivastava et al., 1993], TFII-Ip107/E2F [Luo et al., 2004] and NF-Y [Izumi et al., 2001].

1.3.3. Myc-induced apoptosis

Among its many functions Myc can also elicit apoptosis, which is thought to be a protective mechanism against oncogenic transformation [Askew et al., 1991; Evan et al., 1992; Murphy et al., 2008; Pelengaris et al., 2002]. Apoptosis induction by Myc involves transcriptional activation of the pro-apoptotic proteins Bax [Mitchell et al., 2000] and Bim [Egle et al., 2004] and repression of the anti-apoptotic proteins Bcl2 and Bcl-xL [Eischen et al., 2001a,b]. Elevated levels of c-Myc additionally increase expression of the tumor suppressor Arf and thus lead to stabilization of p53 [Zindy et al., 1998], which can either induce a reversible cell cycle arrest or apoptosis. High levels of Myc repress the cell cycle inhibitor p21 via

Miz1, which also is a prime target of p53 to induce G1 arrest [El-Deiry et al., 1993]. The anti-apoptotic Bcl2 is also a Miz1 target gene which is repressed by formation of the Miz1/Myc complex [Patel and McMahon, 2006, 2007]. Elevated Myc levels could thus favor the outcome of p53 activation against cell cycle arrest and towards activation of pro-apoptotic target genes. This notion is supported by observations based on human tumor samples and mouse models showing that a cooperation of Bcl-2 and Myc takes place during tumorigenesis [Eischen et al., 2001b; Knezevich et al., 2005; Letai et al., 2004; Martín-Subero et al., 2005].

1.3.4. Regulation of Myc function

It is well established that deregulated Myc plays a significant role in human cancer development and maintenance. Normal cells only express the *MYC* gene when dividing actively or upon stimulation by growth factors and reentry of the cell cycle [Kelly et al., 1983; Marcu et al., 1992]. In cancer cells, Myc can be deregulated by any one of several mechanisms that target the expression or activity of Myc directly or indirectly [Meyer and Penn, 2008]. Several means of regulation on a transcriptional, post-transcriptional and post-translational level that normally keep Myc under tight control will be discussed here.

Transcriptional regulation of Myc

Myc was identified as the first eukaryotic cellular gene to be regulated by a transcription elongation block which occurs during cellular differentiation and can be defective in cancer cells. The elongation block is executed as a reduction in the number of RNA polymerase II complexes that read through sites of termination or pausing within exon 1 of the *MYC* gene [Bentley and Groudine, 1986, 1988; Eick and Bornkamm, 1986].

The *MYC* promoter is bound by many different transcription factors (summarized in Wierstra and Alves [2008]). One example is the transcriptional regulation by E2F factors upon stimulation by viral oncoproteins E1A or large T [Hiebert et al., 1989; Thalmeier et al., 1989]. As E2F is also a direct Myc target both factors can thus stimulate each other in a positive feedback loop to allow entry into S phase. This induction by E2F can be repressed again by the TGF-β signalling pathway [Fernandez-Pol et al., 1987].

Post-transcriptional regulation of Myc

MYC mRNA is extremely unstable with a cytoplasmatic half-life of only about 20 minutes [Dani et al., 1984]. An early step in degradation of *MYC* mRNA is poly(A) shortening with subsequent mRNA destabilization and enzymatic decay [Brewer and Ross, 1988; Jones and Cole, 1987]. A mechanism that stabilizes the mRNA is based on binding of CRD-BP (coding region determinant-binding protein) at the carboxy-terminal region which protects the ribonucleic acid from endonuclease attack [Bernstein et al., 1992]. Amplification of CRD-BP was found in a variety of human tumors where it may be responsible for increased Myc levels [Doyle et al., 2000; Ioannidis et al., 2001; Noubissi et al., 2006].

Translational regulation of Myc

There are multiple regulatory mechanisms that regulate translation of the *MYC* mRNA. Its 5'UTR contains an IRES sequence (internal ribosome entry site) which promotes translation [Carter et al., 1999]. Several microRNAs interact with the 3'UTR of the *MYC* mRNA, which either blocks translation or mediates degradation of the mRNA [Cannell et al., 2010; Kress et al., 2011; Sachdeva et al., 2009; Sampson et al., 2007]. It was shown that the microRNAs mir-34b and c which bind to the 3'UTR of Myc are activated in a negative feedback loop by Myc itself. Myc transcriptionally induces the MK5 kinase that phosphorylates and activates FoxO3a which subsequently induces miR-34b and c, thus inducing proliferation arrest by lowering Myc levels. This mechanism can be deregulated in colorectal carcinomas [Kress et al., 2011].

Regulation of Myc via protein stability

Similarly to the *MYC* mRNA, the Myc protein is highly unstable with a half-life of only 20 to 30 minutes [Hann and Eisenman, 1984]. The rapid protein degradation is regulated by phosphorylation and ubiquitination of Myc [Hann, 2006; Vervoorts et al., 2006]. Initially, Myc is phosphorylated by MAP kinases at serine 62, which serves as a priming site for Gsk3 (Glykogen Synthase Kinase 3). Gsk3 phosphorylates Myc at threonine 58 (T58), upon which it is recognized by the Fbw7 ubiquitin ligase and then ubiquitinated and degraded in the proteasome [Lutterbach and Hann, 1994; Sears et al., 2000; Welcker et al., 2004b,a]. This pathway is disrupted in Burkitt lymphomas harboring T58 or S62 mutations in the Myc sequence, leading to reduced ubiquitination and enhanced stability of the Myc protein [Bahram et al., 2000].

The SCF-β-TrCP complex catalyzes attachment of heterotypic ubiquitin chains to the N-terminus of Myc, which antagonizes the SCF-Fbw7 mediated degradation and thereby leads to stabilization of the oncoprotein [Popov et al., 2010]. Finally, the ubiquitin ligase HectH9 catalyzes linkage of K63-linked polyubiquitin chains to Myc which does not elicit proteasomal degradation but recruitment of cofactors and transcriptional activation [Adhikary et al., 2005].

1.4. Objectives of the thesis

(1) Oncogenic activation of the Myc protein is one of the most frequent events on the way to tumor development. To prevent malignant transformation, cells have evolved different protective means of how to react to oncogenic stimuli. Arf triggers a p53-dependent pathway that safeguards cells against hyperproliferative signals, but activation of this pathway does not always have the same outcome. Constitutively active Ras for example activates the *INK4A/Arf* locus and thus induces an irreversible cell cycle arrest named oncogene-induced senescence [Palmero et al., 1998; Serrano et al., 1997]. Elevated Myc levels on the other hand do not induce senescence but rather elicit apoptosis [Evan et al., 1992]. Myc has been shown not only to activate but also to directly interact with the tumor suppressor Arf [Zindy et al., 1998; Qi et al., 2004]. Transcriptional repression by Myc for example via Miz1 also plays a role in Myc-induced apoptosis. Miz1 in turn has nucleophosmin as a coactivator [Wanzel et al., 2008], and nucleophosmin is also major binding partner for Arf. The first aim of this thesis was to explore a possible connection between the three proteins Arf, Myc and Miz1. This may improve our understanding of why Myc primarily elicits apoptosis as an oncogenic stress response.

(2) Posttranslational modifications have been linked to nearly all aspects of tumor development and are highly suitable for use as cancer biomarkers or as therapeutic targets. It is therefore vital to discover new modifications, especially on proteins closely linked to tumorigenesis such as Miz1 and Myc. Both proteins exhibit characteristics making them prone to be modified by sumoylation: nuclear Miz1 perfectly colocalizes with Sumo upon Arf expression, Myc contains a highly conserved region that might act as a Sumo interacting motif.
Therefore, the second aim of this thesis was to investigate wether Miz1 and Myc can be regulated by sumoylation.

Chapter 2.

Materials

2.1. Strains and cell lines

2.1.1. Human cell lines

HeLa
Human cervix carcinoma cell line (ATCC)

U2OS
Human osteasarcoma cell line (ATCC)

Phoenix
Human packaging cell line for MoMuLV-retroviruses (Phoenix-Eco) [Kinsella and Nolan, 1996]

HEK293T
Human embryonic kidney cell line (ATCC)

LS174T
colorectal adenocarcinoma cell line (ATCC)

2.1.2. Bacterial strains

DH5α
Escherichia coli F-, ϕ80dlacZΔM15, Δ(lacZYAargF)U169, deoR, recA1, endA1, hsdR17 (rk-,mk+), phoA, supE44, λ-, thi-1, gyrA96, relA1; for amplification of plasmids

XL1 blue
Escherichia coli, recA1, endA1, gyrA96, thi-1, hsdR17 supE44, relA1, lac [F'proAB lacIqZΔM15Tn10(Tetr)]; for generation and amplification of plasmids

BL21
Escherichia coli, F- ompT gal dcm lon hsdSB(rB- mB-) λDE3 lacI lacUV5-T7 gene 1 ind1 sam7 nin5; for expression of GST fusion proteins

2.2. Cultivation media and supplements

2.2.1. Media for mammalian cell culture

Basal medium DMEM containing L-glutamine (584 mg/ml) was purchased by Sigma. Fetal bovine serum (FBS; from PAA) was heat inactivated for 30 min at 56 °C before use.

Basal medium
DMEM 10 % (v/v) FBS 1 % (v/v) penicillin/ streptomycin (100,000 U/ml; from PAA)

Freezing medium
90 % (v/v) FBS 10 % (v/v) DMSO

2.2.2. Antibiotics for mammalian cell culture

For selection of successfully transfected or infected cells they were treated with the antibiotics given below. A resistance to neomycine was selected with G418, a bleomycine resistance with zeocine.

Blasticidin S (InvivoGen)	5-10 µg/ml
G418 (PAA)	800 µg/ml
Puromycin (InvivoGen)	2 µg/ml
Hygromycin (Merck)	100 µg/ml
Zeocin (InvivoGen)	50-500 µg/ml

2.2.3. Media and antibiotics for bacterial cell culture

Media

LB-medium
10 % (w/v) bacto tryptone
0.5 % (w/v) yeast extract
1 % (w/v) NaCl

LB-agar
LB-medium
1.2 % (w/v) Bacto-Agar
autoclaved, cooled down to 50 °C before adding ampicillin, 20 ml poured into 10 cm dishes

Antibiotics

Depending on the resistance marker on the corresponding DNA plasmid, the following antibiotics were added to the LB-medium or LB-agar:

Ampicillin	100 µg/ml
Kanamycin	100 µg/ml
Chloramphenicol	25 µg/ml

2.3. Nucleic acids

2.3.1. Primer

DNA-primers were synthesized either by Metabion or Sigma (f, fw, for = forward; r, rv, rev = reverse). Primers for quantitative qRT-PCR were designed with the help of the Universal Probe Library by Roche and are all intron-spanning to avoid amplification of genomic DNA.

Table 2.1.: List of primers

name	application	sequence 5' to 3'
Mlu-Bam-Arf	cloning	cgacgcgtggatccatggtgcgcagg
Arf-EcoRI-RV	cloning	cggatatcgaattctcagccaggtccacggg
Miz1-K251R-fwd	mutagenesis	gggcgcagggccagctgaggtcagggaggagggttcccagctgg

Table 2.1 – continued from previous page

Miz1-K251R-rev	mutagenesis	ccagctgggaaccctcctccctgacctcagctggccctgcgccc
Miz1-K138R-Fwd	mutagenesis	ggaggggacaagagagccagagaggagaaggtggccaccagcacgc
Miz-K138R-Rev	mutagenesis	gcgtgctggtggccaccttctcctctctggctctcttgtcccctcc
Miz-K166R-Fwd	mutagenesis	ggccccagcagggacctcagggaggagcgcggcggtcaggccc
Miz-K166R-Rev	mutagenesis	ggccccagcagggacctcagggaggagcgcggcggtcaggccc
Miz1-K229-Fwd	mutagenesis	ggaggtggagcccgcccggagaggggaagaggagcaaaaggagc
Miz-K229R-Rev	mutagenesis	gctccttttgctcctcttcccctctccgggcgggctccacctcc
Miz1-K307R-Fwd	mutagenesis	ccaaggcctacggctccgtcatccacaggtgcgaggactgtgggaagg
Miz-K307R-Rev	mutagenesis	ccttcccacagtcctcgcacctgtggatgacggagccgtaggccttgg
Miz-K696R-Fwd	mutagenesis	gccgatgagacggaagtcctgagggccgagatcagcaaagctgtgaagc
Miz-K696R-Rev	mutagenesis	gcttcacagctttgctgatctcggccctcaggacttccgtctcatcggc
Miz1-K704R-Fwd	mutagenesis	cagcaaagctgtgaggcaagtgcaggaag
Miz1-K704R-Rev	mutagenesis	cttcctgcacttgcctcacagctttgctg
MizV250A-F-S	mutagenesis	gggcgcagggccagctgaggccaaggaggagggttcccagctgg
MizV250A-R-S	mutagenesis	ccagctgggaaccctcctccttggcctcagctggccctgcgccc
MizE253A-F-S	mutagenesis	gggcgcagggccagctgaggtcaaggaggcgggttcccagctgg
MizE253A-R-S	mutagenesis	ccagctgggaacccgcctccttgacctcagctggccctgcgccc
Myc-K326R-f	mutagenesis	ctatcctgctgccaagagggtcaggttggacagtgtcagagtcc
Myc-K326R-r	mutagenesis	ggactctgacactgtccaacctgaccctcttggcagcaggatag
Myc-K355R-f	mutagenesis	cggacaccgaggagaatgtcaggaggcgaacacacaacgtcttgg
Myc-K355R-r	mutagenesis	ccaagacgttgtgtgttcgcctcctgacattctcctcggtgtccg
Myc-K323R-f	mutagenesis	cggaaggactatcctgctgccaagagggtcaagttggacagtgtcag
Myc-K323R-r	mutagenesis	ctgacactgtccaacttgaccctcttggcagcaggatagtccttccg
Sumo1-D15V-f	mutagenesis	ccttcaactgaggacttgggggttaagaaggaaggtg
Sumo1-D15V-r	mutagenesis	caccttccttcttaacccccaagtcctcagttgaagg
Sumo2-K11R-f	mutagenesis	cgaaaagcccaaggaaggagtcaggactgagaacaacgatcatattaatttg
Sumo2-K11R-r	mutagenesis	caaattaatatgatcgttgttctcagtcctgactccttccttgggcttttcg
Sumo2-K33,35R-f	mutagenesis	ggatggttctgtggtgcagtttaggattaggaggcatacaccacttag
Sumo2-K33,35R-r	mutagenesis	ctaagtggtgtatgcctcctaatcctaaactgcaccacagaaccatcc
Sumo2-K42,45R-f	mutagenesis	ggcatacaccacttagtagactaatgagagcctattgtgaacgacagttgg
Sumo2-K42,45R-r	mutagenesis	ccaactgtcgttcacaataggctctcattagtctactaagtggtgtatgcc
Myc-K326R-f	mutagenesis	ctatcctgctgccaagagggtcaggttggacagtgtcagagtcc
Myc-K326R-r	mutagenesis	ggactctgacactgtccaacctgaccctcttggcagcaggatag

Table 2.1 – continued from previous page

Myc-K355R-f	mutagenesis	cggacaccgaggagaatgtcaggaggcgaacacacaacgtcttgg
Myc-K355R-r	mutagenesis	ccaagacgttgtgtgttcgcctcctgacattctcctcggtgtccg
MycK323,326Rf	mutagenesis	ggactatcctgctgccaggagggtcaggttggacagtgtcagagtcc
MycK323,326Rr	mutagenesis	ggactctgacactgtccaacctgaccctcctggcagcaggatagtcc
MycR323,326Kf	mutagenesis	ggactatcctgctgccaagagggtcaagttggacagtgtcagag
MycR323,326Kr	mutagenesis	ctctgacactgtccaacttgaccctcttggcagcaggatagtcc
MycR355K-fw	mutagenesis	cggacaccgaggagaatgtcaagaggcgaacacacaacgtcttgg
MycR355K-rv	mutagenesis	ccaagacgttgtgtgttcgcctcttgacattctcctcggtgtccg
MycR341K-fw	mutagenesis	gacagatcagcaacaaccgaaaatgcaccagccccaggtcc
MycR341K-rv	mutagenesis	ggacctggggctggtgcattttcggttgttgctgatctgtc
MycK341R-f	mutagenesis	gacagatcagcaacaaccgaagatgcaccagccccaggtcc
MycK341R-r	mutagenesis	ggacctggggctggtgcatcttcggttgttgctgatctgtc
cMyc-ADAA-fw	mutagenesis	caagaagatgaggaagaagccgatgctgcttctgtggaaaagaggcagg
cMyc-ADAA-rv	mutagenesis	cctgcctcttttccacagaagcagcatcggcttcttcctcatcttcttg
MycR317K-f	mutagenesis	cgcagcgcctccctccactcggaaggactatcctgctgcc
MycR317K-r	mutagenesis	ggcagcaggatagtccttccgagtggagggaggcgctgcg
MycR289K-f	mutagenesis	cttctgctggaggccacagcaaacctcctcacagcccactg
MycR289K-r	mutagenesis	cagtgggctgtgaggaggtttgctgtggcctccagcagaag
MycR430K-fw	mutagenesis	gacgagaacagttgagacacaaacttgaacagctacggaact
MycR430K-rv	mutagenesis	agttccgtagctgttcaagtttgtgtctcaactgttctcgtc

2.3.2. RNA oligonucleotides

Pools of four RNA oligonucleotides against *UBC9* were purchased from Dharmacon (ON-TARGETplus SMARTpool). As a control the siCONTROL (ON-TARGETplus Non-targeting Pool) was used. Target sequences against *UBC9*:

GGGAAGGAGGCUUGUUUAA
GAAGUUUGCGCCCUCAUAA
GGCCAGCCAUCACAAUCAA
GAACCACCAUUAUUUCACC

2.4. Plasmids

2.4.1. Empty vectors

Table 2.2.: List of empty vectors

pcDNA 3.0 / pcDNA 3.1	Eucaryotic expression vector with CMV (cytomegalovirus)-promoter (Invitrogen)
pBabe hygro/puro/bleo/neo	Eucaryotic retroviral expression vector with LTR-promoter and hygromycin-, puromycin-, bleomycin-, neomycin- resistance (xxx Morgenstern and Land, 1990)
pGEX-4T3	Bacterial expression vector with tac-promoter for expression of GST-tagged recombinant proteins (GE Healthcare)
peGFP N1	Eucaryotic expression vector with CMV (cytomegalovirus)-promoter for generation of C-terminal eGFP-tagged fusion proteins (Clontech)

2.4.2. Expression vectors

Table 2.3.: List of expression vectors

pcDNA3 *MIZ1*	pcDNA3 with CDS of human *MIZ1*
pcDNA3 *MYC*	pcDNA3 with CDS of human *C-MYC*
pcDNA3 *HA-NPM*	pcDNA3 with CDS of human HA-tagged *NPM*
pcDNA3 *His-SUMO2*	pcDNA3 with CDS of human His-tagged *SUMO2*
pcDNA3 *p14ARF*	pcDNA3 with CDS of human *p14ARF*
pcDNA3 *SENP3*	pcDNA3 with CDS of human *SENP3*
pcDNA3 *TOPBP1*	pcDNA3 with CDS of human *TOPBP1*
peGFP *p14ARF* 1-132	peGFP with CDS of human *p14ARF*
peGFP *p14ARF* 65-132	peGFP for expression of an N-terminal deletion mutant of human *p14ARF* (aa 65-132)
pGL2 p15(-113/+160)	pGL2 with the human p15Ink4b- promoter sequence from -113 until +160 followed by the firefly luciferase gene
pGEX *GST-MIZ1*	pGEX-4T2 expression vector (GE Healthcare) with CDS of human *MIZ1*
pGEX *GST-SUMO1*	pGEX expression vector (GE Healthcare) with CDS of human *SUMO1*
pGEX *GST-SUMO2*	pGEX expression vector (GE Healthcare) with CDS of human *SUMO2*
pRRL puro *MIZ1*	pRRL with puromycin resistance and CDS of human *MIZ1* for lentiviral infection
pLV-red *P14ARF*	pLV-red with CDS of human *P14ARF* for lentiviral infection

2.4.3. Lentiviral packaging vectors

Table 2.4.: List of lentiviral packaging vectors

psPAX2	plasmid coding for the lentiviral virion packaging system (HIV gag, pol, rev)
pMD2.g	plasmid coding for the lentiviral envelope (VSV-G env)

2.5. Antibodies

WB: Western blot; IF: immunofluorescence; IP: immunoprecipitation;
mono: monoclonal; poly: polyclonal
m: mouse; r: rabbit

2.5.1. Primary Antibodies

Table 2.5.: List of primary antibodies

protein	type	application	name
β-actin	m, mono IgG1	WB	AC15 (Sigma)
Cdk2	m, mono IgG1	WB	M-2 (Santa Cruz)
GFP	m, mono IgG1	WB	G6539 (Sigma)
HA	m, mono IgG1	WB	16B12 (Covance)
Miz1	m, mono	WB, IF, IP	10E2 (group Eilers production)
c-Myc	m, mono IgG	WB, IF	9E10 (group Eilers production)
p14Arf	r, poly	WB, IF	NB200-111 (Novus Biologicals)
Ubc9	r, poly	WB	Ab33044 (Abcam)
NPM1	m, mono	WB, IF	ab10530 (Abcam)
FLAG (M2)	m, mono IgG1	WB, IF	F3165 (Sigma)
N-Myc	m, mono IgG2a	WB	B8.4.B (BD)
Sumo1	m, mono IgG1	WB	33-2400 (Invitrogen)
Sumo2	r, poly	WB	57-9100 (Invitrogen)

2.5.2. Secondary Antibodies

Table 2.6.: List of secondary antibodies

name	application	description
α-rabbit-HRP	WB	donkey-anti-rabbit-immunoglobulin coupled with horseradish peroxidase (Amersham, NA 934)
α-mouse-HRP	WB	donkey-anti-mouse-immunglobulin coupled with horseradish peroxidase (Amersham, NA 931)
α-mouse-Alexa488	IF	goat-anti-mouse-immunglobulin conjugated with Alexa Fluor 488 (Invitrogen, A11001)
α-mouse-Alexa647	IF	goat-anti-mouse-immunglobulin conjugated with Alexa Fluor 647
α-rabbit-Alexa488	IF	goat-anti-rabbit-immunglobulin conjugated with Alexa Fluor 488
α-rabbit-Alexa647	IF	goat-anti-rabbit-immunglobulin conjugated with Alexa Fluor 647

2.6. Chemicals

All chemicals were purchased from the companies Sigma, Merck, Roth, Acors Organics, Invitrogen and Applichem and used without further purification.

2.7. Enzymes, standards and kits

2.7.1. Enzymes

DNase-free RNase A	Quiagen
M-MLV reverse transcriptase	Promega
Restriction endonucleases	Fermentas, New England Biolabs
RNase-free DNase	Fermentas
T4-DNA-Ligase	Fermentas
Pfu Polymerase	Fermentas
Pfu-Turbo Polymerase	Stratagene
Phusion High Fidelity Polymerase	Fermentas

2.7.2. Standards

Protein marker	PageRuler Prestained Protein Ladder (Fermentas)
DNA marker	1 kb DNA Ladder (Invitrogen)

2.7.3. Kits

JETSTAR 2.0 Plasmid Purification Maxi Kit	Genomed
GeneJET Gel Extraction Kit	Fermentas
RNeasy Mini Kit	Quiagen
SYBR Green qPCR Master Mix	Thermo Scientific
TnT Quick Coupled Transcription/Translation Systems	Promega
Qiaquick PCR Purification Kit	Qiagen

2.8. Buffers and solutions

Bacterial lysis buffer
50 mM NaCl
50 mM Tris base
5 mM EDTA

Bacterial wash buffer
50 mM Tris base
5 mM EDTA
adjust to pH 8 with 6M HCl
1:1000 proteinase inhibitors (freshly added)

Blocking solution for PVDF membrane
5 % (w/v) skim milk powder in TBS-T

Coomassie staining solution
25 % (v/v) isopropanol
10 % (v/v) acetic acid
0.05 % (w/v) Coomassie G250 stain

Coomassie destain solution
10 % (v/v) acetic acid
20 % (v/v) methanol

Crystal violet solution
0.1 % (w/v) crystal violet
20 % (v/v) ethanol

DNA loading buffer
40 % (w/v) saccharose (pH 8.0)
0.2 % (w/v) bromphenol blue
0.2 % (w/v) xylene cyanol
10 mM EDTA

GST binding buffer
25 mM HEPES pH 7.6
100 mM KCl
12.5 mM MgCl2
20 % Glycerin
0.05 % NP40
1 mg/ml BSA
1 mM DTT

GST wash buffer
25 mM HEPES pH 7.6
100 mM KCl
12.5 mM MgCl2
20 % Glycerin
0.1 % NP40
1.5 mg/ml BSA

HBS (2x) for transfection
280 mM NaCl
1.5 mM Na_2HPO_4
50 mM HEPES
adjusted to pH 7.4
sterile filtered

Low salt lysis buffer
25 mM glycylglycine
15 mM $MgSO_4$
4 mM EGTA
1 % (vol/vol) Triton X-100

Luciferase substrate solution
25 mM glycylglycine solution
15 mM K_3PO_4 (pH 8.0)
4 mM EGTA
15 mM $MgSO_4$
75 µM D-luciferine
2 mM ATP
1 mM DTT

Mowiol solution
13.3 % (w/v) Mowiol 4-88
33.3 % (v/v) glycerine
0.13 M Tris (pH 8.5)

NP-40 lysis buffer
50 mM Tris-HCl
150 mM NaCl
1 % NP-40
adjusted to pH 8.0

PBS
137 mM NaCl
2.7 mM KCl
10.1 mM Na_2HPO_4
1.76 mM KH_2PO_4
autoclaved

PI-FACS-buffer
38 mM sodium citrate
54 µM propidiumiodide
24 µg/ml Rnase A

Plasmid prep buffer 1
50 mM Tris-HCl (pH 8.0)
100 mM EDTA
100 µg/ml RnaseA

Plasmid prep buffer 2
200 mM NaOH
1 % (w/v) SDS

Plasmid prep buffer 3
3.1 M potassium acetate (pH 5.5)

RIPA lysis buffer
150 mM NaCl
1 % (v/v) NP-40
0.5 % (w/v) DOC
0.1 % (w/v) SDS
50 mM Tris (pH 7.5)

SDS sample buffer (3x)
187.5 mM Tris (pH 6.8)
30 % (v/v) glycerine
6 % SDS (sodium dodecyl sulfate)
0.03 % (w/v)bromphenol blue
2 M β-mercaptoethanol

SDS running buffer
25 mM Tris Base
250 mM glycine
0.1 % SDS

Stripping buffer
62.5 mM Tris (pH 6.8)
2 % (w/v) SDS
100 mM β-mercaptoethanol

Tank blot buffer (10x)
1.9 M glycine
250 mM Tris Base
0.05 % SDS
adjusted to pH 8.0

TBS (20x)
500 mM Tris Base
2.8 M NaCl
adjusted to pH 7.4

TBS-T
0.2 % Tween-20
25 mM Tris, 140mM NaCl
adjusted to pH 7.4

TE
10 mM Tris
1 mM EDTA
adjusted to pH 8.0

TAE
40 mM Tris
0.114 % (v/v) acetic acid
1 mM EDTA
adjusted to pH 8.0

Separating gel 10-15 %
10 - 15 % (v/v) acrylamide/bisacrylamide
375 mM Tris-Hcl (pH 8.8)
0.1 % (w/v) SDS
0.1 % (w/v) APS
0.1 % (v/v) TEMED

Stacking gel 4 %
4 % acrylamide/bis-acrylamide
125 mM Tris-HCl (pH 6.8)
0.1 % (w/v) SDS
0.1 % (w/v) APS
0.1 % (v/v) TEMED

Sumo buffer A
25 mM Tris-HCl (pH 6.8)
20 mM imidazole
protease inhibitor cocktail (1:1000, Sigma) and 0.1mM NEM (Sigma) freshly added

Sumo buffer B
6 M guanidium hydrochloride
10 mM imidazole
in PBS
protease inhibitor cocktail (1:1000, Sigma) and 0.1mM NEM (Sigma) freshly added

TNN lysis buffer
50 mM Tris-HCl pH 7.4
120 mM NaCl
5 mM EDTA
0.5 % (v/v) NP40
10 mM $Na_4P_2O_7$
100 mM NaF
2 mM $NaVO_4$
protease inhibitor cocktail (1:1000, Sigma), freshly added

trypsin solution
0.25 % trypsin
5 mM EDTA
22.3 mM Tris pH 7.4
125 mM NaCl

2.9. Consumables and equipment

Consumables such as reaction tubes, cell culture and other plastic products were purchased from Applied Biosystems, Eppendorf, Greiner, Kimberley-Clark, Nunc, Sarstedt, B. Braun, Schleicher und Schüll, Millipore and VWR international.

2.9.1. Equipment

Chemiluminescence imaging
LAS-4000 mini (Fujifilm)

Cell culture incubator
BBD 6220 (Heraeus)

Cell counter
CASY cell counter (Innovatis)

Centrifuges
Galaxy MiniStar (VWR International)
Eppendorf 5417 R (Eppendorf)
Eppendorf 542 (Eppendorf)
Multifuge 1S-R (Heraeus)
Avanti J-26 XP (Beckman Coulter)

Fluorcytometer
BD FACS Canto II (BD Biosciences)

Heating block
Dry Bath System (STARLAB)

Incubator shaker
Model G25 (New Brunswick Scientific)

Luminometer
GloMax 96 Microplate Luminometer (Promega)

Microscope for immunofluorescence
DMI 6000 B (Leica)
SP5 (Leica)

Microscope for cell culture
Axiovert 40CFL (Zeiss)

PCR thermal cycler
Mastercycler pro S (Eppendorf)

Photometer
UltrospecTM 3100 pro UV/Visible (Amersham Biosciences)
Spectrofluorometer NanoDrop 3000 (Thermo Scientific)

Power supply
PowerPac HC (Bio-Rad)

Quantitation of RNA
Experion Automated Electrophoresis System (Bio-Rad)
StdSens Experion RNA Chip

Quantitative real-time PCR machine
MXp3000P qPCR system (Stratagene)

SDS-PAGE system
Mini-PROTEAN Tetra Cell (Bio-Rad)

Sterile bench
HeraSafe (Heraeus)

Ultrasonifier
W-250 D (Heinemann)

Universal shaker
SM-30 (Edmund Bühler GmbH)

UV fluorescent table
Maxi UV fluorescent table (PEQLAB)

UV filtered lamp
VL-6.MC with 312nm and 254nm (Vilber Lourmat)

Vortex mixer
Vortex-Genie 2 (Scientific Industries)

Waterbath
ED-5M heating bath (Julabo)

Western blot transfer chamber
Harnischmacher

2.10. Software

Ape plasmid editor
M. Wayne Davis

BD FACSDiva 6.1.2
BD Biosciences

CLC Sequence Viewer 6
CLC bio
DOG visualization of protein domain structures
Lab of Cell Dynamics, Hefei, China

GraphPad Prism
GraphPad Software

LAS AF 2.0
Leica

MxPro qPCR Software
Stratagene

Multi Gauge
Fujifilm

Papers
Mekentosj

SUMOsp 2.0 SUMOylation sites prediction
Lab of Cell Dynamics, Hefei, China

Mac OS X
Apple Inc.

Illustrator™, Photoshop™, Acrobat™
Adobe Inc.

Windows XP™; Excel™, Power Point™
Microsoft Inc.

TeXniCcenter
BCG Soft Ltd.

Chapter 3.

Methods

3.1. Molecular biology methods

3.1.1. Transfection of bacteria with plasmid DNA and plasmid amplification

Circular DNA can be transformed into bacteria to amplify the plasmid. Competent bacteria were thawed on ice and mixed with 1 µg plasmid DNA or ligation mix, then incubated on ice for 30 min followed by a one minute heat shock at 42 °C. The bacteria were plated on an LB agar plate to pick clones from the next day or directly cultivated in 200 ml LB medium to amplify the plasmid on a larger scale. Both procedures were conducted at 37 °C using the appropriate antibiotic to select for bacteria that had been successfully transformed.

3.1.2. Isolation of plasmid DNA from bacteria

A large scale purification of plasmid DNA was performed with the JETSTAR 2.0 Plasmid Purification Maxi Kit according to the manufacturer's instructions. The purified plasmid was dissolved in B. Braun water, diluted to a concentration of 1 µg/µl and stored at -20 °C. For the isolation of small amounts of plasmid (mini prep), 1.5 ml of cultivated bacteria were transferred to a reaction tube, spun down and resuspended in 200 µl plasmid prep buffer 1 to lyse the cells. After a five minute incubation at room temperature 200 µl plasmid prep buffer 2 was added to denature the protein components, these were spun down subsequently (18,000 x g, 5 min, 4 °C). The supernatant was vigorously mixed with 200 µl isopropanol to precipitate the DNA, which was then pelleted through centrifugation (18,000 x g, 10 min, 4 °C). The DNA was washed one with 70 % Ethanol, then dried and resuspended in 50 µl B. Braun water.

3.1.3. Nucleid acid quantitation

The concentration of DNA and RNA in solution was determined with Peqlab's NanoDrop 1000. Purity was determined by assessing the ratio of absorbance at 260 and 280 nm. For pure DNA, A260/280 is $\sim$ 1.8, for RNA $\sim$ 2.

3.1.4. Sequence specific hydrolysis of DNA (restriction digest)

DNA was hydrolyzed in a sequence-specific manner with restriction endonucleases from Fermentas and New England Biolabs using the recommended reaction buffers. The digestions were set up according to the table below and incubated at 37 °C for one hour.

Table 3.1.: Restriction digest mix

2 µg	DNA
1 µl	restriction endonuclease 1
1 µl	restriction endonuclease 2 (if applicable)
2 µl	10 x reaction buffer
ad 20 µl	aqua bidest.

3.1.5. Separation of DNA fragments via gel electrophoresis

DNA fragments of different sizes were separated by agarose gel electrophoresis. Depending on the fragment size, a solution of 1-2 % agarose was boiled in TAE buffer. 0.3 µg/ml ethidium bromide was added and the molten agarose was poured into a gel chamber with combs to form sample wells in the gel. DNA loading buffer was added to the DNA samples which were then pipetted into the wells of the polymerized agarose gel. The size of the nucleotide fragments was determined using 1.5 µl of the 1 kb DNA Ladder from Invitrogen which was separated next to the samples. The gel was run at 120 V for one hour, then the DNA fragments were visualized using a UV transilluminator which detects the intercalator ethidium bromide.

3.1.6. DNA extraction and purification from agarose gels

After separating the DNA by gel electrophoresis the fragment of interest was cut out of the gel with a scalpel. The DNA was extracted from the gel using the Gel Extraction Kit from Qiagen following the manufacturer's protocol.

3.1.7. Ligation of DNA fragments

Double stranded DNA fragments were attached to one another covalently by means of ligation. Insert and plasmid were incubated in a molar ration of 3 : 1 in the ligation mix according to the table below and incubated for four hours at RT or o./n. at 16 °C. To

calculate the optimal amounts of backbone and plasmid the Gibthon ligation calculator was used (http://www.gibthon.org/ligate.html).

Table 3.2.: Ligation mix

$\sim$ 100 ng	linearized plasmid
x ng	DNA fragment (insert)
1 µl	T4 DNA ligase buffer (Fermentas)
1 µl	T4 DNA ligase (Fermentas)
ad 10 µl	aqua bidest.

3.1.8. Isolation of RNA

For the isolation of total RNA from cultured cells TriFast reagent from Peqlab was used. Cells were pelleted by centrifugation (5 min, 400 x g, 4 °C), then resuspended in 1 ml TriFast. After five minutes 200 µl chloroform was added and the mixture was vortexed thoroughly for 15 seconds. After three more minutes of incubation the solution was separated into aqueous and organic phase by centrifugation (10 min, 18,000 x g, 4 °C). The upper, aqueous phase was transferred into a fresh reaction tube and the RNA was precipitated by adding an equal volume of isopropanol followed by vortexing for 15 seconds. The samples were frozen at -20 °C for 30 minutes, then centrifuged (10 min, 18,000 x g, 4 °C) and the pellet was washed in 75 % Ethanol. The final pellet was dried, then resuspended in 20 µl B. Braun water, frozen at -20 °C, then thawed again and the RNA concentration was determined by NanoDrop measurement. The RNA was used for cDNA synthesis and the remainder stored at -80 °C.

3.1.9. DNAse digestion and cDNA synthesis

To remove any residual traces of DNA from the RNA preparations, a DNAse digestion was performed on the total RNA isolated from the cells. 2 µg of RNA were diluted in 8 µl of B. Braun water and mixed with 1 µl of 10 x digestion buffer containing $MgCl_2$, 1 µl of RNAse-free DNAse (both from Qiagen) and 0.2 µl of RNAse inhibitor Ribolock (Fermentas) . This mix was incubated for 30 minutes at 37 °C, then 1 µl of 25 mM EDTA was added and incubated at 65 °C for 10 minutes to stop the digestion.
To quantify specific mRNAs, the RNA was then transcribed into complementary DNA (cDNA) by reverse transcription, using random hexanucleotide primers. For that, 2 µg total RNA in a volume of 10 µl were heated up to 65 °C to dissolve any secondary

structures. The cDNA synthesis mix according to the table below was added and incubated for 10 min at RT, 50 min at 37 °C and 15 min at 70 °C. The generated cDNA was used for qRT PCR and stored at -80 °C.

Table 3.3.: cDNA synthesis mix

10 µl	5 x First Strand Buffer (Invitrogen)
5 µl	dNTPs (2.5 mM, Roth)
2 µl	random primer $p(dN)_6$ (2 µg/ml)
0.2 µl	Ribolock (Fermentas)
1 µl	M-MLV reverse transcriptase (200 U/µl, Promega)
ad 40 µl	B. Braun water

3.1.10. Polymerase chain reaction (PCR)

The polymerase chain reaction [Mullis et al., 1992] was used to amplify specific regions of nucleic acids for different purposes as described below.

PCR to amplify cDNA for cloning

To generate new expression vectors the gene of interest was amplified based on existing expression vectors, which allowed for the addition of new restriction sites.

Table 3.4.: Standard PCR setup

5 µl	10 x Pfu buffer (Stratagene)
1 µl	Pfu polymerase (Stratagene)
100 ng	cDNA template
10 pmol	forward primer
10 pmol	reverse primer
1 µl	DMSO
1 µl	dNTPs (10 mM)
ad 50 µl	B. Braun water

PCR based site directed mutagenesis

To mutate single bases in a PCR template primers were chosen as such to fit the desired target sequence. As such, a product mostly containing the modified bases was generated.

Table 3.5.: Standard PCR thermal cycling profile

temperature	**time**	
95 °C	3 min	
95 °C	30 sec	} *30 cycles*
53 - 65 °C (template dependent)	60 sec	
68 °C	3 min	
72 °C	10 min	

To remove residual wild type template DNA, the PCR product was digested with the enzyme DpnI (1 h, 37 °C), which hydrolyses only methylated DNA.

Table 3.6.: Mutagenesis PCR setup

5 µl	10 x Phusion buffer (Fermentas)
1 µl	Phusion High Fidelity Polymerase (Fermentas)
100 ng	cDNA template
0.25 pmol	forward primer
0.25 pmol	reverse primer
0-5 µl	DMSO
1 µl	dNTPs (10 mM)
ad 50 µl	B. Braun water

Table 3.7.: Mutagenesis PCR thermal cycling profile

temperature	**time**	
98 °C	1 min	
98 °C	30 sec	} *16 cycles*
55 °C	60 sec	
72 °C	2 min	
72 °C	10 min	

Quantitative reverse transcriptase PCR (qRT PCR)

To quantify specific mRNA levels the cDNA synthesized by reverse transcription was amplified by real time PCR. The qPCR SYBR Green Mix from Thermo Scientific was used to set up a reaction mix as described in the table below, and pipetted into the wells of 96-well qPCR plates. Finally, 10 µl of a 1:10 dilution of cDNA was added to each well, the measurement was carried out with the Mx3000P qPCR system (Stratagene).

Table 3.8.: qRT PCR setup

5 µl	SYBR Green Mix (Thermo Scientific)
1 µl	1 µl forward primer (10 pmol/ µl)
1 µl	1 µl reverse primer (10 pmol/ µl)
ad 10 µl	B. Braun water
10 µl	cDNA in a 1:10 dilution added to the respective wells

Table 3.9.: qRT PCR thermal cycling profile

temperature	**time**	
95 °C	15 min	
95 °C 60 °C (template dependent) 72 °C	30 sec 20 sec 15 sec	} *38 cycles*
95 °C	1 min	
60 °C	30 sec	
95 °C	30 sec	

The basis of real time PCR is fluorescent monitoring of DNA amplification, from which target DNA concentration can be determined from the fractional cycle at which a threshold amount of amplicon DNA is produced. The calculation was performed using the relative CT method (Applied Biosystems User Bulletin 2); the housekeeping gene beta-2-microglobulin was used for normalization. The measurements were performed in triplicates to calculate the standard deviation according to the Gaussian law of error.

3.1.11. Microarray

RNA for a genome-wide microarray analysis was extracted from cells using the RNeasy Mini Kit (Qiagen). The quality and quantity of the RNA were examined using the Experion Automated Electrophoresis System with a StdSens Experion RNA Chip (Bio-Rad). Total RNA was labeled with the Quick Amp Labeling Kit (2-Color; Agilent). Agilent SurePrint G3 Human GE 8x60K Microarray (Agilent; Design ID: 028004) was used for the analysis of the gene expression of the different samples in a reference design assay. The reference was generated as a pool of all samples to be analyzed. This reference probe was labeled with Cy3 dye, whereas the samples were labeled with Cy5 dye. After a 17 h hybridization at 65 °C, slides were washed according to the manufacturer's instructions and subsequently scanned using an Agilent DNA microarray scanner G2505C (scan software: Agilent Scan Control version A.8.1.3; quantification software: Agilent Feature Extraction version 10.5.1.1, FE Protocol GE2_105_Dec08).

The resulting intensity values for the red and green channels were normalized using the lowess method within the limma package in R/BioConductor. Regulated probes were selected on the basis that the logarithmic (base 2) average intensity value (A-Value) was $\geq$5. A threshold to indicate probes as differentially expressed between two samples (M-Value) was set at 2-fold change (log2(M) $\geq$1).

3.2. Cell biology methods

All cell culture work was performed at a sterile workbench. Cells were cultivated in CO_2 incubators at 37 °C, 95 % relative humidity and 5 % CO_2.

3.2.1. Passaging of cells

Adherent cells were passaged before completely covering the surface to avoid contact inhibition of growth. The cultivation medium was removed and the cells were washed with PBS. An appropriate amount of trypsin solution was added (e.g. 1 ml on a 10 cm dish) and incubated for 5 minutes at 37 °C to detach the cells. By resuspending the cells in fresh medium the enzymatic activity of trypsin was stopped and a single cell solution was generated. For S2 cells the cell count was determined with a Neubauer counting chamber, for S1 cells with the CASY cell counter. The cells were then seeded for experiments according to their size and proliferation rate in relation to the length of the experiment.

3.2.2. Freezing and thawing cells

For long-term freezer storage cells were detached with trypsin solution as described above, resuspended in fresh medium and then pelleted (5 min, 400 x g, 4 °C). The cells were resuspended in 1 ml freezing medium containing DMSO, transferred to a cryo vial and then slowly frozen at -80 °C using a MrFROSTY freezing container. After 24 h the cells were stored in a liquid nitrogen storage tank.
To unfreeze cells stored in cryo vials these were quickly heated up in a 37 °C water bath, then transfered onto a 10 cm dish containing 10 ml fresh medium. After the cells had attached to the dish the medium was replaced to remove all traces of DMSO.

3.2.3. Transfection of plasmid DNA

To transfect mammalian cells with plasmid DNA one of the following transfection methods was used, depending on the transfection efficiency in different cell lines. An expression of the transiently transfected DNA was observed mostly already after 24 h.

Calcium phosphate transfection

Cells were seeded 24 h before transfection. For 10 cm dishes, 500 µl transfection mix was prepared according to the table below, for dishes with a lower or higher surface area the total volume of transfection agent was scaled appropriately. The transfection mix was

incubated for 5 minutes at RT, then 500 µl 2 x HBS was added dropwise while vortexing to generate calcium phosphate DNA complexes, which were then immediately added to the cells. 12-16 h later the remaining DNA precipitates were removed by washing the cells with PBS upon which fresh medium was added.

Table 3.10.: Transfection mix

5-20 µg	plasmid DNA
50 µl	$CaCl_2$ (2.5 M)
ad 500 µl	B. Braun water

Polyethylenimine (PEI) transfection

Cells were seeded 24 h before transfection in their usual cultivation medium. 5 h before the actual transfection process the basal medium was replaced by transfection medium containing only 2 % FCS and no antibiotics. A transfection mix containing 5-15 µg plasmid DNA and 500 µl PBS as well as 10-30 µl PEI in 500 µl PBS were each set up to incubate 5 min at RT. Then the PEI/PBS solution was added to the DNA mix to incubate another 20 minutes at the same conditions before dropping it onto the cells. 4 h later the remaining DNA precipitates were removed by washing the cells with PBS upon which fresh medium was added.

3.2.4. Transfection of siRNA

For the transfection of synthetic siRNAs cells were seeded at high density in 6 cm dishes using antibiotic-free medium. 24 hours later 5 µl siRNA (20 µg) was diluted with Opti-MEM I (Invitrogen) to 500 µl. 10 µl of of the lipid transfection reagent Lipofectamine RNAiMAX (Invitrogen) was likewise diluted with Opti-MEM I to a volume of 500 µl. RNA and transfection solution were mixed to incubate for 20 min at RT, then dropped onto the cells, leading to a final concentration of 20 nM siRNA and 0,2 % RNAiMAX. 12-16 h later the cells were provided with fresh medium.

3.2.5. Infection of mammalian cells

Cells were infected to stably integrate plasmid DNA into the genome of target cells.

Infection with retrovirus

For infection with retrovirus the moloney murine leukaemia virus (Mo-MuLV) was generated, which infects a range of hosts including mice. The packaging cell line Phoenix-Eco was used to generate this recombinant retrovirus. Phoenix cells originate from HEK 293T cells and express the viral gene fragments gag, env and pol. To infect human cell lines these were transfected with the murine ecotrophic receptor beforehand.

Phoenix cells were seeded at a high density to be transfected 24 h later. The calcium phosphate method was used to transfect the cells with retroviral expression vectors such as pBABE. 15 h later, the cells were provided with a low amount of fresh medium concentrating the virus released by the cells into the supernatant. The virus supernatant was harvested in 15 ml falcons after approximately 40 and 64 h and filtered with a syringe and 45 µm sterile filter (Sarstedt) to remove residual Phoenix cells. The virus was then snap-frozen in liquid nitrogen to be stored at -80 °C.

Target cells to be infected were seeded 24 h prior to infection. The virus supernatant was thawed quickly in the 37 °C waterbath. For 10 cm dishes the old medium was removed, 5 ml of virus supernatant were supplemented with 3 ml fresh medium and added to the cells. To increase the infection efficiency, 5 µl of the cationic polymer polybrene (4 µg/µl hexadimethrin bromide) was added as well. The supernatant was exchanged 12-16 h later for complete medium. To select for successfully transfected cells antibiotics were added 48 h after infection, comparing infected with uninfected cells to determine the completion of the selection process.

Infection with lentivirus

Lentivirus can very efficiently mediate integration of transgenes in dividing and unlike retrovirus also in nondividing cells. HEK 293T cells were used to generate lentivector particles by transfecting them with separate plasmids coding for the virion packaging system, the envelope, and the gene of interest. The structural and enzymatic components of the virion came from HIV-1, the envelope from vesicular stomatitis virus (VSV), using a second generation LV packaging system.

HEK 293T cells were seeded at a high density. 24 h later the cells were transfected with the packaging vector psPAX.2, the envelope vector pMD2G and the gene of interest in an appropriate vector, such as pRRL. 15 h later, the cells were provided with a low amount

of fresh medium concentrating the virus released by the cells into the supernatant. The virus supernatant was harvested in 15 ml falcons after approximately 40 and 64 h and filtered with a syringe and 45 µm sterile filter (Sarstedt) to remove residual Phoenix cells. The virus was frozen at -80 °C for storage.

3.2.6. Colony Assay

The proliferation behavior of cells was determined by colony assay. Cells were infected with different genes of interest and a control and selected with antibiotics if necessary. After selection, the cells from each condition were counted and a defined number was seeded on 6 cm dishes using medium without the selection agent. The cells were grown for six to seven days without allowing them to become confluent. To visualize the colonies cells were washed with PBS, then stained with the triphenylmethan dye crystal violet for at least 1 h. The superfluous dye was washed away with desalted water and the cell culture dishes were dried at room temperature.

3.2.7. Propidium iodide staining for flow cytometry (PI FACS)

Flow cytometry or FACS (fluorescence activated cell sorting) was used to analyze cells based on detection of a fluorescent intercalating agent. The cell cycle stage was determined by measuring fluorescence emission of the intercalating dye propidiumiodide (PI), which relates to the DNA content as follows: G0/G1 (2N), S (>2N, <4N) and G2/M (4N). Polyploid cells (>4N) and apoptotic or necrotic cells (subG1, <2N) could thus be identified as well.

Cells were harvested by trypsinisation including floating cells from the medium supernatant. After resuspension in 1 ml cold PBS the cells were fixed by adding 4 ml ice-cold absolute ethanol while vortexing. The cells were stored at least one night at -20 °C, then washed with PBS and resuspended in FACS buffer containing propidium iodide solution. After at least 1 h of staining in the dark at RT the cells were transferred into FACS tubes and measured with the BD FACSCanto II with the following measurement settings: excitation wavelength of 488nm using a 556 nm longpass- and a 585/42 nm bandpassfilter for propidium idodide (emission at 617 nm). The cell cycle distribution was analysed using the BD FACSDiva 6.1.2 software.

3.3. Protein biochemistry methods

3.3.1. Generation of protein lysates for Western blot

To isolate total protein cells were washed in ice cold PBS, scraped off the cell culture dish and pelleted (400 x g, 5 min, 4 °C). The cell pellet was either frozen in liquid nitrogen to be stored at -80 °C or directly subjected to lysis by resuspending cells in TNN-, NP40- or RIPA-buffer with freshly added proteinase inhibitors (1:1000). The cells were incubated for 30 minutes on ice, then the cell debris was pelleted (18,000 x g, 10 min, 4 °C) and the supernatant transferred to a fresh tube. The protein concentration was determined and the lysate stored at -80 °C until further use.

Alternatively, cells grown in 24- or 6-well plates were lysed directly in hot SDS sample buffer, transferred to a reaction tube and boiled for 15 minutes. The lysates were then used for Western blot analysis or stored at -20 °C.

3.3.2. Protein determination by the Bradford method

Protein concentrations were determined according to Bradford [1976]. 500 µl H_2O was pipetted into Semi-Micro Cells, 1 µl of the protein sample solution was added and mixed with 500 µl Quick Start Bradford dye reagent (Bio-Rad). After an incubation time of 5 min at RT the absorption was measured at a wavelength of 595 nm using an appropriate reference. The measured values were compared to a previously obtained standard curve to calculate the protein concentration of the sample solution.

3.3.3. SDS polyacrylamide gel electrophoresis (SDS-PAGE)

Discontinuous SDS-PAGE (Sodium dodecyl sulfate polyacrylamide gel electrophoresis) was used to separate proteins according to size [Laemmli et al., 1970]. Protein lysates as described in 3.3.1 were filled up with lysis buffer to an equal volume, then mixed with half the volume of 3 x SDS sample buffer. These samples were incubated 5 minutes at 95 °C and spun down afterwards, as were eluates of immunoprecipitations, sumoylation and ubiquitination assays or samples obtained by direct SDS lysis. The protein samples were then transferred into the wells of an SDS polyacrylamide gel consisting of a 7.5-15 % stacking gel and a 4 % resolving gel. The PageRuler Pre-Stained Protein Ladder (Fermentas) was used as a size marker. The electrophoresis was carried out using the Bio-Rad SDS-PAGE chamber with SDS running buffer, first at 80 V for 30 minutes, then at 120 V for 90 minutes.

3.3.4. Staining Protein gels with Coomassie Blue

To visualize proteins obtained by recombinant expression (3.3.9) these were subjected to SDS-PAGE, the gel was then stained in coomassie solution for at least 1 h. To remove excess dye the gel was incubated in destaining solution with gentle shaking until a clear background was obtained.

3.3.5. Western blot

Proteins were separated by SDS-PAGE (3.3.3), followed by electroblotting onto a PVDF membrane using a tank blot system. A PVDF membrane the size of the SDS gel was incubated first in methanol for 1 min, then washed in desalted water for 2 min and finally equilibrated in tank blot buffer for another 2 min. Gel and membrane were neatly layered on top of each other and fixed between Whatman filter papers in a Western blot transfer chamber (Harnischmacher). The electrophoretic protein transfer was carried out at 250 mA for 3 h. All following incubation steps were performed with gentle shaking. The membrane with immobilized proteins was blocked in blocking solution for at least 30 min, then cut into pieces if several proteins from the same membrane were to be visualized. The membrane pieces were incubated o./n. with a dilution of primary antibody in blocking solution, then washed (3 x 10 min in TBS-T), incubated with secondary antibody in blocking solution for 1 h at RT, then again washed (3 x 10 min in TBS-T). Finally, the proteins of interest were visualized via chemiluminescence, induced by the horseradish peroxidase coupled to the secondary antibody. To trigger a specific chemiluminescent signal the Immobilon Western Chemiluminescent HRP Substrate from Millipore was used according to the manufacturer's instructions, the signal was detected with the ImageQuant LAS 400 imager (Fujifilm Global).

3.3.6. Stripping antibodies from PVDF membranes

To release antibodies from a PVDF membrane covered with immobilized proteins the membrane was incubated in stripping buffer for 30 min in a 60 °C water bath. The membrane was washed, blocked and incubated with primary and secondary antibodies as described in 3.3.5.

3.3.7. Immunoprecipitation

Immunoprecipitations (IPs) were performed to detect protein-protein interactions. Cells were lysed in TNN lysis buffer with fresh proteinase inhibitors (1:1000) and sonicated

(4 x 5 sec, 1 min pause, 20 %) using the W-250 D sonifier (Heinemann). The lysate was centrifuged (10 min, 18,000 x g, 4 °C) to spin down the cell debris, the supernatant was transferred to a fresh tube. The protein concentration was determined as described in 3.3.2, the same amount of protein was used in each IP condition, filling up samples with TNN buffer to a volume of 400 µl as needed. A 5 % input of each lysate was collected and boiled with SDS sample buffer. For preclearing, 40 µl of 10 % BSA in TNN was added to each 400 µl sample, as well as 50 µl of a mixture of washed protein A/G sepharose beads (Protein A Sepharose CL-4B from Invitrogen, Protein G Sepharose Fast Flow from Sigma). The samples were incubated on a rotating wheel for 4 h at 4 °C, then the beads were spun down and discarded. 2 µg of specific antibody was added to each IP sample and these were rotated o./n. at 4 °C. The next day 50 µl fresh protein A/G sepharose beads ware added to the IP samples to incubate on a rotating wheel for 2 h. The beads loaded with protein-bound antibodies were washed four times with TNN buffer, then 40 µl of SDS sample buffer were added to elute the protein at 95 °C for 5 min and the samples were subjected to SDS-PAGE and Western blot using the input as a reference for IP efficiency .

3.3.8. *In vivo* sumoylation assay

To detect if a protein of interest could be modified by Sumo *in vivo* cells were transfected with plasmids expressing His-tagged Sumo and the protein of interest. The cells were harvested 48 h after transfection, 10 % of each sample was collected separately and boiled in SDS sample buffer to be used as an input. The remaining cells were lysed in 1 ml Sumo buffer A containing proteinase inhibitors and freshly prepared NEM. To completely disrupt the cells these were sonicated (4 x 5 sec, 10 sec pause, 20 %) and cleared of the cell debris by centrifugation (10 min, 6000 x g, 4 °C). The supernatant was transferred to a fresh tube, 100 µl of a 50 % slurry of previously washed Ni^{2+}-NTA-agarose were added and incubated on a rotating wheel o./n. at 4 °C. The next day the beads were spun down by centrifugation (2 min, 1000 x g, 4 °C) and washed two times with 1 ml Sumo buffer A, two times with a 1:4 mixture of buffer A and B, and two times with Sumo buffer B. To elute sumoylated proteins from the beads these were boiled in 100 µl of SDS sample buffer for 5 min and centrifuged (1 min, 1,000 x g). The supernatant was subjected to SDS-PAGE and Western blot side by side with the input sample.

3.3.9. Bacterial expression and purification of GST fusion proteins

The gene of interest was cloned into a pGEX expression vector to enable expression of a GST fusion protein in E.cli BL21 cells, which perform high-efficiency protein expression

upon induction by IPTG. The transfection and cultivation of bacteria was performed as described in 3.1.1 A clonal overnight culture of BL21 containing the pGEX construct was diluted 1:20 and incubated shaking at 25 °C. As soon as the culture reached an optical density of A_{600nm}=0.6 IPTG (isopropyl-β-D-thiogalactopyranoside) was added to a final concentration of 1 mM to induce expression of the GST fusion protein. The culture was grown for another 6 h before pelleting of the bacteria (7.700 x g, 10 min, 4 °C), which were either stored at -80 °C or directly subjected to lysis. To lyse the cells 100 ml of bacterial culture were resuspended in 2 ml bacterial lysis buffer with fresh proteinase inhibitors, then sonicated (10 x 10 sec, 1 min pause, 40 %). The lysate was centrifuged at high speed (10,000 x g, 20 min, 4 °C) to pellet the bacterial cell debris and insoluble protein, this pellet was solubilized in 2 ml bacterial wash buffer. A fraction of each the solubilized pellet and the supernatant was mixed with SDS sample buffer and analyzed on a coomassie gel to verify the expression of the GST fusion protein and determine its solubility.

3.3.10. GST pulldown

To analyze the interaction of *in vitro* translated proteins with recombinant GST tagged Sumo a GST pulldown experiment was performed. GST-Sumo1, 2 and 3 were expressed and purified according to 3.3.9. 300 µl of a 50 % slurry of glutathion sepharose beads were washed in 10 ml PBS/ 1 % Triton X-100 and added to each GST-Sumo lysate to be incubated for two hours at 4 °C on a rotating wheel. The beads were washed three times with 10 ml PBS/ 1 % Triton X-100 and then resuspended in 150 µl PBS. 2 µl of the beads in PBS were boiled in 200 µl SDS loading buffer for 5 min and analyzed via SDS-PAGE and coomassie gel to quantify the fraction of glutathion-bound Sumo1, 2 and 3. The remaining beads were spun down (1 min, 200 x g, 4 °C), resuspended in glycerine and stored at -20 °C. For the *in vitro* transcription and translation the TNT Quick Coupled Trancription/Translation System from Promega was used according to the manufacturers instructions with twice the recommended amount of plasmid and kit reagents. The DNA template originated from pcDNA3 expression plasmids with T7 RNA polymerase promoter. From the *in vitro* translated samples 2 % were kept as an input and boiled in SDS sample buffer, the remainder divided into four reaction tubes and diluted to 500 µl with GST binding buffer. Equal volumes of GST only, GST-Sumo1, 2 and 3 bound to the sepharose beads were added according to the quantification from the coomassie gel and incubated rotating for 4 h at 4 °C. The beads were washed five times with each 1 ml of GST washing buffer, then boiled in 20 µl SDS sample buffer and centrifuged (3 min, 1,000 x g). Finally, the

supernatant from the beads and the 2 % input was analyzed via SDS-PAGE and Western blot.

3.3.11. Indirect immunofluorescence

Cells were cultivated and transfected on cover slips to be processed for indirect immunofluorescence. To fix the cells they were incubated in 3.7 % paraformaldehyde for 15 min at RT after an initial wash with ice-cold PBS. To permeabilized the cells they were washed with PBS/ 0.1 M Glycin (3x 10 min, RT) and PBS/ 0.1 % NP-40 (3x 10 min, RT), to be blocked with PBS/ 0.5 % NP-40/ 5 % FCS (blocking buffer) for 45 min at 37 °C. The cover slips were transferred into a wet chamber with the cells facing upwards and 40 µl of primary antibody diluted in blocking buffer was pipetted on top. After an incubation time of 45 min at 37 °C the cells were washed three times with blocking buffer. Next the cells were incubated with a 40 µl dilution of secondary antibody (1:400) and Hoechst nuclear stain (1:5000) in blocking solution, again for 45 min at 37 °C in the dark. Unbound antibody was removed by washing three times with blocking buffer. Finally the cover slips were washed with distilled water and mounted on a glass slide using a small drop of mounting medium, the slides could be stored in the dark at 4 °C before analyzing them with the fluorescence microscope. Confocal images were obtained as described in detail in Herkert et al. [2010].

3.3.12. Luciferase reporter gene assay

Cells in 6-well plates were transfected with reporter constructs and additional expression plasmids. 24 h later, the cells were washed with ice cold PBS and disrupted in 250 µl passive lysis buffer (Promega) for 15 min at RT while shaking. The lysate was transferred into a reaction tube and cleared of the cell debris by centrifugation (1 min, 400 x g, 4 °C). To determine the luciferase activity, 50 µl of lysate was pipetted into a clear bottom 96-well plate and placed into the Glomax 96 Microplate Luminometer. The device automatically added 100 µl of freshly prepared luciferase substrate solution and measured light emission at 562 nm two seconds later for an interval of ten seconds (in relative light units, RLU). To normalize the obtained values the protein concentration was determined as described in 3.3.2.

3.3.13. UV treatment of cells

Before irradiation of attached cells, the medium supernatant was completely removed, the cells were irradiated for 60 seconds after which the very same medium was restored. Cells

on 6 cm or 10 cm dishes were treated with a dose of 500 J/m^2 UV-B all at the same time and then harvested at different time points by trypsiniation, including floating cells in the medium supernatant.

Chapter 4.

Results

4.1. The tumor suppressor Arf interacts with Miz1 to antagonize its function

4.1.1. Miz1 recruits Arf into the nucleoplasm and is itself sequestered into subnuclear foci

Nucleophosmin (NPM) has been identified as an essential coactivator of Miz1 [Wanzel et al., 2008]. In unstressed cells, the majority of NPM resides in the nucleolus, but it also shuttles into the nucleoplasm and cytoplasm [Yu et al., 2006]. NPM accumulates in the nucleoplasm upon induction of stress such as DNA damage and also upon expression of Miz1 [Wanzel et al., 2008]. In the nucleolus NPM acts as a chaperone for the tumor suppressor protein Arf [Bertwistle et al., 2004] and Arf is known to interact with Myc [Qi et al., 2004]. Since both NPM and Myc are binding partners of Miz1 it was investigated if there was also an interaction between Miz1 and Arf.

Expression of Miz1 in HeLa cells recruited endogenous and overexpressed p14Arf out of the nucleoli into the nucleoplasm (Fig. 4.1 A). The intranuclear distribution of Miz1 markedly changed from a homogenous distribution to an accumulation in subnuclear structures in about 80% of all transfected cells. These foci partially overlapped with the nucleoplasmic Arf, indicated by a Pearson's correlation coefficient (R_r) of 0.519 as a mean value of ≥ 5 cells. The Pearson correlation describes similarity between shapes to indicate colocalization; 1.0 indicates perfect positive correlation, -1.0 complete negative correlation [Zinchuk et al., 2007].

4.1.2. Arf and Miz1 associate with each other

To determine if Arf binds to Miz1, immunoprecipitation assays were conducted, the results of which are summarized in Figure 4.2. It could be shown that both human p14Arf as well as mouse p19Arf bind to Miz1 *in vivo* [Herkert et al., 2010]. This interaction is independent

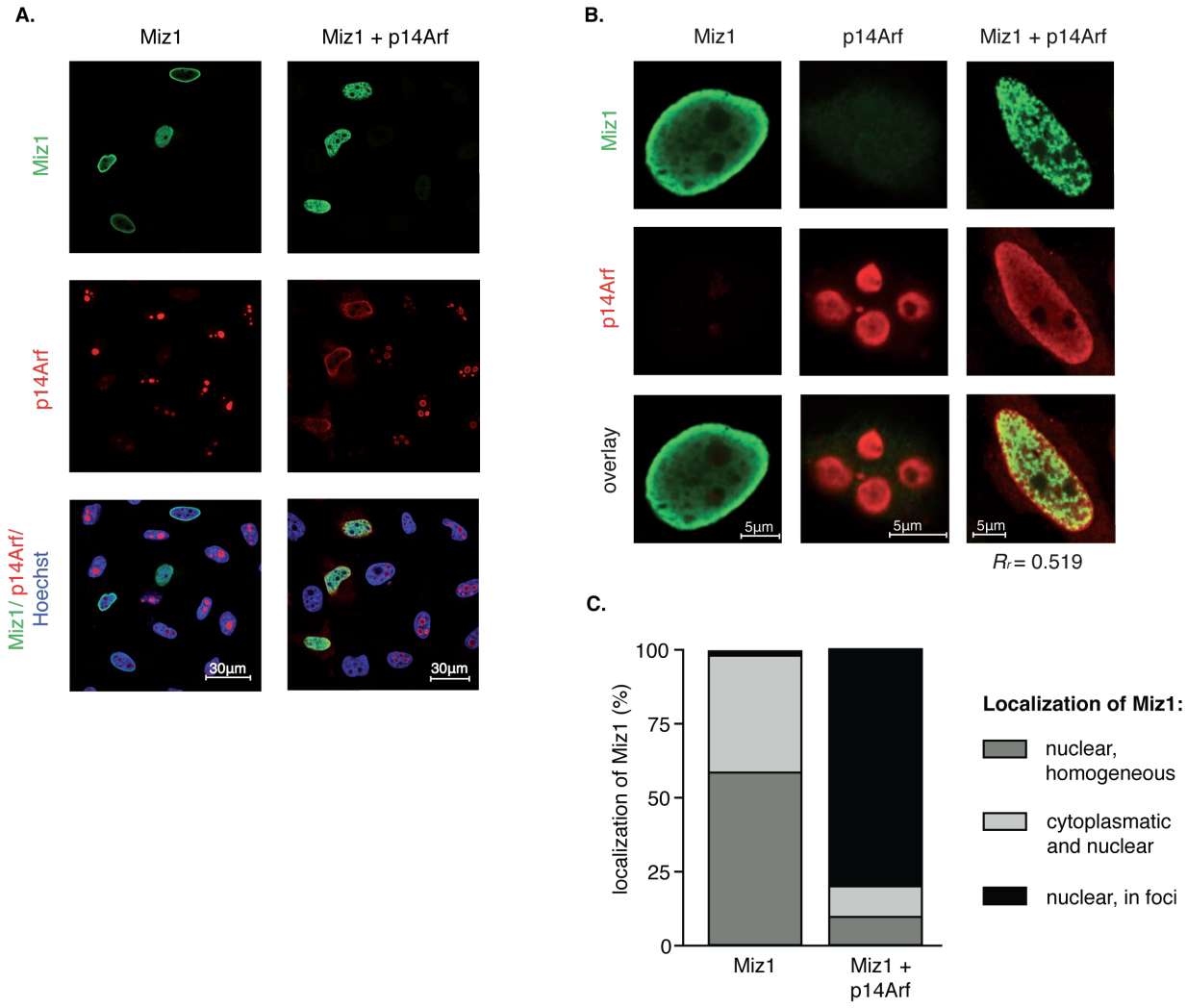

Figure 4.1.:
Miz1 recruits endogenous and exogenous Arf into the nucleoplasm and is itself sequestered into subnuclear structures [1]

A.-B. HeLa cells grown on cover slips were transfected with expression plasmids for Miz1 and p14Arf and fixed for immunofluorescence 48 h later. Miz1 and p14Arf proteins were detected with specific antibodies, Hoechst 33258 was used to stain chromatin. The Pearson correlation coefficient was calculated as a mean value of ≥ 5 cells.

C. The localization of Miz1, either homogeneously distributed in the nucleus and/or cytoplasm or in heterogenous subnuclear foci was quantified counting ≥ 40 transfected cells.

[1] These Figures were published in similar form in Herkert et al. [2010] (see also following pages).

of nucleophosmin, as it is still valid in NPM$^{-/-}$ MEFs. On the contrary, enforced expression of NPM in these cells severely impaired the interaction between Miz1 and Arf. Myc both

binds to Miz1 and Arf but does not simply act as a scaffold for the association of Miz1 and Arf, as Myc and Miz1 bind to Arf in different regions (see 4.1.7 on page 64).

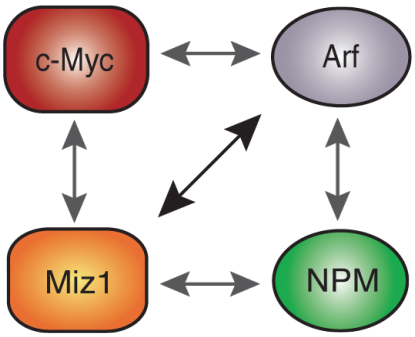

Figure 4.2.:
Arf directly interacts with Miz1 which is antagonized by nucleophosmin

Immunoprecipitation experiments in Herkert et al. [2010] showed the previously known interactions between Myc/Arf, Myc/Miz1, Arf/NPM and Miz1/NPM (grey arrows). In addition, a direct interaction between Miz1 and Arf which is not dependent on Myc or NPM was discovered (black arrow).

4.1.3. Arf reduces the solubility of Miz1

Verification of Miz1 and Arf protein expression showed that Arf markedly decreased Miz1 levels that could be detected via Western Blot. This occurred using lysis buffers containing low salt concentrations and relatively mild detergents such as NP-40. This effect could be ascribed neither to an influence of Arf coexpression on the Miz1 expressing vector nor an Arf-induced proteasomal degradation of Miz1 [Wanzel, 2010]. In fact, lysing cells in sample buffer containing 6 % SDS at 95 °C revealed that Arf merely reduced the solubility of Miz1, which could be retained with harsher lysis conditions (Fig. 4.3).

4.1.4. Nucleophosmin inhibits the Arf-induced foci formation and solubility change of Miz1

To activate transcription, Miz1 forms a soluble complex with its coactivator nucleophosmin [Wanzel et al., 2008]. Myc competes with NPM for association to Miz1 and induces a less soluble repressive complex [Peukert et al., 1997]. As elevated expression of nucleophosmin inhibits the binding of Arf to Miz1 (see 4.1.2 on page 59), I analyzed the effect of NPM on subnuclear localization and solubility of Miz1. I could reproduce in immunofluorescence assays that Miz1 recruits nucleophosmin out of the nucleoli into the nucleoplasm as shown in Wanzel et al. [2008]. Strikingly, elevated expression of NPM completely abrogated the

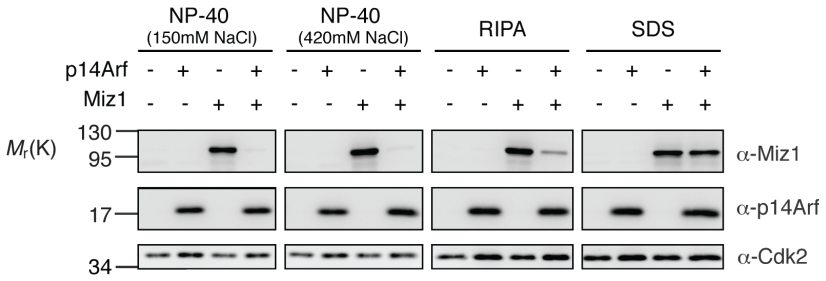

Figure 4.3.:
Arf markedly reduces the solubility of Miz1[1]

HeLa cells were transfected with the indicated plasmids and harvested 24 h later using different lysis conditions, from a mild lysis in NP-40 containing buffers over a harsh lysis in RIPA buffer to a complete lysis in boiling SDS sample buffer. The protein extracts were analyzed by Western Blot, Cdk2 was used as a loading control.

formation of subnuclear structures upon expression of Miz1 and Arf (Fig. 4.4 A). Likewise the Arf-induced solubility change of Miz1 was abolished entirely (Fig. 4.4 B).

4.1.5. Arf inhibits transactivation by Miz1

To analyze the functional outcome of the interaction between Miz1 and Arf I performed luciferase reporter assays. As seen in previous studies, Miz1 induced the expression of a *P15INK4B* promoter plasmid [Staller et al., 2001]. Arf alone did not influence the basal reporter activity, however it severely inhibited Miz1-dependent transactivation in a dose-dependent manner (Fig. 4.5). I obtained concurrent results using a *P21CIP1* reporter construct (data not shown).

4.1.6. Arf induces sumoylation of Miz1

Arf is primarily know for its function in stabilizing the tumor suppressor p53. More recently also p53-independent functions of Arf have been described, for example its ability to induce sumoylation of proteins to which it binds, such as NPM and Mdm2 [Tago et al., 2005]. Interestingly, sumoylation of transcription factors has often been linked to the establishment of repressive heterochromatic complexes on the DNA [Garcia-Dominguez and Reyes, 2009].
I therefore aimed to investigate if sumoylation might be involved in the Arf-mediated effects on Miz1. The immunofluorescence analysis showed that Flag-tagged Sumo2 indeed colocalized with the Arf-induced Miz1 foci to an exceptional degree (Fig. 4.6 A, R_r =

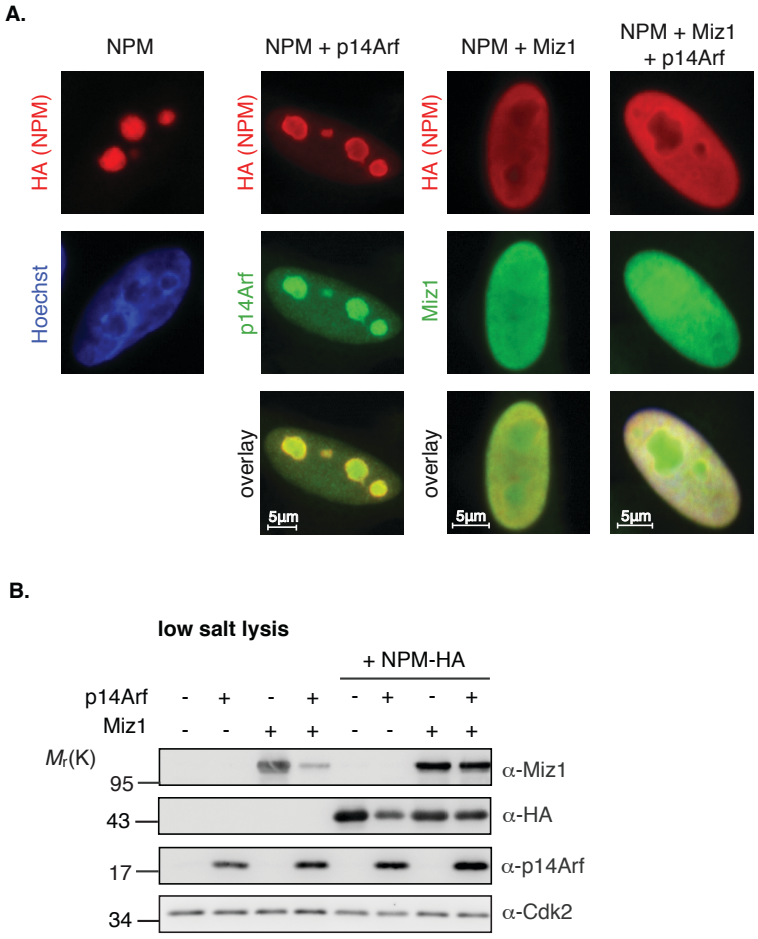

Figure 4.4.:
Nucleophosmin inhibits Arf-induced foci formation and solubility change of Miz1 [1]

A. Immunofluorescence was performed as described in Fig. 4.1, HA-tagged NPM was detected with an HA antibody.

B. HeLa cells were transfected with the indicated plasmids and harvested 24 h later using a low salt lysis buffer (containing NP-40 and 150 mM NaCl). The protein extracts were analyzed by Western Blot, Cdk2 was used as a loading control.

0.903). To examine if Arf induced the sumoylation of its binding partner Miz1, we set up an *in vitro* sumoylation assay. His-tagged Sumo2 in addition to Miz1 and p14Arf was expressed in HeLa cells and sumoylated protein species were pulled down using Ni^{2+}-NTA-agarose. Subsequent Western Blot analysis revealed that Miz1 is sumoylated upon His-Sumo2 expression, which is increased quite significantly by Arf (Fig. 4.6 B, further results in 4.2.1 on page 70). Next I analyzed if sumoylation is the cause for the formation of intranuclear Miz1 foci upon Arf expression. In addition to expressing Miz1, Arf and

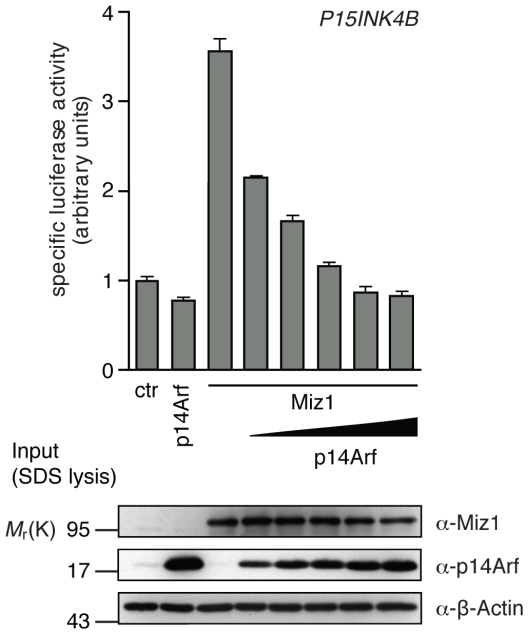

Figure 4.5.:
Arf inhibits Miz1-dependent transactivation of the *P15INK4B* promoter [1]

HeLa cells were transfected with the indicated plasmids and a luciferase reporter construct containing the *P15INK4B* promotor. 48 h after transfection the specific luciferase activity was determined and normalized to the protein content in each condition. Immunoblots after SDS sample buffer lysis document the expression of transfected proteins, β-Actin was used as a loading control. Error bars represent standard deviation of biological triplicates.

Flag-Sumo2 I depleted the Sumo E2 enzyme Ubc9 for immunofluorescence experiments using siRNA. Depletion of Ubc9 as the only E2 enzyme in the sumoylation cascade has been shown to effectively disrupt the cellular sumoylation machinery [Lin et al., 2003]. However, this did not abolish the sequestration of Miz1 into intranuclear structures, but merely suppressed the colocalisation of Sumo2 in those (Fig. 4.6 C). Furthermore we could show that the change in solubility by Miz1 through Arf was also not abrogated upon depletion of the sumoylation machinery [Herkert, 2010]. Taken together, the sumoylation of Miz1 shows every sign of being independent of the foci formation and solubility change.

4.1.7. An Arf domain binding to Myc is necessary for the effects of Arf on Miz1

Myc is a potent repressor for Miz1 transactivation, inhibits the binding of Miz1 to NPM and induces a complex of Miz1 and Myc which is resistant to mild extraction [Peukert et al., 1997; Wanzel et al., 2008].

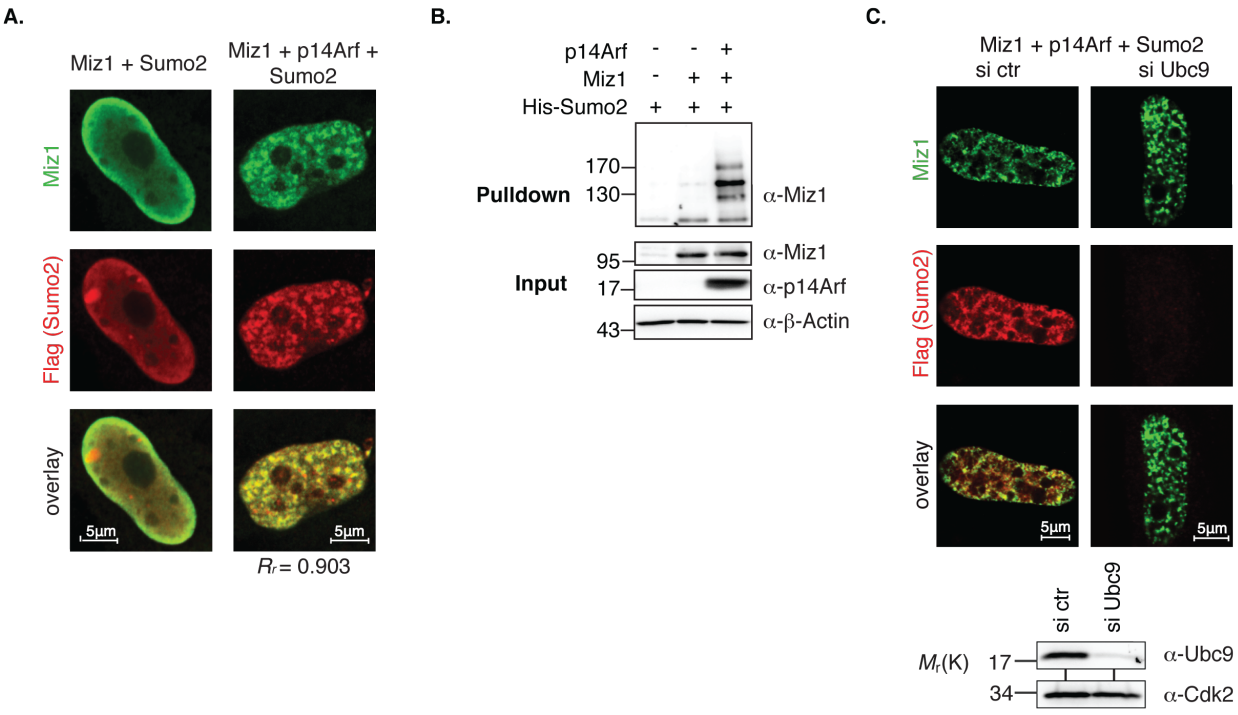

Figure 4.6.:
Arf recruits Sumo2 into Miz1 foci and induces the sumoylation of Miz1 [1]

A. Immunofluorescence was performed as described in Figure 4.1, Flag-Sumo2 was detected with a Flag antibody.

B. HeLa cells were transfected with the indicated plasmids and harvested 24 h later under denaturing conditions. His-Sumo modified proteins were pulled down using Ni^{2+}-NTA-agarose and analyzed via Western Blot with a 7.5% input sample.

C. HeLa cells were first transfected with a combination of four siRNAs directed against Ubc9 or a control siRNA, 24 h later with the indicated protein expression plasmids. Immunofluorescence was performed another 24 h later as described in Figure 4.1. Protein depletion of Ubc9 was verified by Western Blot using Cdk2 as a loading control.

Arf also binds to both Miz1 and Arf which is further explained in 4.1.2 on page 59. Therefore, the Arf-mediated effects on Miz1 might reflect an assembly of the Myc-Miz1 complex. To further investigate this notion we examined wether Miz1 and Myc interact with Arf in different regions using Arf deletion mutants. We could reproduced, that c-Myc interacts with the N-terminus of Arf [Qi et al., 2004]. In contrast, Miz1 still binds to an Arf mutant devoid of the first 65 amino acids. Even though the C-terminal part of p14Arf is sufficient for the interaction with Miz1, this mutant cannot repress the transactivation, induce the sequestration into less soluble complexes (summarized in Figure 4.7 A) or induce the sumoylation of Miz1 (Fig. 4.7 B). Immunofluorescence showed that the GFP-tagged

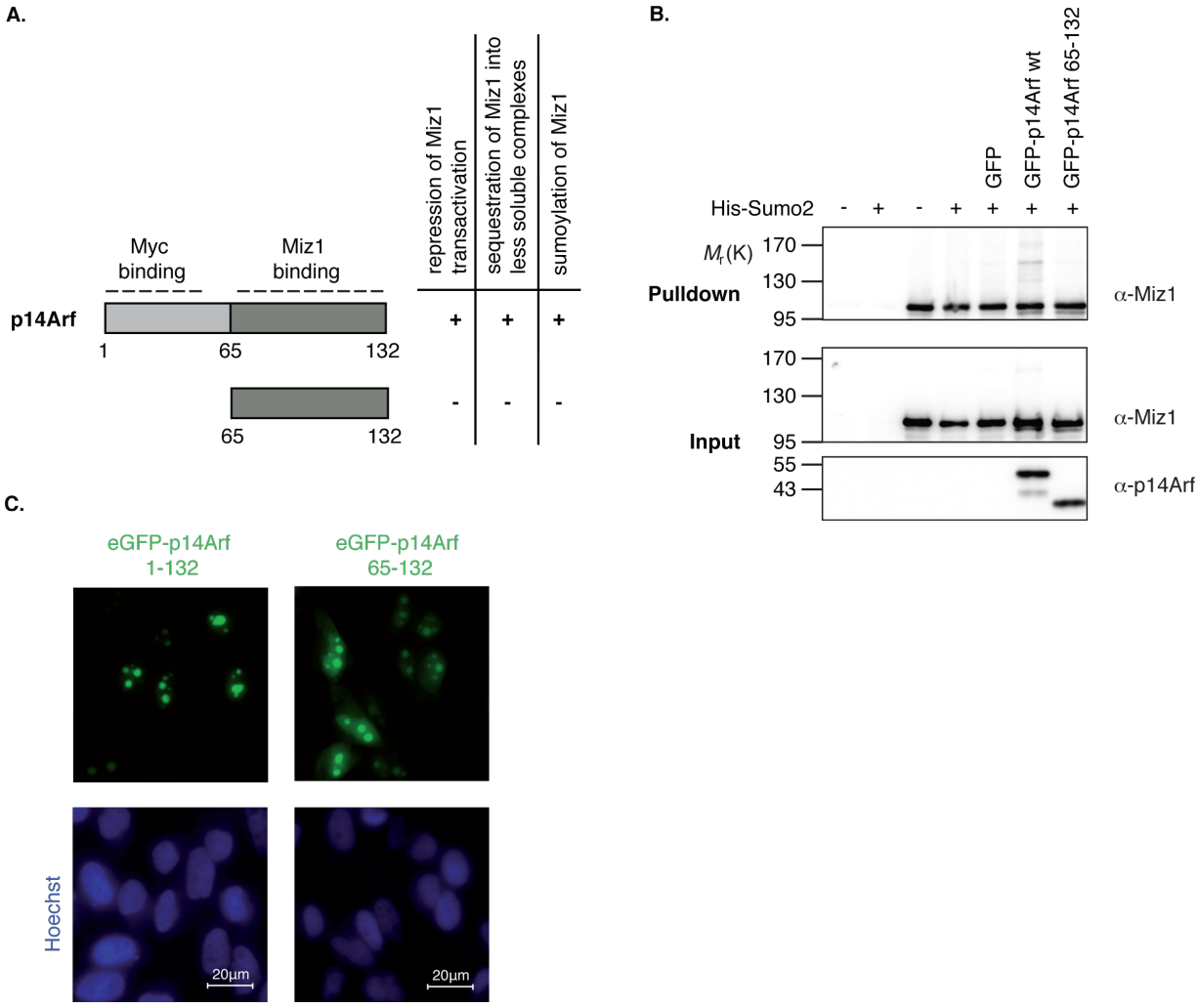

Figure 4.7.:
The N-terminal half of Arf mediates the effects of Arf on Miz1 [1]

A. The diagram summarizes findings from Herkert et al. [2010] and B: The N-terminal, Myc-binding domain of Arf is needed to mediate repression, sequestration and sumoylation of Miz1.

B. His-Sumo2 pulldown was performed as described in 4.6 B. The weaker sumoylation signal might be ascribed to the comparably large GFP-tag fused to the Arf protein.

C. Immunofluorescence was performed as described in Figure 4.1, except that the fluorescence signal was emitted directly from the GFP-tagged Arf proteins.

N-terminal deletion mutant of p14Arf used for the analysis localizes to the nucleoli to a similar extent as wild type GFP-p14Arf (Fig. 4.7 C).

4.1.8. A Myc mutant that cannot bind to Miz1 fails to colocalize in Arf-induced Miz1 foci

Immunofluorescence analysis expressing c-Myc in addition to Miz1 and p14Arf provides further evidence for an involvement of Myc as part of the complex. Wild type c-Myc recruits Arf out of the nucleoli into the nucleoplasm very much like Miz1. More importantly, c-Myc also colocalizes significantly in Arf-induced Miz1 foci (Fig. 4.8 A) with a Pearsons correlation coefficient of $R_r = 0.848$.

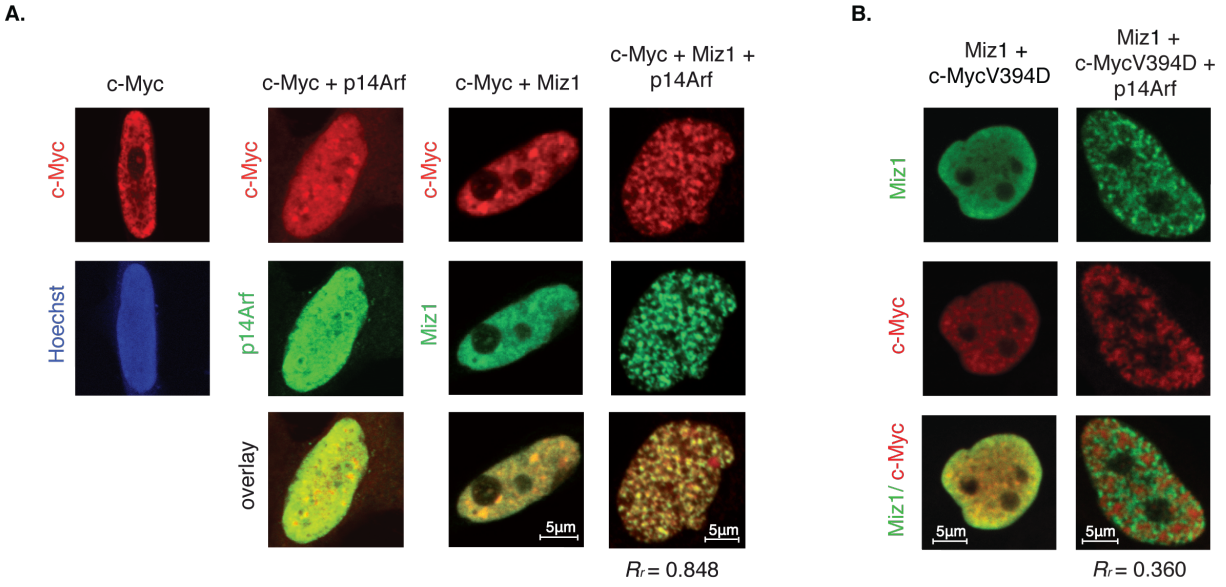

Figure 4.8.:
Myc V394D which cannot bind to Miz1 fails to colocalize in Arf-induced Miz1 foci [1]

A.-B. Immunofluorescence was performed as described in Figure 4.1. Enforced expression of c-Myc wild type and c-Myc VD in each case dominated the immunofluorescence signal over endogenous wild type c-Myc.

Furthermore I analyzed the c-Myc V394D mutant, which can no longer bind to Miz1 [Herold et al., 2002], in this context. Myc VD largely fails to colocalize to the Arf-induced subnuclear structures of Miz1 (Fig. 4.8 B; $R_r = 0.360$). Please note that enforced expression of c-Myc wild type and MycVD in each case dominated the immunofluorescence signal, however endogenous Myc also colocalizes to the Miz1 foci (data not shown).

4.1.9. Miz1 mutants show that the Arf effects on Miz1 are mediated by recruitment of Myc

To substantiate the assumption that Myc is required for Arf to inhibit Miz1 function, we used three previously characterized Miz1 mutants which are impaired in binding to

Myc [Peukert et al., 1997]. The Miz1 Δ33 deletion still retains some binding affinity to the Myc-binding domain localized between the 12th and 13th zinc finger. In contrast to that, the Miz1 Δ75 deletion and the quintuple point mutation Miz1 4Pro completely abrogate Myc binding. All three mutants still bind to p14Arf (summarized in Figure 4.9 A). The solubility analysis showed that Miz1 mutants which cannot bind to Myc are not sequestered into less soluble complexes upon overexpression of Arf (Fig. 4.9 B). This directly correlates with any remaining binding ability of the Miz1 mutant to Myc, as Miz1 Δ33 becomes less soluble still. I also tested if the Miz1 mutants can still be repressed by Arf in their ability to transactivate the *P15INK4B* reporter. The depiction as fold repression shows that the Myc binding domain of Miz1 is also needed for Arf to repress the Miz1 transactivation function (Fig. 4.9 C). In addition, immunofluorescence analysis revealed that a Miz1 mutant devoid of Myc binding does not form intranuclear foci upon Arf expression (Fig. 4.9 D). Finally, Miz1 Δ75 cannot be sumoylated anymore. Please note that expression of NPM also inhibits the sumoylation, which adds up to the effects presented in 4.1.4 on page 61.

In sum, the ability of Miz1 to bind to Myc is needed for the Arf-induced change in solubility, repression of transactivation, foci formation and sumoylation of Miz1.

Figure 4.9. *(facing page)*:
Miz1 mutants not binding to Myc fail to respond to Arf [1]

A. Overview of Miz1 mutants, all of them being capable of binding to p14Arf [Herkert et al., 2010]. ZF = zinc finger
B. The solubility assay was performed as in Figure 4.3.
C. The luciferase assay was performed as in Figure 4.5. Error bars represent standard deviation of biological triplicates.
D. Immunofluorescence analysis was performed as in Figure 4.1.
E. His-Sumo2 pulldown was performed as described in 4.7 B. Note that for this assay Sumo1 instead of Sumo2 was used, which is further analyzed in section 4.2.1.

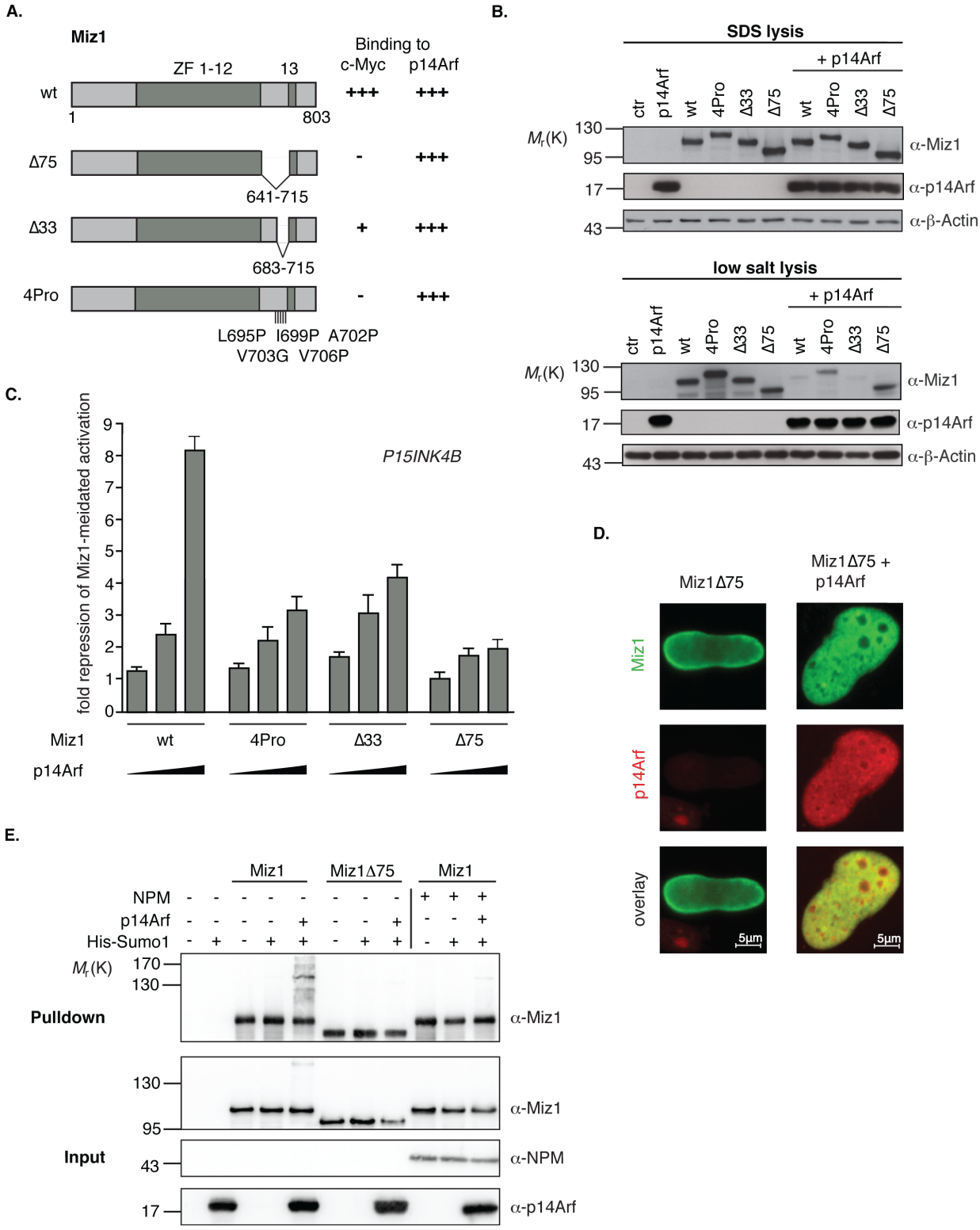
A.
Miz1
ZF 1-12
13
Binding to
c-Myc
p14Arf
wt
1
803
+++
+++
Δ75
641-715
-
+++
Δ33
683-715
+
+++
4Pro
L695P I699P A702P
V703G V706P
-
+++
B.
SDS lysis
+ p14Arf
ctr
p14Arf
wt
4Pro
Δ33
Δ75
Mr(K)
130
95
17
43
α-Miz1
α-p14Arf
α-β-Actin
low salt lysis
C.
fold repression of Miz1-meidated activation
P15INK4B
Miz1
wt
4Pro
Δ33
Δ75
p14Arf
D.
Miz1Δ75
Miz1Δ75 +
p14Arf
Miz1
p14Arf
overlay
5μm
E.
Miz1
Miz1Δ75
NPM
p14Arf
His-Sumo1
Mr(K)
170
130
Pulldown
α-Miz1
95
Input
43
α-NPM
17
α-p14Arf

4.2. Sumoylation of Miz1

4.2.1. Miz1 can be modified by both main Sumo isoforms

There are three isoforms of Sumo expressed in higher eucaryotes. Sumo1 is 50 % identical in sequence to Sumo2/3, which form a distinct subfamily being very similar in sequence and function [Hay, 2005]. Hence, I only considered the specific Sumo1 and Sumo2 isoforms for the sumoylation analysis. I performed *in vivo* sumoylation assays in HeLa cells by expressing His-tagged Sumo1 or Sumo2 in addition to proteins involved in the sumoylation, either as targets, inducers or inhibitors of this modification. Upon denaturing lysis, sumoylated protein species were pulled down using Ni^{2+}-NTA-agarose. Subsequent Western Blot analysis showed the modification status of the protein of interest, a higher migrating band after pulldown being indicative for a Sumo modification.

In vivo sumoylation assays with overexpression of Miz1, p14Arf and His-Sumo revealed that Miz1 can be sumoylated by Sumo1 and Sumo2, and that this is strongly induced by Arf (Fig. 4.10 A). Miz1 antibody staining of pulldown samples showed that also unmodified Miz1 of a size of about 100 kDa sticks to the agarose beads used for this kind of experiment. However, three to four higher migrating bands, the most prominent one at around 150 kDa, could clearly be distinguished and are in part also visible in the input samples. To validate that this size shift really signifies sumoylation, I performed an *in vivo* sumoylation assay upon depletion of the E2 enzyme Ubc9 (Fig. 4.10 B). Expression of a set of four siRNAs against Ubc9 completely abrogated any higher migrating bands of Miz1 in the pulldown samples in contrast to expression of control siRNA.

4.2.2. Miz1 is sumoylated at lysine 251

Sumo proteins can be covalently attached to lysine residues in a target protein. The majority of sumoylation sites follow the consensus motif Ψ-K-X-E/D, with Ψ being a bulky hydrophobic amino acid [Bernier-Villamor et al., 2002]. To find the major sumoylation site in Miz1, I applied the SUMOsp software tool for *in silico* sumoylation site prediction [Xue et al., 2006]. The algorithm suggested five possible sumoylation sites in Miz1 (Fig. 4.11 A). To analyze if sumoylation occurred at one of these lysines, I generated five different mutants of Miz1. In each mutant a single lysine was replaced with an arginine, mimicking an unmodified lysine at the respective site (K{*number*}R). Additionally I created a Miz1 mutant combining all lysine to arginine replacements (KR5). I analyzed these mutants in a His-Sumo2 pulldown which showed sumoylation of all single KR mutants except K251R,

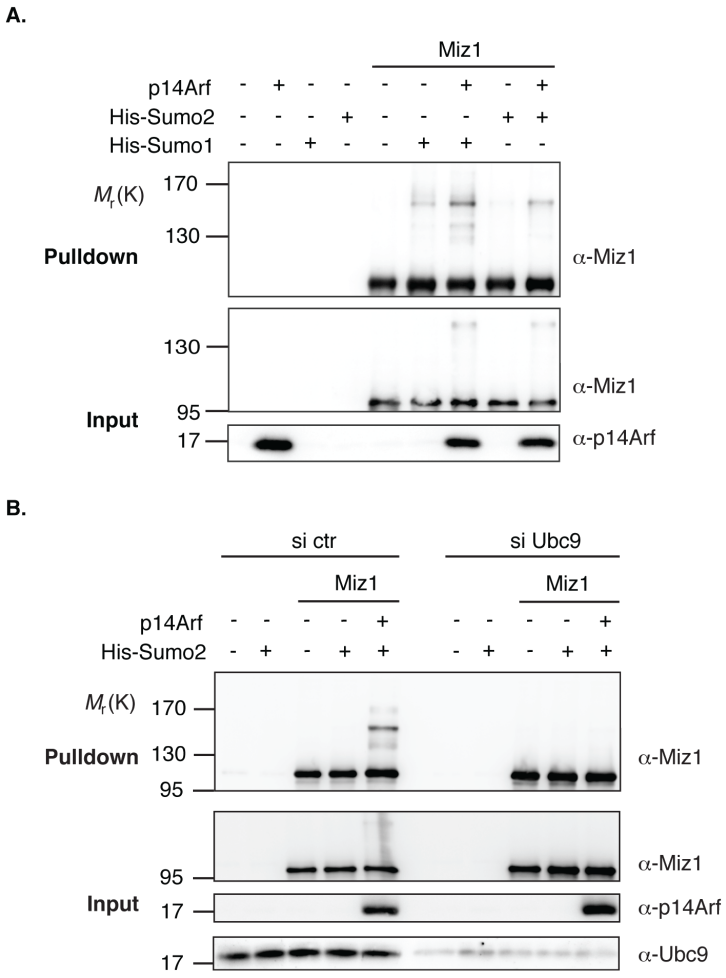

Figure 4.10.:
Miz1 can be sumoylated by Sumo1 and Sumo2 which is induced by Arf

A. HeLa cells were transfected with the indicated plasmids and harvested 24 h later under denaturing conditions. His-Sumo modified proteins were pulled down using Ni^{2+}-NTA-agarose and analyzed via Western Blot using a 7.5% input sample.

B. HeLa cells were first transfected with a combination of four siRNAs directed against Ubc9 or a control siRNA, 24 h later with the indicated protein expression plasmids. His-Sumo assays were performed as described in A, protein depletion of Ubc9 was verified via Western Blot.

where the strong shifted band of about 150 kDa was no longer detectable (Fig. 4.11 B). The KR5 mutant recapitulated the K251R phenotype without further decrease in sumoylation.

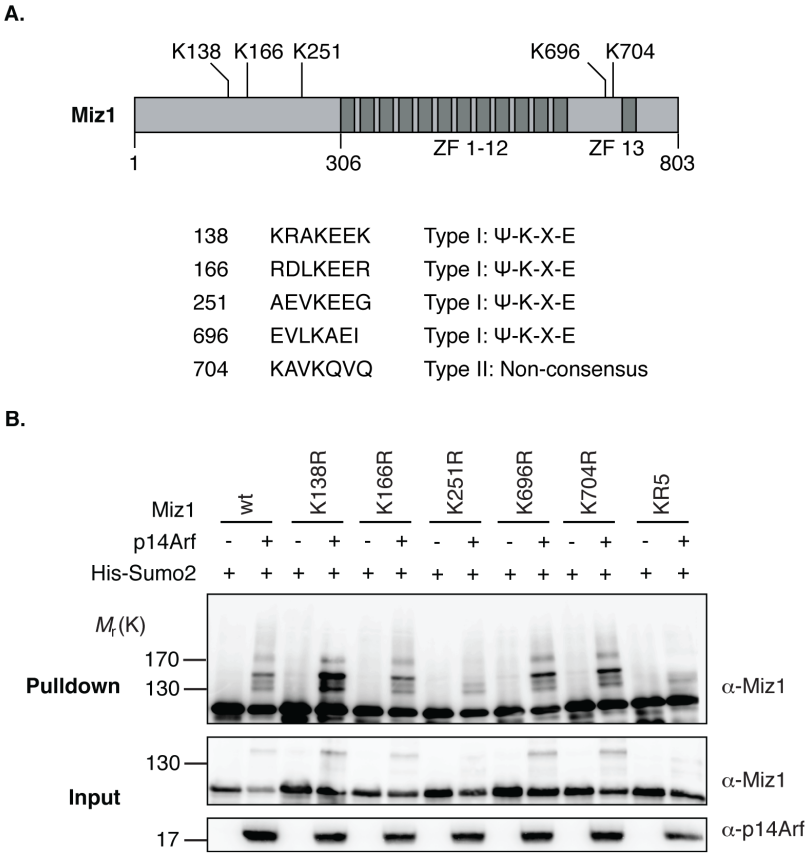

Figure 4.11.:
Miz1 can be sumoylated at lysine 251

A. The diagram illustrates the lysines in Miz1 predicted to be sumoylated. The corresponding sumoylation motifs are shown below. ZF = zinc finger

B. Five Miz1 mutants with single lysines replaced by arginines were generated (K{*number*}R). Additionally, a mutant comprising all five replacements was used (K5R). *In vivo* sumoylation assays were performed as described in Figure 4.10 A.

4.2.3. Validation of the sumoylation site in Miz1

To confirm the notion that the sumoylation machinery is recruited to the sumoylation consensus motif around lysine 251, I generated two more Miz1 mutants. I replaced the two other crucial amino acids of the same motif, valine 250 and glutamic acid 253 with alanines. His-Sumo pulldown experiments showed that mutation of either of the three vital amino acids in the consensus motif lead to a significant loss in sumoylation, with mutation of valine 250 displaying the mildest effect (Fig. 4.12 A). Moreover, lysine 251 in Miz1 was confirmed as the target amino acid for sumoylation not only by Sumo2 but by both the Sumo1 and Sumo2 isoforms (Fig. 4.12 B).

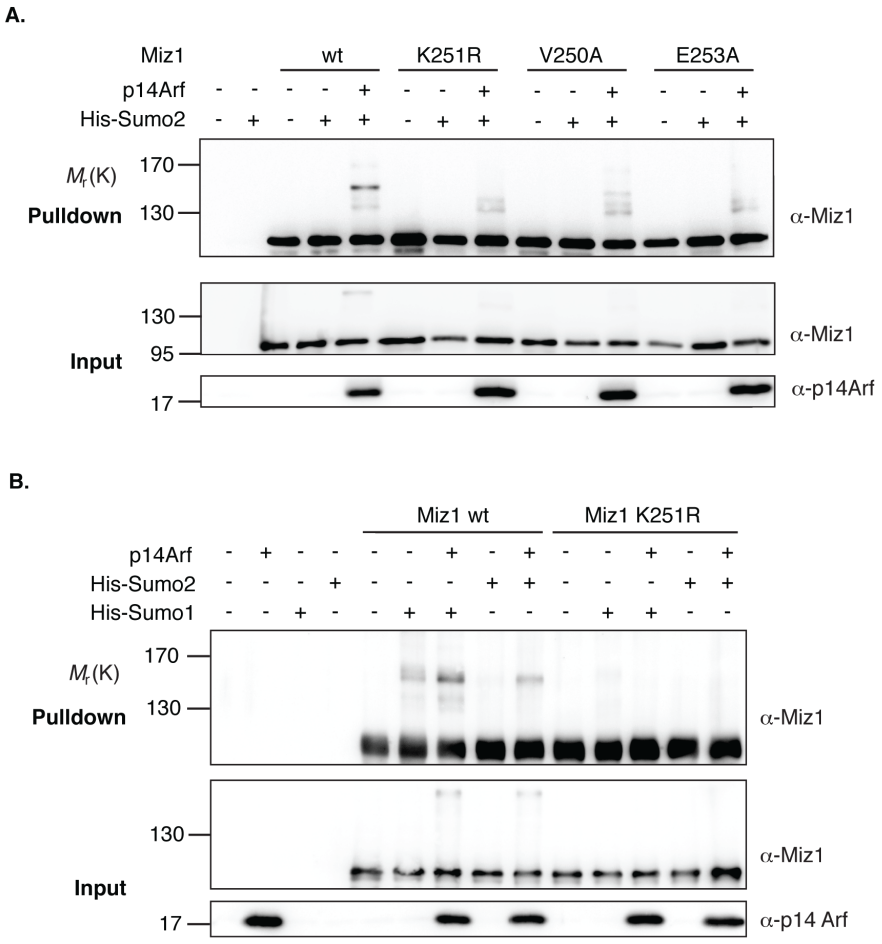

Figure 4.12.:
Validation of the sumoylation site in Miz1

A. Two Miz1 point mutants with valine 250 or glutamic acid 253 replaced by alanine were generated (V250A, E253A). *In vivo* sumoylation assays were performed as described in Figure 4.10 A.

B. *In vivo* sumoylation assays were performed as described in Figure 4.10 A, using both the Sumo1 and Sumo2 isoforms.

4.2.4. Arf induces sumoylation of Miz1 by inhibiting Senp3

Arf can mediate the sumoylation of proteins through its ability to inhibit the Sumo-specific protease Senp3 [Haindl et al., 2008]. To do so, Arf triggers sequential phosphorylation, ubiquitination and subsequent proteasomal degradation of Senp3 [Kuo et al., 2008]. To test if Senp3 might be involved in inhibiting sumoylation of Miz1, I performed His-Sumo pulldowns while expressing Senp3 wild type and the catalytically inactive mutant Senp3 C352S in addition to Miz1 and p14Arf. Strikingly, overexpression of Senp3 inhibited the sumoylation of Miz1, both with and without induction by p14Arf. In contrast, expression

of the catalytically inactive mutant of Senp3 further promoted the sumoylation of Miz1. The Senp3 C352S mutant most likely acts as a dominant-negative protein for the endogenous Senp3 as has been shown before using another catalytically inactive mutant of this enzyme [Gong and Yeh, 2006]. Thus, Arf induces the sumoylation of Miz1 by inhibiting its desumoylation by the Sumo protease Senp3.

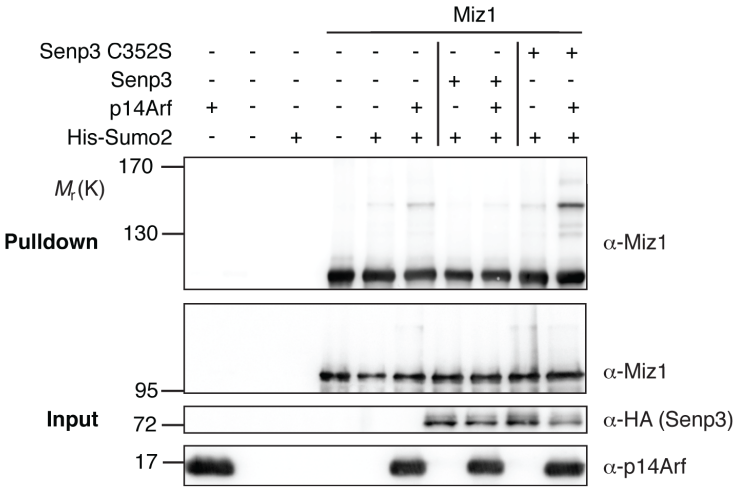

Figure 4.13.:
Arf induces sumoylation of Miz1 by inhibiting the Sumo protease Senp3

Senp3 wild type and the catalytically inactive mutant Senp3 C352S were expressed in addition to Miz1 and p14Arf. *In vivo* sumoylation assays were performed as described in Figure 4.10 A. Half the amount of Arf was transfected compared to the previous experiments to possibly allow further upregulation in the sumoylation extent of Miz1.

4.2.5. Miz1 sumoylation is not increased upon exposure to various stress stimuli

In all previous experiments, sumoylation was analyzed upon transfection of Sumo and its target protein Miz1. To verify sumoylation on an endogenous level, I performed His-Sumo pulldown experiments either without any kind of enforced expression or by infecting near to endogenous amounts of Miz1. However, I could not verify sumoylation of endogenous or virally infected Miz1 in pulldown experiments (data not shown). This might be due to the short half-life and the usually very low steady-state level of the Sumo modification [Johnson, 2004; Hay, 2005] which makes it hard to be detected on an endogenous level.

Overall sumoylation is increased upon exposure to various stresses such as heat shock, osmotic or ethanol stress [Saitoh and Hinchey, 2000]. The response to oxidative

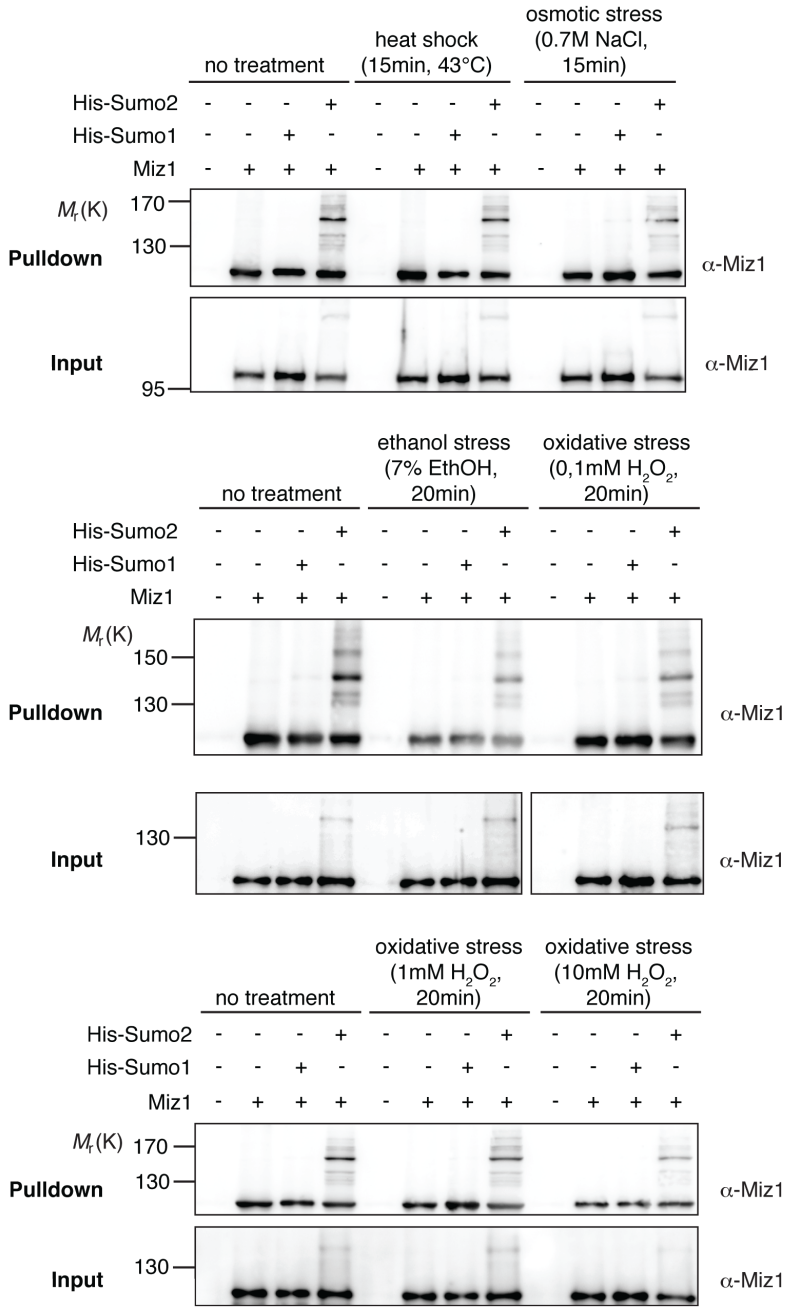

Figure 4.14.:
Miz1 sumoylation is not increased upon treatment with various stress stimuli

In vivo sumoylation assays were performed as described in Figure 4.13, using a lower amount of p14Arf. HeLa cells were treated with the indicated stress conditions before harvesting by scraping off cells from the dish.

stress varies depending on the concentration of H_2O_2 [Bossis and Melchior, 2006]. A concentration of 1 mM H_2O_2 induces a Uba2-Ubc9 crosslink and rapid loss of overall sumoylation by Sumo1 and Sumo2. Higher H_2O_2 concentrations such as 100 mM again induce accumulation of Sumo conjugates by now also inhibiting the Sumo peptidases.

I performed *in vivo* sumoylation assays assays upon various kinds of stress treatments to determine a condition which might be used to visualize endogenous sumoylation of Miz1. I transfected HeLa cells with Miz1, p14Arf and either His-Sumo1 or His-Sumo2. The stress treatment was either applied before scraping the cells off the dish (Fig. 4.14) or after detaching the cells by trypsinisation and treating them in a reaction tube (obtaining essentially the same results, data not shown). All stresses which had been shown to trigger overall sumoylation did not visibly upregulate the extent of Miz1 sumoylation under these conditions, but rather diminished it. Treatment with low concentrations of H_2O_2 (0.1 mM) reduced the sumoylation as expected. In sum, none of the stresses previously shown to trigger overall sumoylation had an inducing effect on the sumoylation of Miz1.

4.2.6. Miz1 K251R cannot phenotypically be distinguished from Miz1 wild type in inhibiting cell growth

Next I assessed if the K251R mutant of Miz1, which displayed a defective sumoylation in the *in vivo* sumoylation assays, shows a different phenotype compared to Miz1 wild type in growth behaviour. U2OS cells do not actively express p14Arf, as their INK4a/Arf locus is silenced by DNA methylation [Badal et al., 2008]. I used these osteosarcoma cells for the following experiments, infecting relatively low levels of Arf compared to the previous transfection assays.

Miz1 has been shown to repress cell growth in colony formation assays due to expression of CDK inhibitors [Staller et al., 2001]. I lentivirally infected U2OS cells with Miz1 wild type and K251R in combination with p14Arf and monitored the cell growth in a growth curve and by colony assay. Miz1 and p14Arf alone induced an inhibition of growth as expected, the combination of the two revealed a more severe arrest phenotype. However, I could not distinguish Miz1 wild type and the non-sumoylatable K251R mutant within this experimental setup (Fig. 4.15). I obtained the same results using lentiviral infection in the p14Arf expressing HeLa cells and retroviral infection of LS174 cells (data not shown). It should be noted that the extent of the growth arrest induced by Miz1 is dependent on serum conditions and varies from mild growth inhibition (as seen in Figure 4.15) to

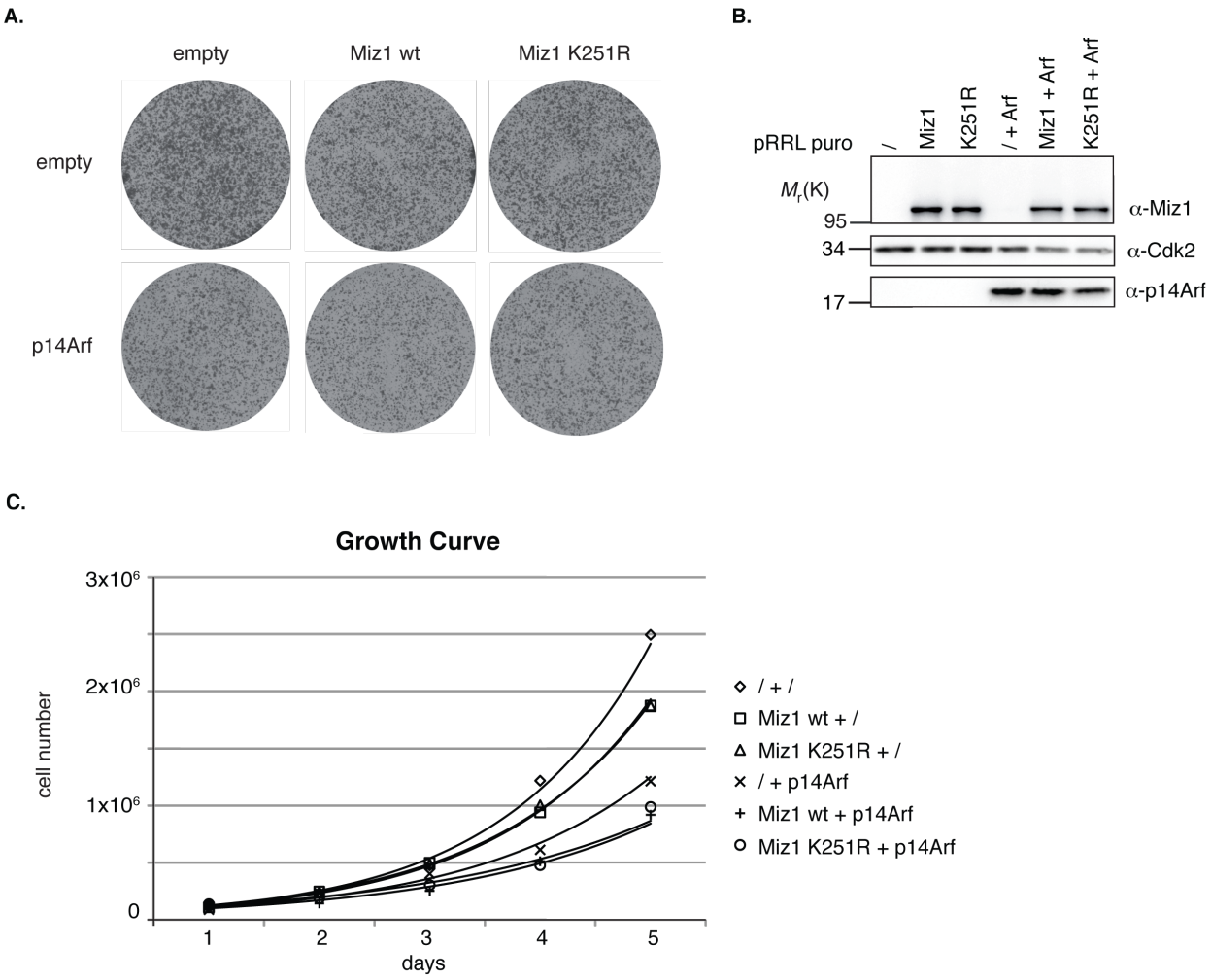

Figure 4.15.:
Miz1 wild type and K251R show the same growth arrest phenotype

A. U2OS cells were lentivirally infected with empty vector, Miz1 wild type or Miz1 K251R and selected for expression of these proteins by a two-day puromycin treatment. Then either p14Arf or an empty construct were infected and 25,000 cells seeded on 6cm dishes. After 6 days cells were subjected to crystal violet staining.

B. Expression of proteins was detected by Western Blot analysis two days after Arf infection.

C. Cell growth was monitored by seeding 100.000 U2OS cells onto 6cm dishes one day after Arf infection and counting cells each of the five following days.

a complete block in proliferation (as shown by Staller et al. [2001]). This was discovered through direct experimentation using twelve different kinds of sera (data not shown).

4.2.7. Miz1 wild type and the non-sumoylatable mutant show the same phenotype upon DNA damage

It is known that Miz1 plays a role in DNA damage, for example upon treatment of cells with ultraviolet radiation (UV). Miz1 activates transcription of the *p21cip1* gene upon UV-B irradiation. Miz1 also releases a fraction of the topoisomerase II binding protein 1 (TopBP1) from the chromatin where it is kept in unstressed cells to be protected from degradation by HectH9. TopBP1 activates the Atr master kinase in the DNA damage response which leads to activation of downstream targets such as Chk1 and p53 [Herold et al., 2008].

To determine if sumoylation of Miz1 may play a role in this process, I compared Miz1 wild type and the non-sumoylatable mutant in their response to UV-B. I lentivirally infected LS174T human colon adenocarcinoma cells also used in Herold et al. [2008] with an empty vector control, Miz1 wild type and the K251R mutant. I treated cells with UV-B for 60 seconds, then harvested them for FACS analysis and Western Blot after 0, 1, 2, 4 or 6 hours. The Western Blot shows expression of the two Miz1 variants, as well as expression of activated Chk1 (phosphorylated at Ser 345) which is indicative of active Atr signaling (Fig. 4.16 A). In the empty vector situation, phospho-Chk1 levels increase shortly after UV-B treatment, then rapidly decline again. Expression of both Miz1 wild type and the K251R mutant induce a stronger increase of phospho-Chk1 which is retained active for a longer time as has been observed before. The FACS analysis shows a decrease in G2/M phase and a slight increase of the subG1 content for the empty vector infected cells over time, reflecting a previously characterized G1 and S phase arrest with mild apoptosis upon UV-B treatment (Fig. 4.16 B). Infection of Miz1 wild type and the K251R mutant again shows a similar phenotype, both inducing a decrease of cells in G2/M phase as well as a fairly strong apoptotic response at the later time points. All in all, I could not detect major differences between overexpression of Miz1 wild type and the non-sumoylatable mutant combined with UV-B treatment with this experimental setup.

4.2.8. Global gene expression pattern induced by Miz1 wild type and the non-sumoylatable mutant

To assess if the global gene expression pattern that results from overexpression of Miz1 wild type is different to the one induced by the Miz1 non-sumoylatable mutant, we performed a genome-wide microarray analysis. I lentivirally infected U2OS cells with Miz1 wild type and K251R in combination with an empty vector construct or p14Arf (Fig. 4.17 A).

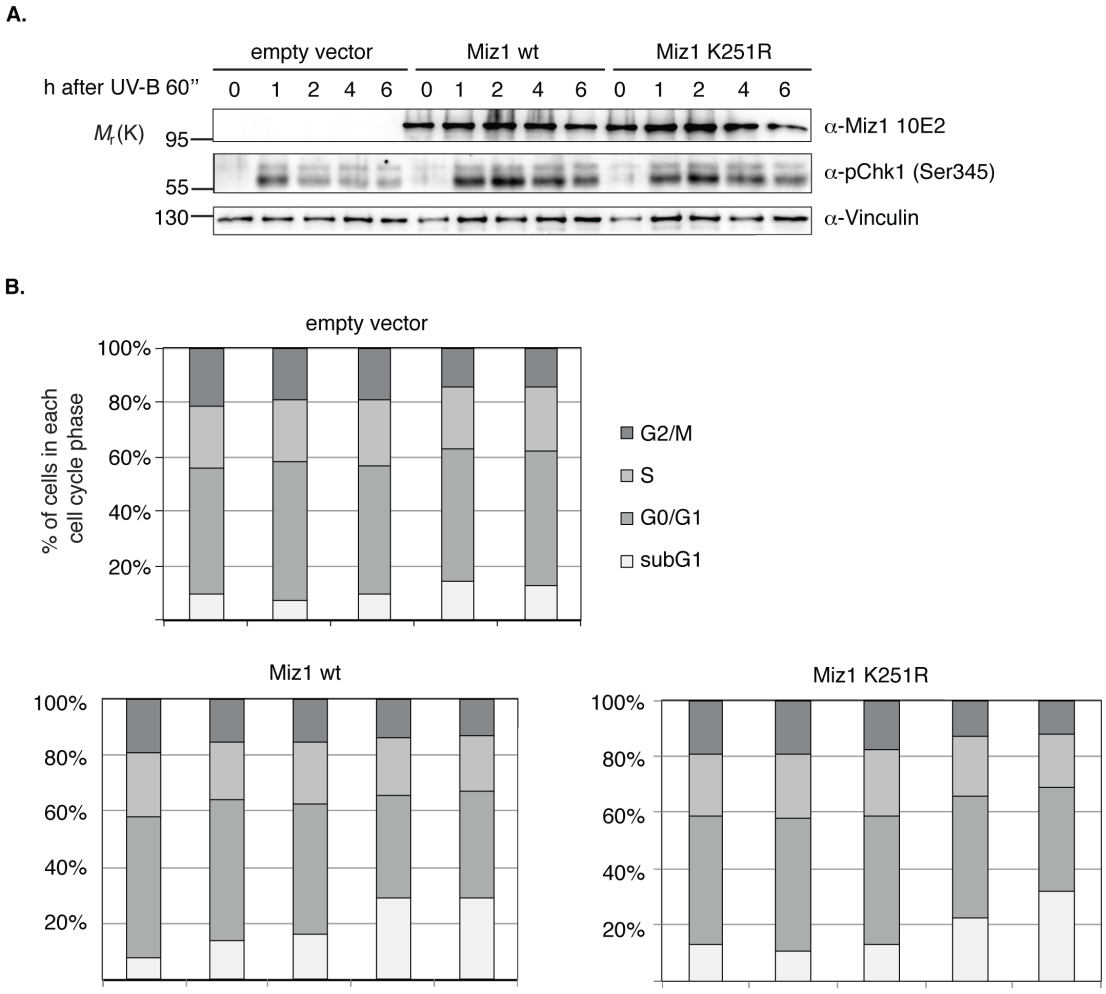

Figure 4.16.:
Miz1 wild type and K251R respond to UV-B irradiation in the same way

A,B. LS174T cells were lentivirally infected with empty vector, Miz1 wild type or Miz1 K251R and selected for expression of these proteins by a two-day puromycin treatment. Cells on 10 cm dishes were treated with a dose of 500 J/m^2 UV-B all at the same time and then harvested 0, 1, 2, 4 or 6 hours later by trypsination, including floating cells in the medium supernatant. Cells were split up, one half was boiled in hot SDS sample buffer and subjected to Western Blot, using Vinculin as a loading control (A). The other half was fixed in ethanol and subjected to PI-FACS (B).

I harvested the cells and isolated the RNA which was subjected to microarray analysis performed by Michael Krause. Bioinformatician Lukas Rycak analyzed the raw data (both from IMT Marburg).

A.

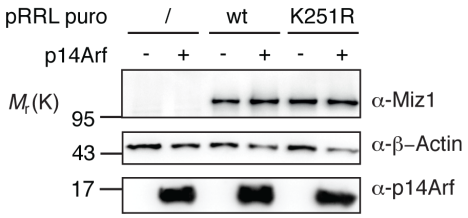
pRRL puro
/
wt
K251R
p14Arf
- + - + - +
M_r(K)
95
43
17
α-Miz1
α-β–Actin
α-p14Arf

B.

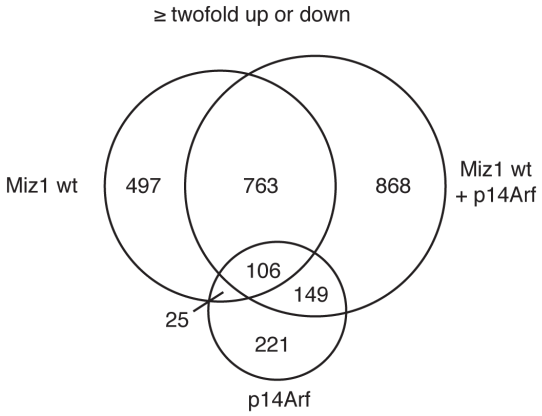
≥ twofold up or down
Miz1 wt
497
763
868
Miz1 wt
+ p14Arf
106
149
25
221
p14Arf

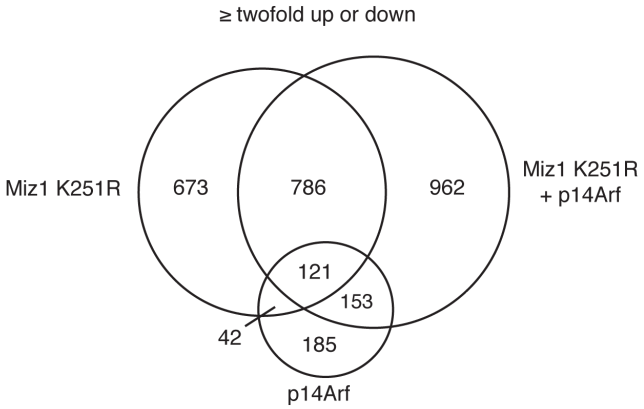
≥ twofold up or down
Miz1 K251R
673
786
962
Miz1 K251R
+ p14Arf
121
153
42
185
p14Arf

C.

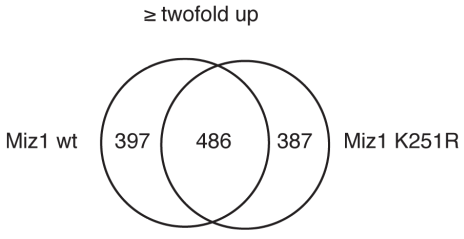
≥ twofold up
Miz1 wt
397
486
387
Miz1 K251R

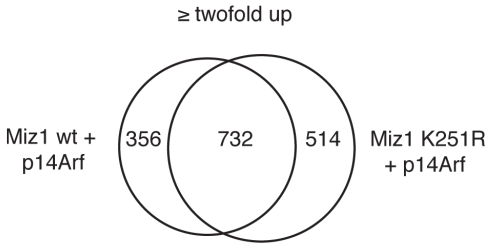
≥ twofold up
Miz1 wt +
p14Arf
356
732
514
Miz1 K251R
+ p14Arf

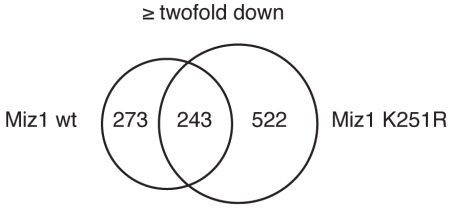
≥ twofold down
Miz1 wt
273
243
522
Miz1 K251R

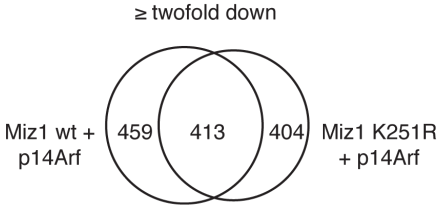
≥ twofold down
Miz1 wt +
p14Arf
459
413
404
Miz1 K251R
+ p14Arf

The Venn diagrams in Figure 4.17 B give a first impression of the number of regulated genes and their distribution. All genes that are twofold up- or downregulated in comparison to the empty vector situation were considered. The analysis reveals that expression of Arf strongly enhances the ability of both Miz1 wild type and the K251R mutant to modulate transcription, which is independent of the effects induced by Arf alone (as already observed in Herkert et al. [2010]). Specifically, Miz1 wild type modulates 1886 genes more than twofold in the presence of Arf, but only 1391 in its absence. Similarly, expression of Arf enhanced the number of Miz1 K251R-modulated genes from 1622 to 2022. To see if Miz1 wild type and the non-sumoylatable mutant have different effects on either repression or activation of genes, I generated Venn diagrams for either twofold up- or downregulation of genes in the presence or absence of Arf (Fig. 4.17 C). The overlap between genes regulated by Miz1 wild type and the K251R mutant is highly significant in each of the four Venn diagrams. However, there are also several genes only regulated in either of the two Miz1 conditions. Most prominently, Miz1 K251R downregulates 765 genes in comparison to 516 genes downregulated by Miz1 wild type. Also, overexpression of Miz1 wild type together with Arf leads to upregulation of 1088 genes while K251R together with Arf upregulates 1246 genes. Taken together, the expression patterns of Miz1 wild type and the non-sumoylatable mutant are highly similar but also exhibit some differences.

Validation of the microarray

Gene Ontology (GO) term analysis using DAVID revealed no apparent groups of genes that are differentially regulated when comparing Miz1 wild type with the K251R mutant (data not shown). However, if assumed that infection of Miz1 wt + Arf but not Miz K251R + Arf leads to sumoylation of Miz1, it should be possible to identify a set of genes that is regulated differently comparing sumoylated and non-sumoylated Miz1. If this kind

Figure 4.17. ***(facing page)*:**
Microarray results summarized in Venn diagrams

A. U2OS cells were infected with lentiviruses expressing the indicated proteins or with empty vector controls. After selection, cells were harvested and a fraction of them analyzed via hot SDS lysis and Western Blot. From the remaining cells the RNA was extracted and examined for quality and quantity, then used for a microarray experiment.
B. Two Venn diagrams depicting the overlap in genes up- or downregulated twofold in comparison to the empty vector condition are shown.
C. The overlap of genes that are either up- or downregulated are depicted in separate Venn diagrams for the different infection conditions comparing Miz1 wild type and the non-sumoylatable K251R mutant.

of sumoylation-based differential regulation would occur, a set of four regulation patterns considering the six infection conditions could be imagined. A certain group of genes could show up- or downregulation only when Miz1 is sumoylated ("only Miz1+Arf up, only Miz1+Arf down"), another group of genes could be regulated only in absence of Miz1 sumoylation ("all up except Miz1+Arf, all down except Miz1+Arf"). I sorted the list of all $\geq$ twofold regulated genes from the microarray, each in comparison to the empty vector condition, according to these four regulation patterns.

In Figure 4.18 A, these patterns become apparent: Each of the four panels represent a list of genes picked out as described above. The bars represent an average of the logFC values of all genes in the respective group. The "all up except Miz1+Arf, all down except Miz1+Arf" groups count only comparably few genes (30 and 18 genes), which when averaged do also not reflect strong differences among the distinct infection conditions. In contrast to that, the "only Miz1+Arf up, only Miz1+Arf down" groups of genes are considerably larger (211 and 341 genes) and the Miz1+Arf condition stands out more clearly as being regulated in a different manner. Thus, I focused on these two groups of genes for further analysis.

To validate the microarray, I analyzed several top regulated genes which showed a strong up- or downregulation in one of the infection conditions by qRT PCR. All of these reflected the same regulation in microarray and qRT PCR (data not shown). Next, I picked several

---

Figure 4.18. ***(facing page)*:**
Grouping of genes and validation of the microarray data by qRT PCR

A. Genes were picked that show a differential regulation for the Miz1 + Arf condition, where Miz1 is possibly sumoylated. Four groups of genes were generated that either showed a $\geq$ twofold regulation only in the Miz1 + Arf condition ("only Miz1+Arf up, only Miz1+Arf down") or in all conditions except Miz1 + Arf ("all up except Miz1+Arf, all down except Miz1+Arf"). The number of genes in each list is specified in the heading. The bars in each of the four panels represent the averaged logFC values of all genes in the respective group which were analyzed for the different infection conditions. wt = Miz1 wild type, K251R = Miz1 K251R

B. Six genes were picked out of the "only Miz1+Arf down" group and validated by qRT PCR with the same RNA used for the microarray. The upper panel shows the microarray data for each gene compared to the empty vector control, the reference point at zero is set as the average value of all analyzed samples from the whole array. The lower panel shows the qRT PCR analysis with the same genes normalized to beta-2-microglobulin. The relative mRNA levels were each set in reference to the value of the empty vector infection which was arbitrarily set to 1.

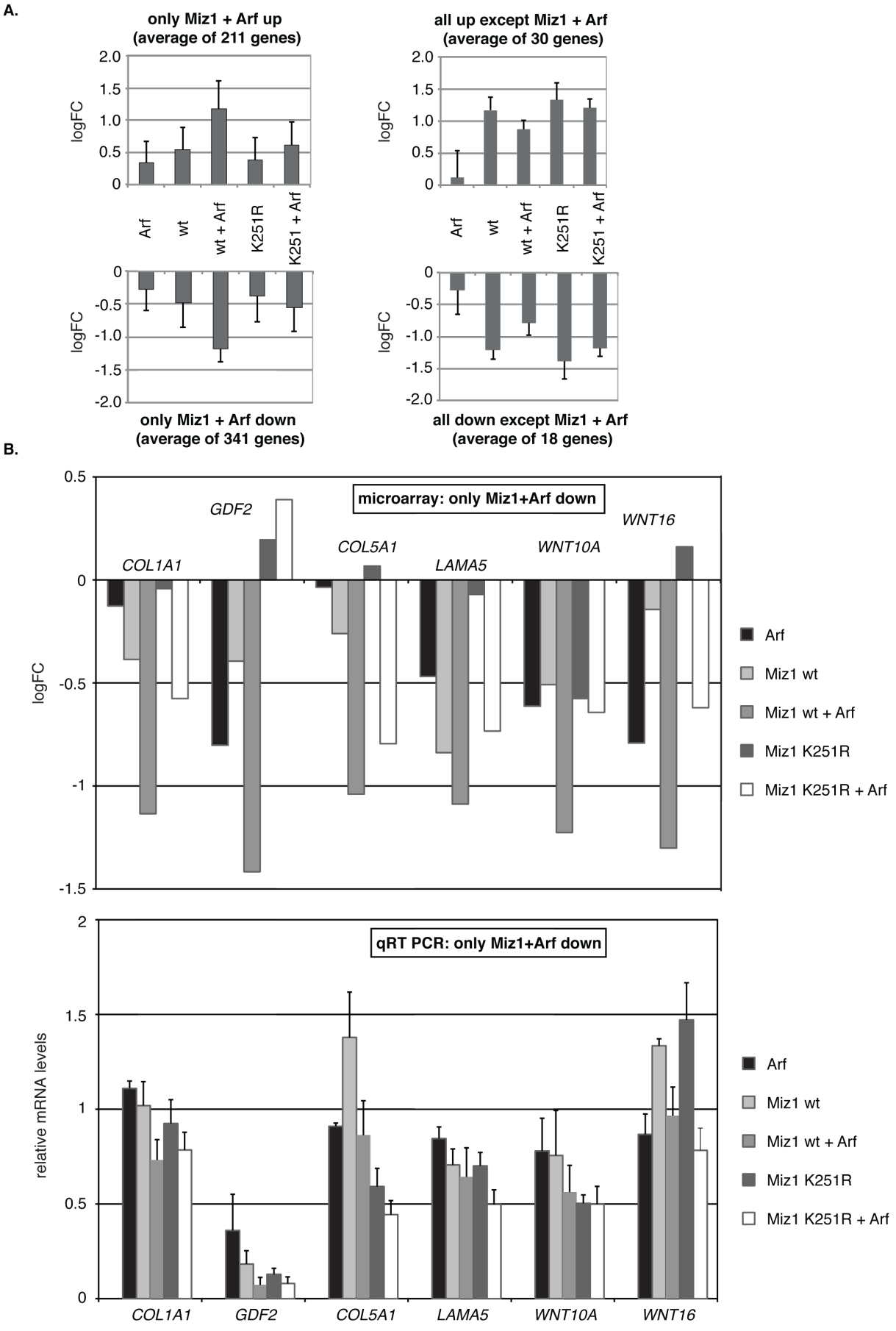
A.
only Miz1 + Arf up
(average of 211 genes)
all up except Miz1 + Arf
(average of 30 genes)
logFC
Arf
wt
wt + Arf
K251R
K251 + Arf
only Miz1 + Arf down
(average of 341 genes)
all down except Miz1 + Arf
(average of 18 genes)
B.
microarray: only Miz1+Arf down
COL1A1
GDF2
COL5A1
LAMA5
WNT10A
WNT16
Miz1 wt
Miz1 wt + Arf
Miz1 K251R
Miz1 K251R + Arf
qRT PCR: only Miz1+Arf down
relative mRNA levels

genes out of the aforementioned two groups of genes and also analyzed them by qRT PCR, focusing on genes which show the most divergent regulation in the sumoylated Miz1 condition. In Figure 4.18 B the microarray data of the validation targets from the "only Miz1+Arf down" group is shown together with the qPCR analysis. While the microarray exhibits a twofold repression only in the Miz1+Arf condition for these genes, this cannot be observed for the qRT PCR validation in the same manner. Even though repression does occur, except for Wnt16, the ratio between the different conditions in the qPCR does not reflect the microarray output. I also observed this for genes validated from the "only Miz1+Arf up group" and in an independent experiment with RNA isolated from newly infected cells (data not shown). With this analysis, I could not identify a group of genes that are differentially regulated in the Miz1+ Arf condition.

4.3. Sumoylation of Myc

4.3.1. C-Myc and N-Myc can be modified by both Sumo isoforms

In the previous chapter I could show that Arf-induced complex formation of Miz1, Arf and Myc goes along with sumoylation of Miz1 at a specific lysine. To reveal if Sumo modification of Myc is possible as well, I performed a sumoylation analysis using the two best characterized Myc isoforms, the abundant c-Myc and the neuronal N-Myc. *In vivo* sumoylation assays were performed in HeLa cells as described in 4.2.1 on page 70.

The pulldown experiments revealed that upon overexpression of c-Myc together with His-Sumo2, a whole ladder of higher migrating Myc species can be pulled down (Fig. 4.19 A). Arf expression does not stimulate an increase of the sumoylation of Myc as it does for Miz1 (data not shown). Unmodified c-Myc with a size of about 55 kDa sticks to the agarose beads, which I had already observed for Miz1. N-Myc can also be sumoylated by both the Sumo1 and Sumo2 isoforms, which is later shown for c-Myc as well (4.3.6 on page 90). The major N-Myc sumoylation band at around 90 kDa can already be detected in the input samples, the overall sumoylation pattern in the pulldown samples is characterized by a ladder of higher migrating bands (Fig. 4.19 B). Substantially less unmodified N-Myc sticks to the agarose beads used in the *in vivo* sumoylation assays, thus I performed the first part of the sumoylation analysis using the N-Myc isoform.

I blotted the pulldown samples for N-Myc sumoylation in addition directly with Sumo1 and Sumo2 antibodies, showing a major increase in sumoylated proteins upon N-Myc overexpression for both Sumo1 and Sumo2 (Fig. 4.19 C). The proteins detected in the Sumo blots exhibit the same band pattern with and without transfection of N-Myc, including a characteristic 90 kDa protein which likely is RanGap [Saitoh and Hinchey, 2000]. HeLa cells do not endogenously express N-Myc, which leads to the conclusion that transfection of N-Myc together with Sumo increases sumoylation of other targets.

4.3.2. Myc is subjected to multisumoylation

The His-Sumo pulldown with both c- and N-Myc does not show clearly distinguishable higher migrating bands which are indicative for attachment of a single or a few Sumo molecules. Instead, a first prominent band shifted up about 45 kDa is followed by a ladder of bands reaching up to the 170 kDa range. To verify this as sumoylation and to explore the nature of the modification, I first performed an *in vivo* sumoylation assay with and without

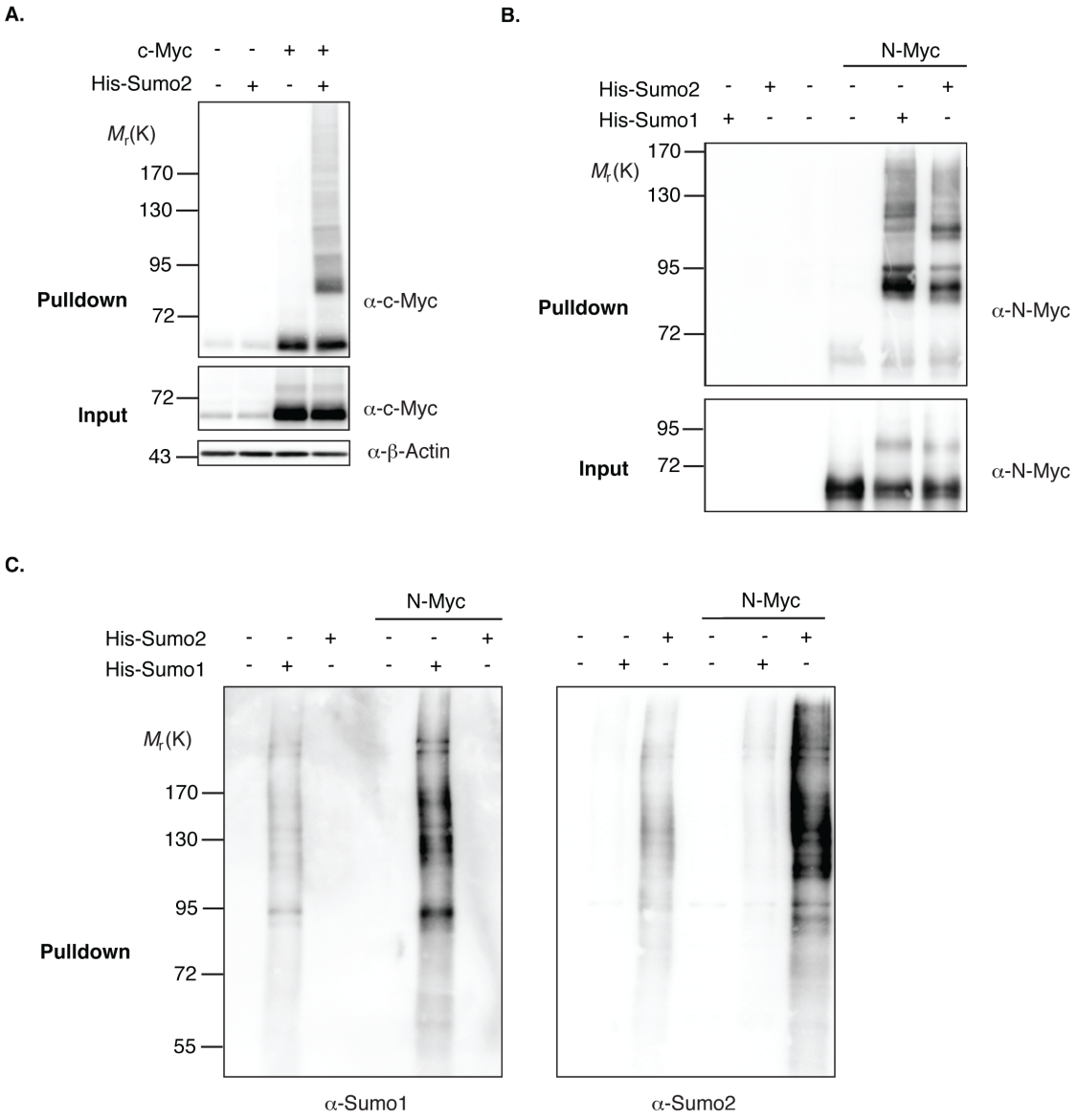

Figure 4.19.:
c-Myc and N-Myc can get sumoylated by Sumo1 and Sumo2

A. Sumoylation of c-Myc by Sumo2. HeLa cells were transfected with the indicated plasmids and harvested 24 h later under denaturing conditions. His-Sumo modified proteins were pulled down using Ni^{2+}-NTA-agarose and analyzed via Western Blot with a 7.5 % input sample. This procedure applies to all sumoylation assays in the following Figures, any changes will be specified.

B. Sumoylation of N-Myc by Sumo1 and Sumo2 in the His-Sumo pulldown.

C. His-Sumo pulldown samples of the experiment in B were blotted for Sumo1 and Sumo2, respectively.

depletion of the E2 enzyme Ubc9. Expression of an siRNA pool against Ubc9 severely diminished higher migrating bands of pulled-down N-Myc throughout the whole size range (Fig. 4.20 A). Next, I tested if the unusual pattern of many higher migrating bands results from poly-Sumo chains or ubiquitination of a Sumo molecule that is attached to Myc. I generated two mutants of Sumo2, which either lack the internal sumoylation site or all sites that have been shown to be possible targets for ubiquitination [Tatham et al., 2008]. Both Sumo2 mutants showed the same ability to modify N-Myc as wild type Sumo2 (Fig. 4.20 B). Therefore, polysumoylation as well as formation of mixed Sumo/ubiquitin chains can be excluded as the reason for the distinctive size shift. This is further supported by the fact that Sumo1 modification of Myc also shows a ladder of shifted bands, even though Sumo1 lacks an internal sumoylation site which is necessary for poly-Sumo chain formation.

Sumoylation of Myc could result in subsequent ubiquitination at internal lysines in the Myc sequence. To investigate if sumoylation promotes ubiquitination of Myc, I performed a His-ubiquitin assay. To prevent degradation of ubiquitinated Myc I treated cells with proteasome inhibitor before harvesting. Otherwise the same setup and protocol as used for the His-Sumo pulldown was applied. Overexpression of an HA-tagged version of Sumo2 resulted in a visible band shift in the N-Myc input sample and an accumulation of sumoylated species in the high kDa range on the HA-Sumo blot. Coexpression of N-Myc and ubiquitin resulted in polyubiquitination of N-Myc as expected, but this did not increase upon additional expression of Sumo2 (Fig. 4.20 C). Proteasome inhibition never resulted in accumulation of sumoylated Myc using differently tagged constructs of Sumo1 and Sumo2 (data not shown).

4.3.3. Sumoylation consensus sites in Myc

Sumoylation often occurs within the defined consensus motif Ψ-K-X-E/D (see also 4.2.2 on page 70). The SUMOsp software tool for *in silico* sumoylation site prediction proposed one non-consensus sumoylation site in c-Myc which overlapped with one of the two predicted consensus sites in N-Myc. To verify if these sites could be preferred targets for modification by Sumo, I generated two N-Myc mutants. For the KR3 mutant I replaced two adjacent lysines in addition to the predicted lysine 351 by arginines, the K413R mutant just contains one replacement (Fig. 4.21 A). An *in vivo* sumoylation assay revealed that the KR3 and K413R mutant can both be sumoylated like wild type N-Myc, even though the KR3 mutant shows minor changes in the sumoylation pattern in the lower kDa range, which is also reflected in the input (Fig. 4.21 B). Sumoylation consensus lysines in Myc are therefore

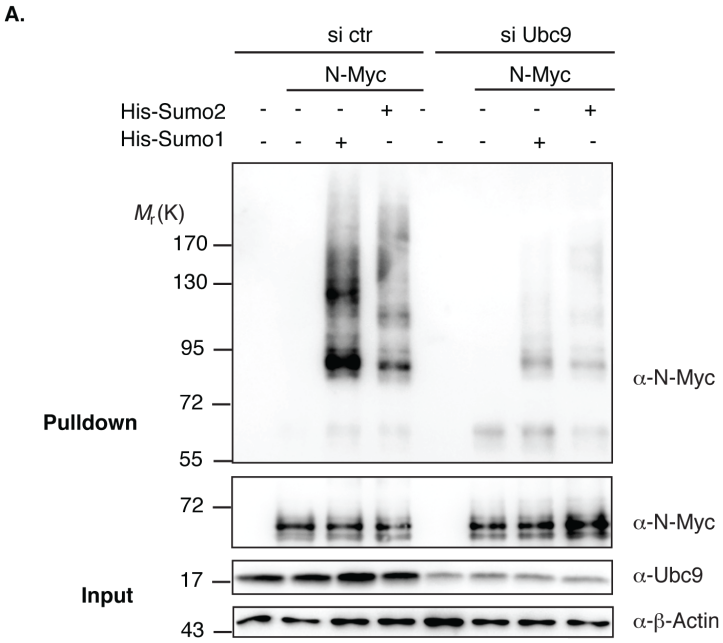
A.
si ctr
si Ubc9
N-Myc
N-Myc
His-Sumo2 - - - + - - - - +
His-Sumo1 - - + - - - + -
M_r(K)
170
130
95
72
55
Pulldown
α-N-Myc
72
α-N-Myc
Input
17
α-Ubc9
43
α-β-Actin

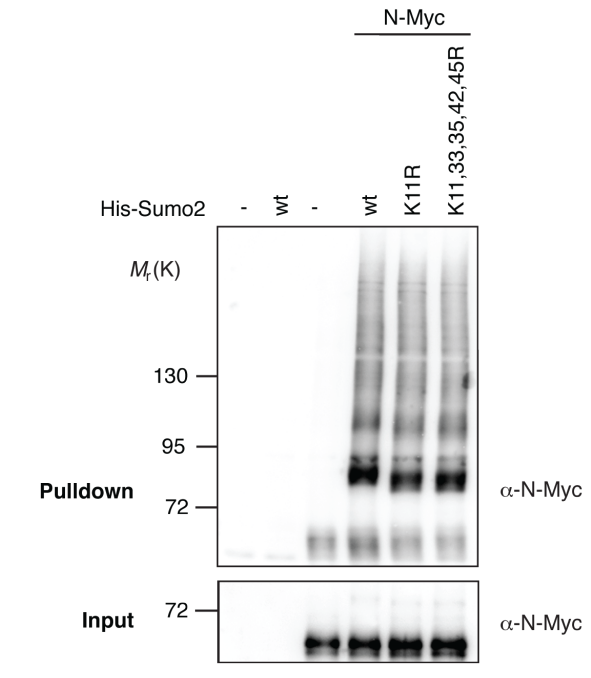
B.
N-Myc
His-Sumo2 - wt - wt K11R K11,33,35,42,45R
M_r(K)
130
95
Pulldown
72
α-N-Myc
Input
72
α-N-Myc

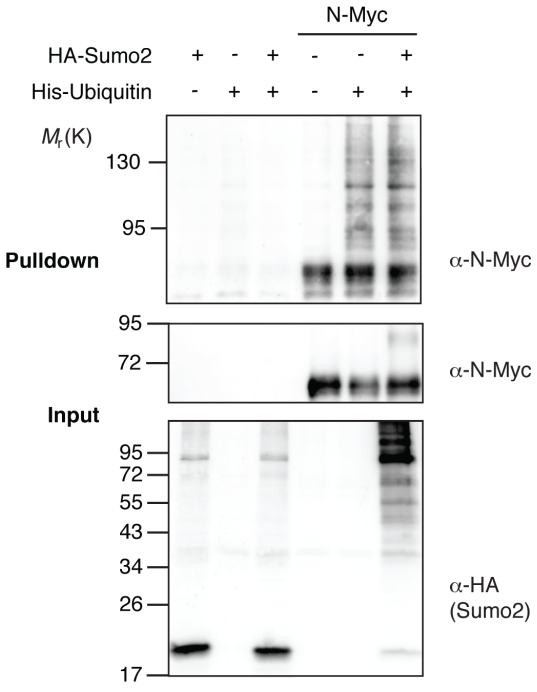
C.
N-Myc
HA-Sumo2 + - + - - +
His-Ubiquitin - + + - + +
M_r(K)
130
95
Pulldown
α-N-Myc
95
72
α-N-Myc
Input
95
72
55
43
34
26
17
α-HA
(Sumo2)

not exclusive targets for sumoylation, as already expected from the notion that Myc must be multisumoylated.

4.3.4. Determining a preferred region for sumoylation in Myc

To analyze if sumoylation of Myc plays a biological role, a mutant of Myc refractory to sumoylation that could be compared to wild type Myc would be very useful. From the previous experiments it coud be concluded that sumoylation must take place at multiple lysines in the Myc sequence. I therefore investigated if these lysines could be reliably determined to generate a non-sumoylatable Myc mutant.

C-Myc contains 25 lysines. Two mutants of c-Myc were provided by Laura A. Jänicke, which only contain lysines in either the N-terminal or the C-terminal half, the remaining lysine residues replaced by arginines. *In vivo* sumoylation assays with Sumo1 and Sumo2 revealed that both mutants were severely depleted for sumoylation, especially in the higher kDa range. This was far more prominent for the mutant that lacks the lysines in the C-terminus, which contains 18 out of the total 25 lysines (Fig. 4.22 A).

4.3.5. Using single lysine mutants of Myc to find target sites for sumoylation

Mutants of c-Myc containing either only C- or N-terminal lysine residues did not reveal a preference for sumoylation considering the different numbers of lysines in either half of the protein. To investigate the sumoylation sites in Myc more thoroughly, I used mutants of c-Myc provided by Nikita Popov which either contain no lysines at all (K-less) or only single lysines (Kx). All remaining lysine residues were replaced by arginines. I compared the 25 mutants each to wild type Myc and the non-sumoylatable K-less mutant as a negative control for their potential to be sumoylated, several examples are shown in Figure 4.23 A

Figure 4.20. ***(facing page)*:**
Myc is multisumoylated by Sumo1 and Sumo2

A. HeLa cells were first transfected with a pool of four siRNAs directed against Ubc9 or a control siRNA, 24 h later with the indicated protein expression plasmids. *In vivo* sumoylation assays were performed as described in Figure 4.19 A, protein depletion of Ubc9 was verified via Western Blot.
B. *In vivo* sumoylation assays were performed using a Sumo2 mutant unable to form poly-Sumo chains (K11R) or one that is refractory to chain-formation and internal ubiquitination (K 11, 33, 35, 42, 45 R).
C. The His-ubiquitin assay was performed following the same protocol as used for the His-Sumo pulldown. Cells were treated with 10 µM MG-132 for 6 hours before harvesting to prevent degradation of ubiquitinated Myc in the proteasome.

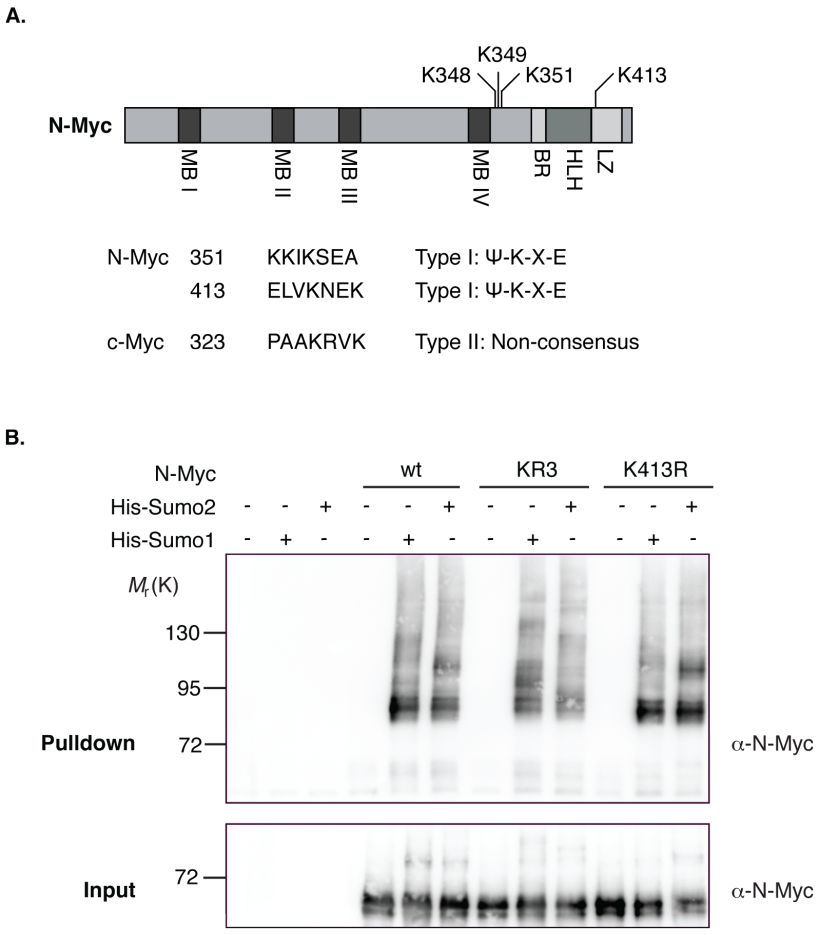

Figure 4.21.:
Sumoylation consensus sites in Myc are not exclusive targets for sumoylation

A. Possible sumoylation sites in N-Myc and c-Myc are listed. The diagram illustrates the lysines replaced by arginines for the KR3 (K 348, 349, 351 R) and the K413R mutant in relation to important functional motifs in the Myc protein. Lysine 323 in c-Myc aligns with lysine 348 in N-Myc. MB = Myc box, BR = basic region, HLH = helix-loop-helix, LZ = leucine zipper

B. *In vivo* sumoylation assays were performed using the N-Myc KR3 and K413R mutants described in A.

and B. The extent of sumoylation was quantified for each mutant and plotted in Figure 4.23 C. The analysis revealed a cluster of preferred sumoylation sites between lysine 289 and 355. This region overlaps with the sumoylation consensus site in N-Myc around lysine 351.

4.3.6. Central target lysines play an important role in the sumoylation of c-Myc

To verify if the central sumoylation cluster in c-Myc is decisive for sumoylation of the full-length protein, I generated two additional mutants. One had six lysines from the cluster

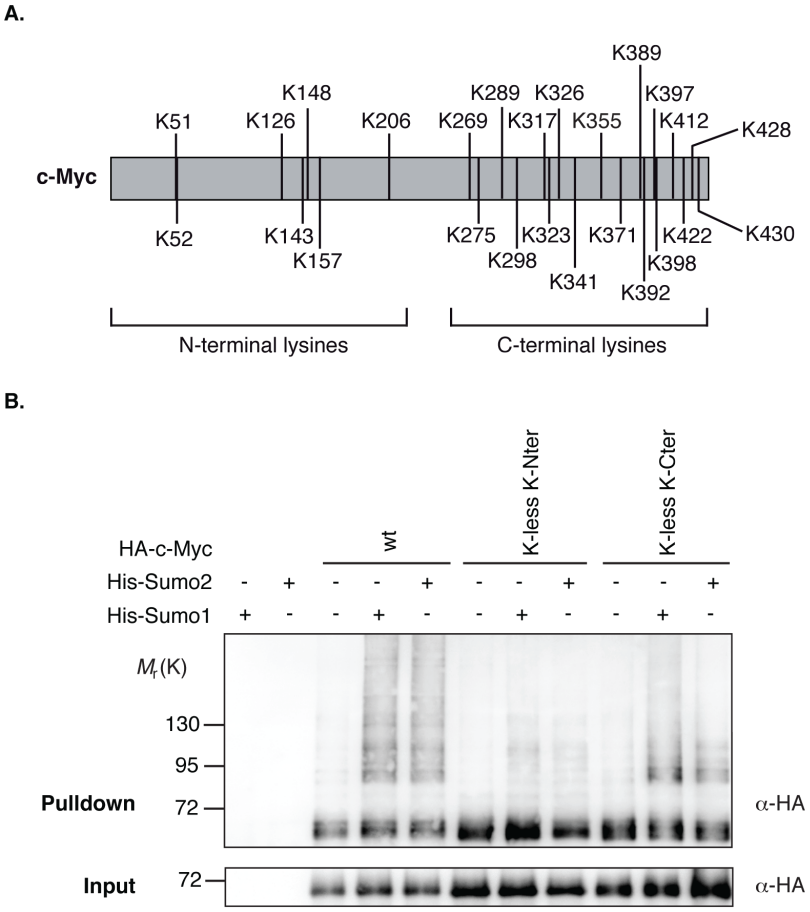

Figure 4.22.:
Myc mutants lacking C- or N-terminal lysines in the sumoylation assay

A. The diagram depicts the localization of all 25 lysines in c-Myc. Brackets indicate which lysines were mutated to arginines in the C- or N-terminal half of c-Myc.

B. *In vivo* sumoylation assays were performed using c-Myc mutants containing only N-terminal lysines (K-less K-Nter) or only C-terminal lysines (K-less K-Cter) respectively. Note that these and the following lysine mutants of c-Myc all contain an N-terminal HA-tag.

mutated to arginines (KR6), the other one exclusively contained seven lysines from the same region (K-less R7K). The KR6 mutant could still be sumoylatated to a significant extent in comparison to wild type c-Myc and the lysine-less mutant (Fig. 4.24 A). The mutant with the reconstituted lysines showed some sumoylation, but the extent of the modification did not reach the same level as for wild type c-Myc (Fig. 4.24 B). It can thus be concluded that the previously identified cluster for c-Myc modification by Sumo is important for the sumoylation of c-Myc without being the sole Sumo target region.

4.3.7. Myc sumoylation is not increased upon exposure to various stress stimuli

I could not detect sumoylation of Myc without overexpression of the protein when performing His-Sumo pulldowns. Increasing the sumoylation of Myc might enable visualization of an endogenous Sumo modification. Therefore, I applied different kinds of stress treatments which are known to induce overall sumoylation to cells before harvesting them for the pulldown experiments (see also 4.2.5 on page 74).

None of the stresses which had been shown to trigger overall sumoylation visibly induced the extent of Myc sumoylation. Treatment with high concentrations of H_2O_2 (100 mM) abrogated the sumoylation of c-Myc completely and increased its nonspecific binding to the agarose beads used for the pulldown (Fig. 4.24 A). Lower concentrations of H_2O_2 neither induced nor diminished Sumo modification of Myc to a distinguishable extent (Fig. 4.24 B).

4.3.8. Myc contains the sequence of a possible Sumo interacting motif

The *MYC* family of oncogenes is evolutionary well conserved from insects to vertebrates, although sequence conservation is limited to a few short domains [Schwinkendorf and Gallant, 2009]. The most conserved domains are Myc box II and III, but there is an almost equally conserved sequence in the central part of Myc. This has been first described as a PEST sequence (amino acids 226 to 270 of murine c-Myc) which is necessary for ubiquitin-mediated degradation but not as a region of direct ubiquitin attachment [Gregory and Hann, 2000].
Interestingly, this highly conserved region fulfills all criteria for being a reverse Sumo interacting motif (SIMr). SIMs interact with Sumo non-covalently and thus often mediate the effects of sumoylation [Wimmer et al., 2012]. The sequence in the human c-Myc and

Figure 4.23. ***(facing page)*:**
Single c-Myc lysine mutants reveal a cluster of preferred sumoylation sites

A.-B. *In vivo* sumoylation assays were performed using c-Myc mutants containing only single lysines (K-less Kx), shown here are examples for ten mutants. The extent of sumoylation was compared by quantifying higher migrating bands in relation to c-Myc sticking to the agarose beads in the pulldown samples, as this proved to be more accurate than comparing with the input values.

C. The extent of sumoylation of each K-less Kx mutant was set in relation to the sumoylation of wild type Myc, which was arbitrarily set to 1. Sumoylation clusters in a central domain of Myc at lysines 289, 298, 326 and 355.

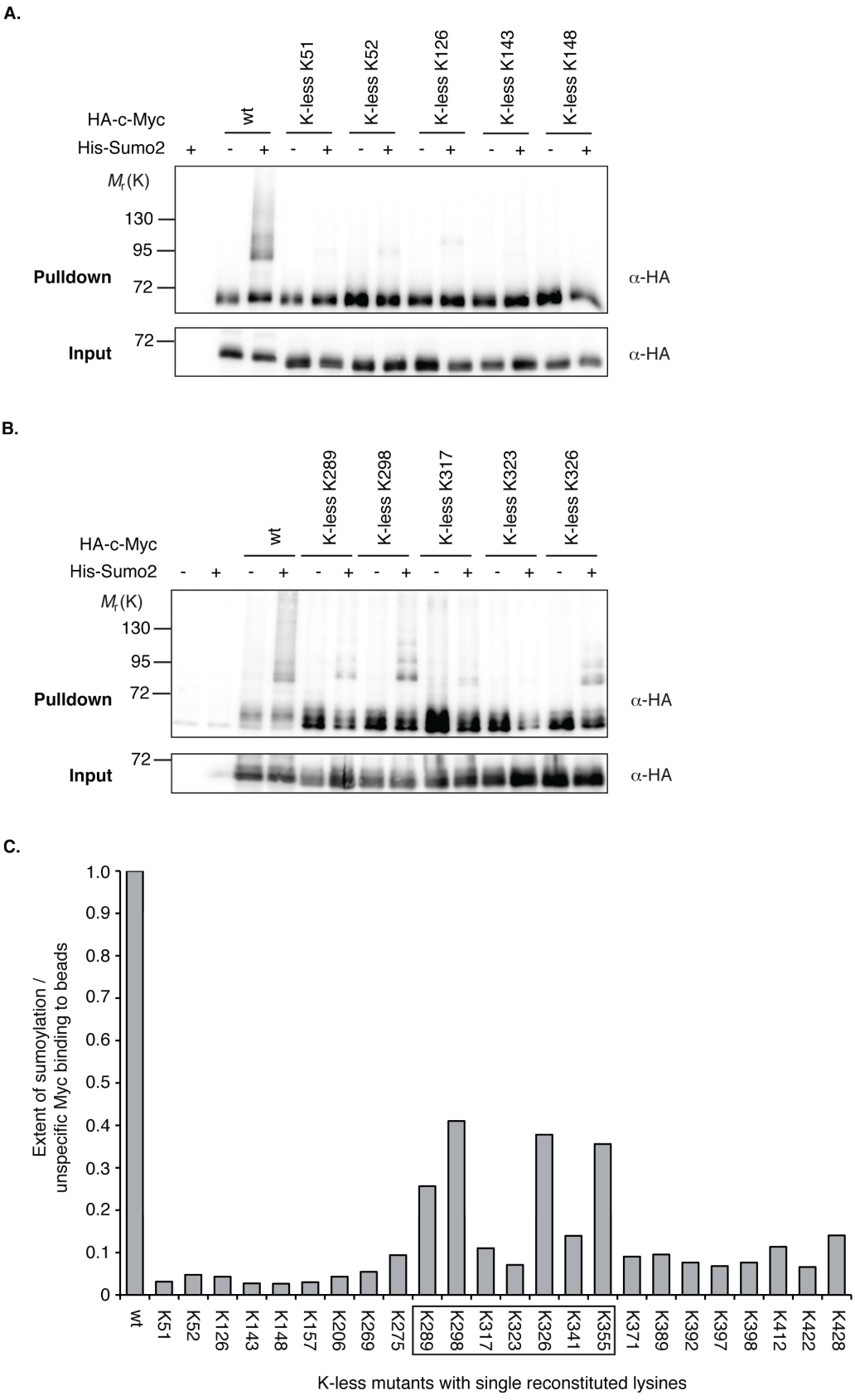
A.
HA-c-Myc
His-Sumo2
wt
K-less K51
K-less K52
K-less K126
K-less K143
K-less K148
M_r(K)
130
95
72
Pulldown
Input
α-HA
B.
HA-c-Myc
His-Sumo2
wt
K-less K289
K-less K298
K-less K317
K-less K323
K-less K326
M_r(K)
130
95
72
Pulldown
Input
α-HA
C.
Extent of sumoylation / unspecific Myc binding to beads
1.0
0.9
0.8
0.7
0.6
0.5
0.4
0.3
0.2
0.1
0
wt
K51
K52
K126
K143
K148
K157
K206
K269
K275
K289
K298
K317
K323
K326
K341
K355
K371
K389
K392
K397
K398
K412
K422
K428
K-less mutants with single reconstituted lysines

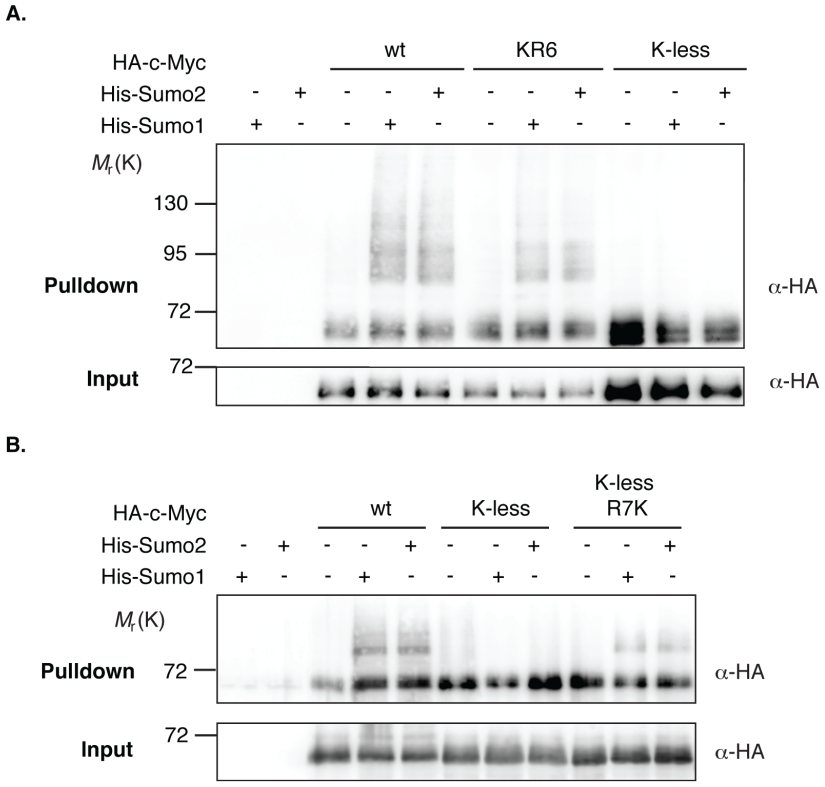

Figure 4.24.:
A cluster of lysines in the central region of c-Myc is an important target region for sumoylation

A. *In vivo* sumoylation assays were performed using a c-Myc mutant lacking six lysines from the sumoylation cluster (KR6 = K 289,298,323,326,341,355 R) and [B.] one that only contained lysines in the cluster region (K-less R7K = R 289,298,317,323,326,341,355 K).

N-Myc homologues and in orthologues from other species contains a core sequence of three hydrophobic amino acids (IDVV) which complies with the SIM consensus sequence V/I-X-V/I-V/I. This core is either followed by either a serine or a threonine and preceded by an acidic stretch of aspartic and glutamic acids (Fig. 4.26 A).

Sumo interacting motifs often provide an interaction platform for sumoylated target and effector proteins. As Myc is sumoylated at many different non-consensus sites, the internal

Figure 4.25. *(facing page)*:
Sumoylation of c-Myc is not upregulated upon treatment with various stress stimuli

A.-B. HeLa cells were treated with the indicated stress conditions before harvesting by scraping off cells from the dish and subjecting them to the usual His-Sumo pulldown procedure.

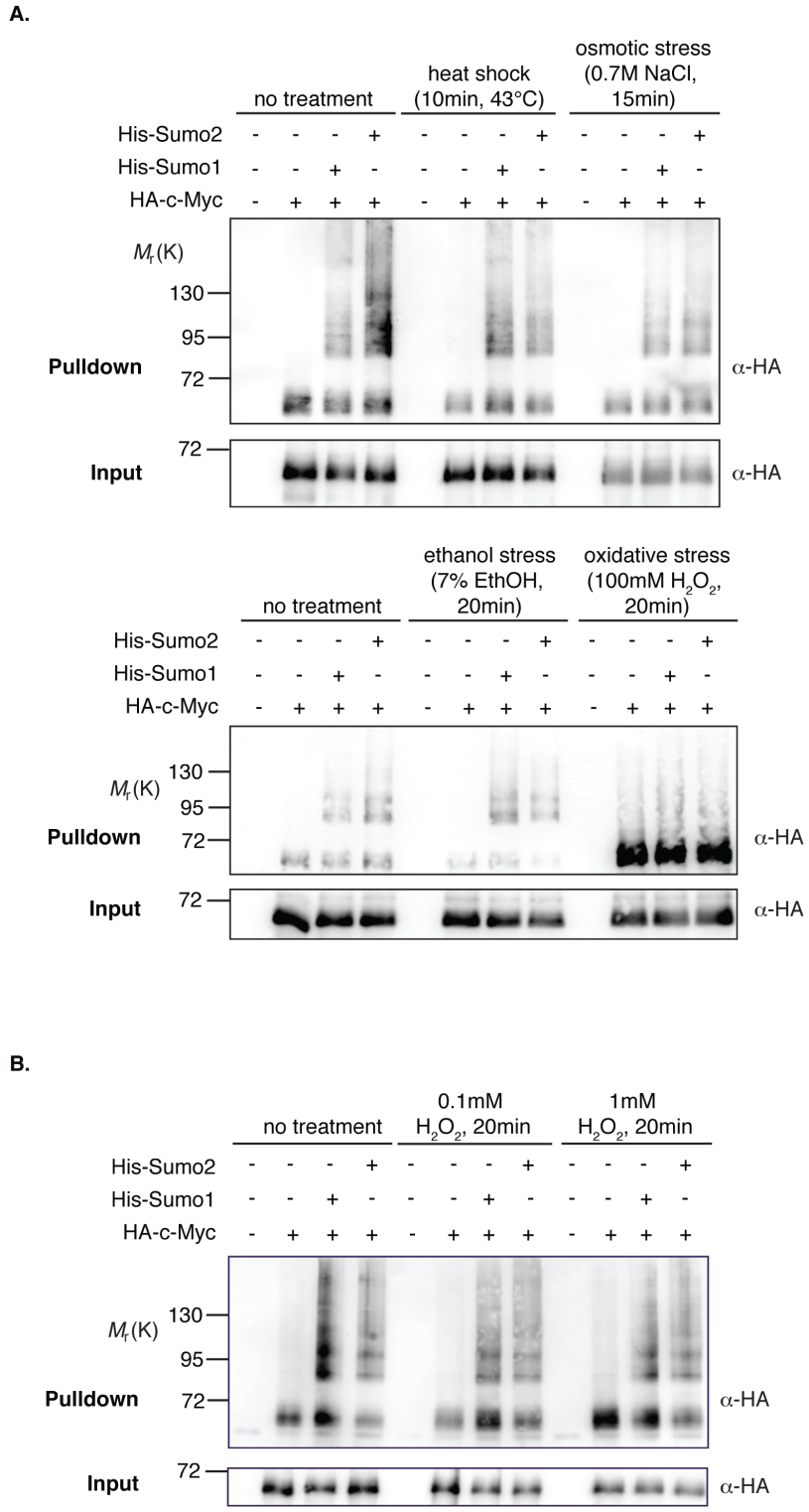
A.
no treatment
heat shock (10min, 43°C)
osmotic stress (0.7M NaCl, 15min)
His-Sumo2
His-Sumo1
HA-c-Myc
M_r(K)
130
95
72
Pulldown
α-HA
72
Input
α-HA
no treatment
ethanol stress (7% EthOH, 20min)
oxidative stress (100mM H_2O_2, 20min)
His-Sumo2
His-Sumo1
HA-c-Myc
M_r(K)
130
95
72
Pulldown
α-HA
72
Input
α-HA
B.
no treatment
0.1mM H_2O_2, 20min
1mM H_2O_2, 20min
His-Sumo2
His-Sumo1
HA-c-Myc
M_r(K)
130
95
72
Pulldown
α-HA
72
Input
α-HA

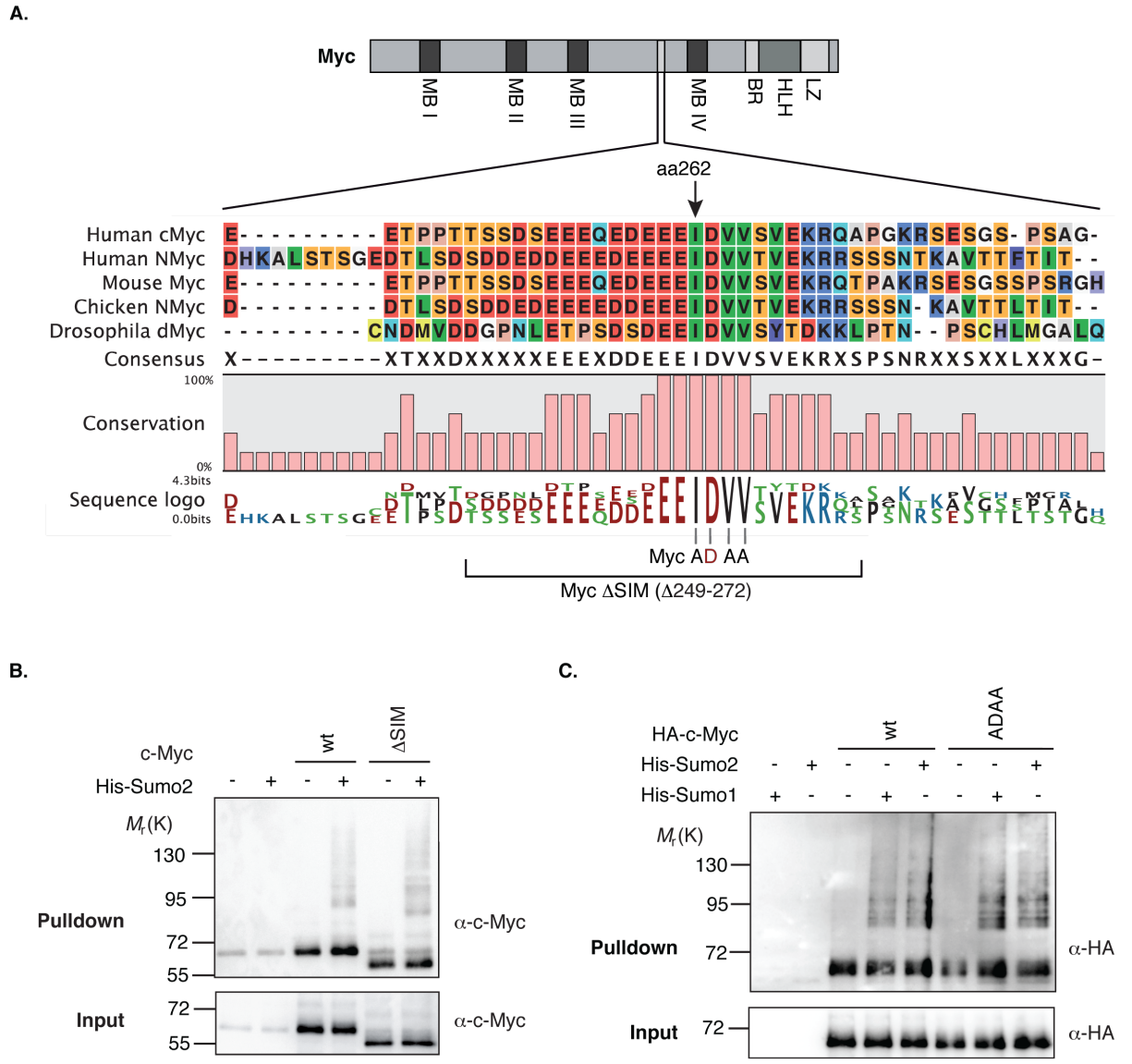

Figure 4.26.:
Myc contains a highly conserved sequence which could be a Sumo interacting motif but which is not needed for internal sumoylation of Myc

A. Sequence alignment between human Myc homologues and paralogues from different species reveals a highly conserved sequence which fulfills all criteria for a reverse Sumo interacting motif (graph created with CLC sequence viewer 6).

B.-C. *In vivo* sumoylation assays with a c-Myc ΔSIM deletion mutant lacking amino acids 249-272 and a Myc ADAA point mutant with the hydrophobic isoleucine and the two valines replaced by alanines.

SIM could recruit a Sumo-loaded Ubc9 to the protein to enable sumoylation of Myc. This has been shown for the ubiquitin ligase USP25 [Mohideen and Lima, 2008]. To test this,

I generated two mutants of c-Myc, a deletion mutant lacking the whole conserved SIM sequence area (Myc ΔSIM: Δ249-272) and a point mutant with the core hydrophobic amino acids replaced by alanines (Myc ADAA). *In vivo* sumoylation assays revealed that both mutants can be sumoylated to the same extent as wild type c-Myc (Fig. 4.26 B-C). Thus, sumoylation of Myc is independent of its possible SIM sequence.

4.3.9. Non-covalent Sumo binding to Myc *in vitro*

To verify if the Sumo interacting motif is a veritable domain for non-covalent binding of Myc to Sumo proteins, I performed *in vitro* binding assays. GST-tagged Sumo1, 2 and 3 isoforms were recombinantly expressed, then affinity purified with glutathione sepharose beads. N-Myc, c-Myc and its ADAA mutant and two control proteins RNF4 and Ubc9 were generated by *in vitro* translation. The recombinant Sumo proteins bound to sepharose beads were incubated with the *in vitro* translated proteins, the beads were washed and the precipitates analyzed by Western Blot.

The binding analysis shows a clear but weak binding of c-Myc and N-Myc to the Sumo1 isoform, but not to Sumo2 or 3. This is however independent of the conserved domain in Myc which was hypothesized to be a Sumo interacting motif (Fig. 4.26 B-C). RNF4 and Ubc9 which contain validated Sumo interacting motifs both bind preferably to Sumo2 and Sumo3 as expected and thus prove the assay to be functional (Fig. 4.26 D-E).

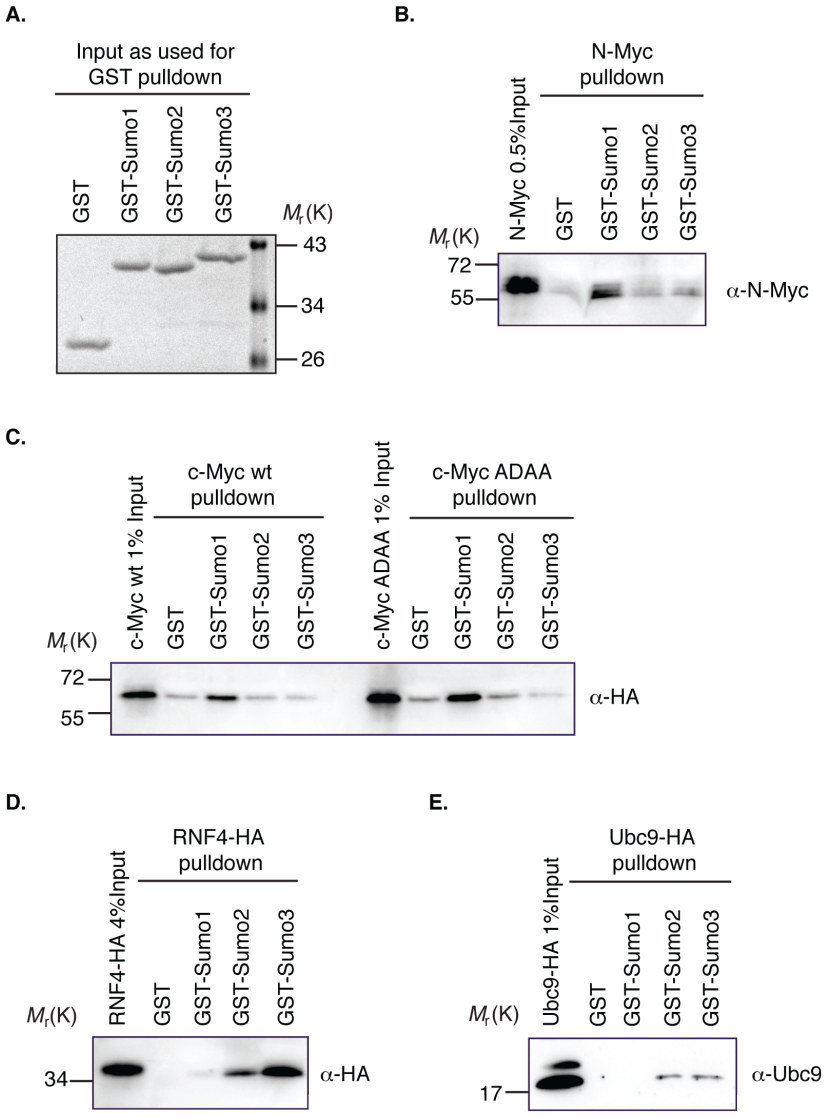

Figure 4.27.:

Non-covalent binding of c-Myc and N-Myc to Sumo in an in vitro binding assay

A. GST-tagged Sumo1, 2 and 3 was expressed recombinantly in bacteria and affinity purified using glutathione sepharose beads. Quantification by SDS-PAGE followed by coomassie staining verified equal amounts of the different Sumo isoforms used for the following binding assay, GST served as an internal control.

B.-E. Equal amounts of *in vitro* translated N-Myc, c-Myc wild type, c-Myc ADAA, HA-tagged RNF4 and Ubc9 were incubated with either GST alone or the different GST-Sumo isoforms bound to sepharose beads. The precipitates on the beads were washed gently and visualized via Western Blot, comparing it to a 1% input of each *in vitro* translated sample.

Chapter 5.

Discussion

5.1. Arf inhibits Miz1 function by inducing a repressive Myc/Miz1 complex

The first objective of this thesis was to study a possible interaction between the three proteins Arf, Myc and Miz1. The tumor suppressor p14Arf (p19Arf in mice) is encoded by the *INK4A/ARF* locus and shares exon 2 with p16(Ink4a) in an alternate reading frame, which gave Arf its name [Quelle et al., 1995]. While p16(Ink4a) inhibits cyclin D-dependent kinases and thus regulates the retinoblastoma (Rb) protein to block G1-S transition, Arf stabilizes p53 by inhibiting the ubiquitin ligase Mdm2 [Lin and Lowe, 2001]. Consequently, the two transcripts play a major role in protecting cells from oncogenic transformation, which is underlined by the fact that the *INK4A/ARF locus* is frequently deleted, mutated or epigenetically silenced in a wide array of human tumors [Lowe and Sherr, 2003]. Arf can be activated by oncogenic signals such as elevated Myc activity, which is counteracted by p53-dependent apoptosis [Zindy et al., 2003]. However, Arf has been shown also to possess tumor suppressive p53-independent functions. This becomes apparent in the higher tumor incidence of triple knockout mice lacking Arf, Mdm2 and p53 in comparison to double knockout animals merely lacking p53 and Mdm2 [Weber et al., 2000]. In reaction to oncogenic Myc for example, Arf does not only activate p53 but directly binds to Myc to inhibit its transactivation function on genes that activate hyperproliferation and transformation [Qi et al., 2004].

The Arf protein has an unusual amino acid composition with more than 20 % arginine residues making it highly basic. Arf is unstructured and highly unstable unless bound to other proteins, primarily to nucleophosmin (NPM) in the nucleolus [Sherr, 2006]. NPM acts as a molecular chaperone to form stable high-molecular mass complexes with Arf. Nucleophosmin itself is also affected in its function as a endoribonuclease by this interaction. It normally induces 28S rRNA maturation but this is inhibited by Arf which promotes ubiquitination and degradation of NPM [Itahana et al., 2003]. Additionally,

Arf stimulates sumoylation of NPM which again blocks its function in rRNA processing [Haindl et al., 2008; Kuo et al., 2008].

5.1.1. Miz1 interacts with Arf and relocalizes it from the nucleoli into the nucleoplasm

It has been established that Arf directly interacts with Myc in response to oncogenic stress, and it is also known that Myc binds to Miz1 to repress transcription. It does so for example by displacing an important coactivator of Miz1, nucleophosmin, which again is a major interactor of Arf in the nucleolus. It was thus investigated, whether Arf and Miz1 could interact as well and if they influence each others localization.

The immunofluorescence analysis clearly showed that overexpressed Miz1 recruits endogenous and exogenous Arf out of the nucleoli into the nucleoplasm (Fig. 4.1 on page 60). It has been described that Arf is highly unstable and rapidly degraded in the proteasome upon ubiquitination by the E3 ligase ULF, unless stabilized by nucleophosmin in the nucleoli [Chen et al., 2010]. Even though it is generally accepted that nucleolar localization may be a means of stabilizing and storing Arf, forms of Arf that do not accumulate in the nucleolus retain the capacity to stabilize MDM2 [Llanos et al., 2001]. Other publications even postulate that Arf primarily functions outside the nucleolus, and that sequestering by NPM holds it inactive. This is supported by the fact that NPM and Mdm2 both bind to the same N-terminal domain of Arf, probably in a competitive manner [Korgaonkar et al., 2005]. Thus, it can be assumed that the recruitment of Arf out of the nucleoli by Miz1 does not lead to degradation of Arf, as implicated by its strong nucleoplasmic detection of both the endogenous and exogenous protein in the immunofluorescence.

While Arf is recruited out of the nucleoli into the nucleoplasm, the normally homogenous distribution of Miz1 is also altered upon overexpression of Miz1 and Arf. In about 80 % of transfected cells, Miz1 is sequestered into subnuclear, foci-like structures. These partially overlap with the Arf distribution indicated by a Pearson's coefficient of about 0.5. Miz1 has already been shown to be sequestered upon overexpression of Myc [Peukert et al., 1997], but the resulting structures appear as larger pools of aggregated protein and do not resemble the Arf-induced structures in direct comparison (not shown). I furthermore tested if the Arf-induced Miz1 foci represent paraspeckles, several components of which can bind to the Miz1-interacting protein TopBP1 [Kuhnert et al., 2012], or if they were PML

bodies which show a similar phenotype to the Miz1 foci. Immunofluorescence analysis upon overexpression of GFP-tagged proteins, PSF or P54nrb as protein components of the paraspeckles or SP100 as part of the PML bodies, did not reveal a substantial colocalisation of any of these in the Arf-induced Miz1 structures (data not shown).

Immunoprecipitation assays described in detail in Herkert et al. [2010] confirmed an interaction between Miz1 and both human and mouse Arf. This interaction is independent of nucleophosmin, which could act as a bridging protein between Miz1 and Arf, as the reciprocal binding was also detected in $NPM^{-/-}/p53^{-/-}$ MEFs. Quite the contrary, reconstitution of NPM in these cells antagonized binding between Arf and Miz1, which I further analyzed in Figure 4.4 on page 63. It should be noted, that Miz1 attachment to Arf could be mediated by Myc, which is known to bind to Arf and Miz1 and according to recent reports also to nucleophosmin [Li et al., 2008]. Indeed Myc plays an important role in mediating the Arf effects on Miz1 as will be discussed below (see 5.1.5).

5.1.2. Arf reduces the solubility of Miz1 and inhibits its transactivation function, which is counteracted by nucleophosmin

Arf expression markedly reduced the solubility of Miz1 (Fig. 4.3 on page 62). Such a reduced extractability often goes along with formation of repressive histone modifications such as trimethylated histone H3K9 [Kouzarides, 2007]. Chromatin immunoprecipitation experiments indeed showed a strongly increased signal for $H3K9^{triMe}$ around the Miz1 binding site of the *P15INK4B* promoter upon Arf expression without affecting the Miz1 binding itself [Herkert et al., 2010].

To test wether Arf affects Miz1 function as a transcription factor, I performed luciferase reporter assays using a *P15INK4B* promoter plasmid (Fig. 4.5 on page 64). Arf clearly inhibited the Miz1-dependent transactivation, I obtained the same result using a *P21CIP1* construct (data not shown). Nucleophosmin has been shown to act in the opposite direction, it is an essential coactivator of Miz [Wanzel et al., 2008]. As NPM and Arf bind to Miz1 in a competitive manner, it was not surprising to find that overexpression of NPM abrogated formation of subnuclear Miz1 foci upon Arf expression. Likewise the reduced extractability could also not be observed when NPM was expressed.

Expression of Arf also repressed Miz1 function *in vivo*. We expressed combinations of Miz1 and p19Arf in $Arf^{-/-}$, $p53^{-/-}$, $Mdm2^{-/-}$ MEFs by retroviral infection. Flow cytometric

analysis revealed that expression of Miz1 led to a G1 arrest, triggered by elevated amounts of the cell cycle inhibitor p21Cip1, a direct Miz1 target [Wanzel et al., 2008]. Coexpression of p19Arf abolished the G1 arrest and led to a transcription-independent S phase arrest via Miz1 [Herold et al., 2002].

In sum, Arf represses Miz1 transactivation function which is accompanied by reduced solubility of Miz1 and which may be accounted for by formation of heterochromatin on its target promoters. The biological relevance of this repressive mechanism could be verified *in vivo* by expressing Miz1 and Arf in $p53^{-/-}/Mdm2^{-/-}/Arf^{-/-}$ MEFs. Arf notably diminished the Miz1-induced G1 arrest which normally follows upregulated p21 levels upon overexpression of Miz1.

5.1.3. Arf induces anoikis via Miz1 target genes

A genome-wide gene expression study in U2OS cells showed a strong increase in the number of repressed genes upon Miz1 and Arf overexpression [Herkert et al., 2010]. These repressed genes comprise a subgroup of factors involved in cell adhesion, such as several different integrins, which mediate contact between cells and the surrounding extracellular matrix [Hynes, 2002]. Interestingly, many of these cell adhesion genes presented a $H3K9^{triMe}$ signature close to the Miz1 binding sites on their promoters. As many epithelial cells are dependent upon proper contact to the extracellular matrix, repression of this set of genes leads to loss of cell adhesion and subsequently to a type of apoptosis called anoikis [Reginato et al., 2003]. Indeed, retroviral overexpression of Miz1 and Arf in U2OS cells which were additionally stressed by the selection process with two different antibiotics died shortly after selection. To verify that detachment of cells is the cause and not the result of apoptosis, we expressed the anti-apoptotic protein Bcl2 in these cells, which reduced apoptosis measured by PI-FACS but did not impair the loss of cell adhesion [Herkert, 2010].

5.1.4. Arf induces sumoylation of Miz1 independently of other Arf-induced Miz1 phenotypes

It was proposed that one of the p53-independent functions of Arf is its ability to induce sumoylation of proteins to which it binds, such as Mdm2 [Xirodimas et al., 2002], p53 [Chen and Chen, 2003], Werners helicase [Woods et al., 2004] and notably also nucleophosmin [Xirodimas and Lane, 2008]. The effects of sumoylation on Mdm2 and

p53 are largely unknown, the Werners helicase is relocalized from the nucleolus to the nucleoplasm upon sumoylation by Arf. Nucleophosmin is inhibited by sumoylation in its function in rRNA processing, the detailed mechanism of this inhibition will be discussed in 5.2.2. Sumoylation of transcription factors in most cases leads to transcriptional repression, often through establishment of heterochromatic DNA complexes such as of a H3K9$^{\mathrm{triMe}}$ and H4K20$^{\mathrm{triMe}}$ signature around binding sites of sumoylated Sp3. I thus examined if Arf also induces sumoylation of Miz1.

I used His-Sumo pulldowns to extract all sumoylated proteins and subsequently detect a protein of interest out of this pool with a specific antibody. The analysis revealed that Miz1 is sumoylated by Sumo2, which is substantially increased by expression of Arf (Fig. 4.6 on page 65). Details about the nature of the sumoylation of Miz1 will be discussed in 5.2. The sumoylation-promoting effect of Arf is specific, as it does not induce sumoylation of Myc (data not shown).

Further immunofluorescence experiments showed that exogenous Miz1 colocalized with Sumo2 in the Arf-induced Miz1 foci to an exceptional degree, with a Pearsons's correlation coefficient of about 0.9 (Fig. 4.6 on page 65). To validate if sumoylation is the cause and not the result of foci formation, I depleted the Sumo E2 ligase Ubc9 via siRNA, which effectively disrupts the sumoylation machinery [Lin et al., 2003]. The immunofluorescence analysis showed that depletion of Ubc9 completely abrogated detection of any Sumo signal, which might be due to its relative instability when not attached to a target protein. However, the relocalization of Miz1 into subnuclear foci by Arf was unchanged. Additionally, depletion of Ubc9 did not affect sequestration of Miz1 into insoluble complexes [Herkert, 2010].

A complete Ubc9 knockout in mice is embryonic lethal, but animals with just one allele are unaffected [Nacerddine et al., 2005]. Indeed, cells only need 20 % of physiological Ubc9 levels to survive [Melchior, 2010a]. Thus an inefficient knockdown of Ubc9 in the aforementioned experiments could prevent detection of the role of sumoylation in Miz1 sequestration into insoluble nuclear foci. This however seems unlikely regarding the major effect of an Ubc9 knockdown on sumoylation of Miz1 in the His-Sumo pulldowns as seen in Figure 4.10 on page 71.

5.1.5. The effects of Arf on Miz1 require formation of a trimeric complex with Myc

There are various reports describing a connection between Myc and Arf as well as Myc and Miz1, which will be shortly reviewed below. Myc mediates repression of Miz1 just like Arf does, thus it is possible that these three proteins act together in one complex which was tested through direct experimentation.

Oncogenic stress such as elevated Myc activity induces expression and enhanced stability of Arf. Precisely, Myc activates Arf transcription via FoxO [Bouchard et al., 2007] and inhibits the ubiquitin E3 ligase Ulf which mediates degradation of Arf [Chen et al., 2010]. Arf in turn represses Myc transactivation on genes that activate hyperproliferation and transformation by directly binding to it, while it does not affect Myc-mediated repression [Qi et al., 2004; Datta et al., 2004]. Furthermmore, Myc competes with NPM for binding to Miz1 just like Arf (see also 5.1.1), and this effectively blocks transactivation by Miz1 [Wanzel et al., 2008]. Miz1 is a main mediator of Myc-induced repression, and overexpression of both proteins leads to subnuclear sequestration and reduced solubility of Miz1 [Peukert et al., 1997], similarly to what was observed in this work.

Based on this knowledge, I examined if Arf induces formation of a repressive Arf/Myc/Miz1 complex. N-terminal mutants of Arf revealed that it interacts with Myc and Miz1 through different domains. Myc interacts with the highly conserved N-terminal part of the Arf protein (as shown before by Datta et al. [2004]), which is the same domain that also binds to NPM [Bertwistle et al., 2004] and Mdm2 [Zhang et al., 1998]. In contrast, Miz1 can still interact with an N-terminal deletion mutant of Arf (Fig. 4.7 on page 66). Even though the interaction with Miz1 is not impaired, this Arf mutant is no longer able to repress transactivation, induce sequestration into insoluble complexes or promote sumoylation of Miz1. All these effects obviously require the presence of the N-terminal domain of Arf.

To check if Myc colocalizes in the Arf-induced Miz1 foci, I performed an immunofluorescence analysis with overexpression of Miz1, Arf and c-Myc. Myc also recruits Arf out of the nucleoli into the nucleoplasm as has been observed before [Datta et al., 2004] but which is still under debate in the literature [Amente et al., 2006]. Upon overexpression of Miz1, Myc evidently colocalizes in the subnuclear structures induced by Arf, with a Pearson's correlation coefficient of about 0.85. This is highly dependent on the interaction

of Myc with Miz1. A mutant of Myc that cannot bind to Miz1 (c-Myc V394D) does not colocalize in a comparable manner with a Pearson's correlation coefficient of only 0.36. In sum, Arf induces a highly significant colocalization of Miz1 with Myc in subnuclear foci, Arf itself is part of these foci but to a slightly lesser extent (Pearson's correlation coefficient of about 0.52, Fig. 4.1 on page 60). This could lead to the assumption that the primary role of Arf is to induce the Myc/Miz1 repressive complex.

To further substantiate the notion that complex formation between Miz1 and Myc is necessary for the effects of Arf on Miz1, we analyzed several mutants of Miz1 that are impaired in Myc binding. These mutants of Miz1 were largely refractory to sequestration into insoluble subnuclear complexes, failed to be repressed in reporter assays and could also not be sumoylated in response to Arf expression. This is underlined by the fact that only the Miz1 Δ33 mutant, which showed residual Myc binding activity, reacted to some extent like wild type Miz1.

The importance of Myc in these mechanisms was furthermore supported by the observation, that not only coexpression of Miz1 and Arf but also of c-Myc and Arf induced the anoikis phenotype described in 5.1.3 on page 102. This is dependent on the interaction with Miz1, as c-Myc V394D does not have the same phenotype [Herkert et al., 2010].

5.1.6. Relevance and interpretation of Myc as part of an Arf-induced repressive complex on Miz1

Myc has been shown before to repress cell adhesion via Miz1, namely in hematopoietic and epithelial cells [Frye et al., 2003; Gebhardt et al., 2006; Wilson et al., 2004]. This mechanism is vital for example for keratinocyte stem cells to exit from their niche and differentiate. Decrease in keratinocyte adhesion is dependent on formation of the Myc/Miz1 complex, as Myc V394D fails to do so.

Additionally, the repressive Myc/Miz1 complex is already known to participate in induction of apoptosis. Transcriptional repression of the anti-apoptotic Bcl2 and the cell cycle inhibitor p21Cip1, which are normally induced by Miz1, is an essential step towards Myc-induced apoptosis [Patel and McMahon, 2006; Seoane et al., 2002].

Miz1 and Arf can both inhibit cell cycle progression. Miz1 does so by activating transcription of p15ink4b, p21Cip1 and p57Kip2 [Seoane et al., 2001, 2002; Adhikary et al., 2003],

Arf can induce stabilization of p53 which also activates p21Cip1 [El-Deiry et al., 1993]. Still, the two interaction partners do not cooperate in inducing cell cycle arrest but rather collectively inhibit cell adhesion which leads to apoptosis. Myc is the critical factor that mediates this outcome.

The discovered mechanism may provide one answer to the question why oncogenic stress induced by Ras or c-Myc has such different outcomes. Despite the fact that both oncogenes activate the Arf/p53 signaling pathway, Ras induces senescence and c-Myc apoptosis. Even though Arf inhibits Myc transactivation in a negative feedback loop, Myc's repressive function remains unaffected so that a Myc/Miz1 complex can repress cell adhesion genes and induce apoptosis.

5.1.7. Summary and model

Arf induces formation of a repressive Myc/Miz1 complex in characteristic subnuclear structures, which exhibit a decreased solubility. In an independent next step, Arf induces sumoylation of Miz1, which might be the cause for the observed heterochromatinisation on the promoters around Miz1 binding sites. Participation of Myc is necessary and decisive in all these steps. Effectively, a set of Miz1 target genes involved in cell adhesion is repressed which finally leads to cell death via anoikis.

In a cellular context, these findings propose the following model (Fig. 5.1): In unstressed cells, Arf is retained in the nucleolus by the abundant nucleophosmin, the latter can also shuttle to the cytoplasm to act as a coactivator of Miz1. Oncogenic levels of Myc induce relocalization of Arf into the nucleoplasm, where Arf and Myc outcompete NPM for binding to Miz1 and induce a repressive Arf/Myc/Miz1 complex. Additionally, Arf induces sumoylation of Miz1 which could lead to the recruitment of corepressors such as histone methyltransferases which induce formation of heterochromatin on the promoters of cell adhesion genes. The resulting loss of contact to the extracellular matrix finally leads to anoikis.

In this model the formation of an Arf/Myc/Miz1 complex can be assigned with a tumor suppressor function, as it leads to death of cells with increased Myc activity. But what happens when apoptosis as the final outcome of the loss of cell adhesion is impaired?

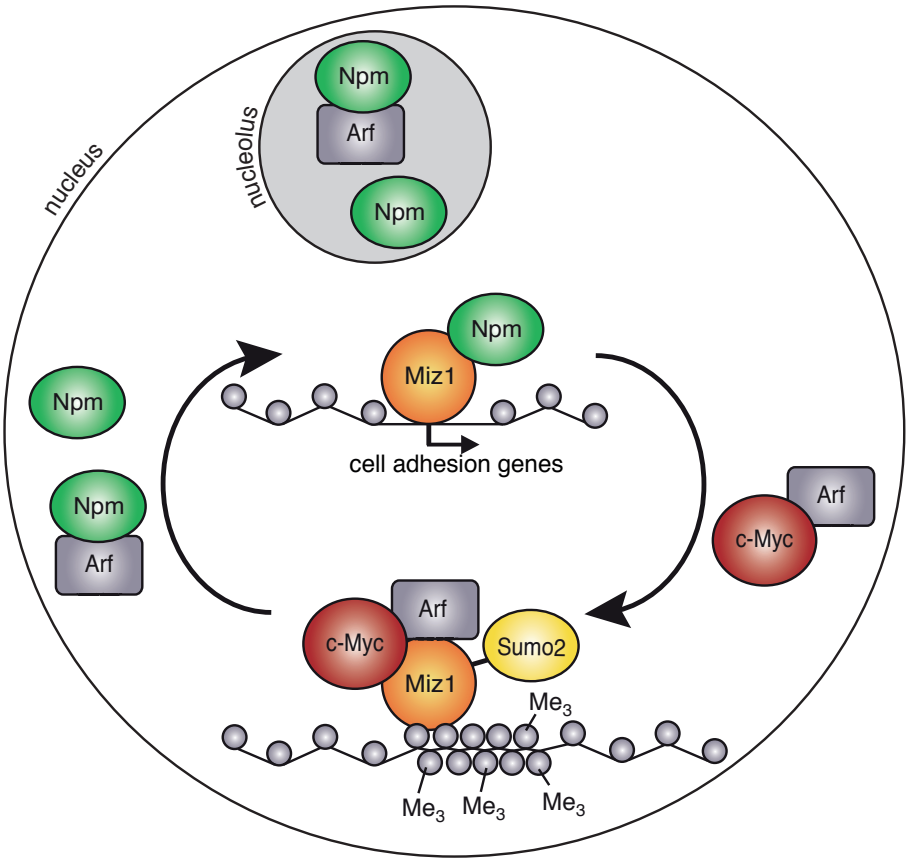

Figure 5.1.:
Model of Arf-mediated repression via a Myc/Miz1 complex
See text for explanation. Me_3 = $H3K9^{triMe}$

There are several reports in the literature describing that breakdown of anoikis contributes prominently to the malignancy of mammary and colon cancers [Yawata et al., 1998; Streuli and Gilmore, 1999; Shanmugathasan and Jothy, 2000]. The exact mechanism how cell death via anoikis is executed proves to be quite complex [Frisch and Screaton, 2001]. Integrin signaling molecules such as the focal adhesion kinase (FAK) or the integrin-linked kinase (ILK) activate the PI3K survival pathway directly by activating Akt but also through indirect mechanisms [Giancotti and Ruoslahti, 1999; Dedhar, 2000]. Inadequate expression of integrins abrogates this pro-survival signaling. Another mechanism depends on apoptosis regulators that serve as sensors for cytoskeletal integrity which is closely linked to cell adhesion. Bim for example is normally sequestered by microtubule-associated dynein light chain 1 (DLC1), when released (for example after taxol treatment). Bim interacts with Bcl2 to inhibit it, which stimulates release of cytochrome C from the mitochondria [Puthalakath et al., 1999; Strasser et al., 2000]. Bmf is sequestered by

actin/myosin-associated dynein light chain-2 (DLC-2), and transferring cells from the attached state into suspension allows for Bmf to complex and neutralize Bcl2 [Puthalakath et al., 2001]. Both activation of Bim [Egle et al., 2004] as well as repression of Bcl2 [Eischen et al., 2001a] have also been reported to be fundamental steps on the way to Myc-induced apoptosis.

If cell death upon loss of cell adhesion is impaired by failure of one of the mechanisms described above, formation of the Arf/Myc/Miz1 complex could indeed support tumorigenesis instead of inhibiting it. Cells would detach but stay alive, which may promote invasiveness and metastasis. Anoikis resistance has been documented to enable cells to survive after detachment from their primary site while travelling through the lymphatic and circulatory systems, thereby significantly increasing their malignant potential [Simpson et al., 2008; Voulgari and Pintzas, 2009]. Myc has already been shown to play an important role in regulating invasiveness and metastasis, for example by promoting epithelial-mesenchymal transition [Wolfer and Ramaswamy, 2011]. One source reveals that transcriptional repression of integrin α1 by N-Myc promotes invasiveness of human neuroblastoma cells [Tanaka and Fukuzawa, 2008]. Another recent report describes that Myc cooperates with Skp2 to recruit Miz1 and p300 into a transcriptional complex that activates RhoA, which is necessary for migration, invasion, and lung metastasis *in vivo* [Chan et al., 2010]. This was substantiated by the analysis of human prostate carcinomas, which showed a significant correlation between expression of RhoA, Myc, Skp2 and Miz1 and metastasis.

All in all, formation of a repressive Arf/Myc/Miz1 complex may be the tumorsuppressive response to elevated Myc levels, but could lead to promotion of metastasis if the apoptotic outcome is impaired.

5.2. Miz1 can be sumoylated at a specific lysine which is induced by Arf

In the course of the experiments leading to the identification of a repressive Arf/Myc/Miz1 complex we also discovered that Arf can induce sumoylation of Miz1 by Sumo2. To learn more about this so far unknown modification of Miz1, I analyzed which Sumo isoforms bind to Miz1 at which site and tried to elucidate the exact function of this modification.

5.2.1. Arf induces sumoylation of Miz1 at lysine 251

I used *in vivo* sumoylation assays to pull down sumoylated proteins from a cell lysate and subsequently compare the protein input with the sumoylated fraction. Concomitant expression of Miz1, Arf and Sumo1 or Sumo2 showed several higher migrating bands in the Western Blot analysis of Miz1 protein. These ranged from a shift in size of about 30 kDa to the most prominent band moving up about 50 kDa to a weaker band with a 70 kDa shift (Fig. 4.10 on page 71). The theoretical molecular weight of the Sumo proteins is 11 kDa, however the size increase for each Sumo added is typically in the range of 15-17 kDa [Hilgarth and Sarge, 2005]. In all experiments Sumo1 which cannot form chains sumoylated Miz1 with the same modification pattern as Sumo2. Thus, chain formation cannot explain the unexpectedly big size shifts. Furthermore, depletion of Ubc9, the only E2 ligase in the sumoylation process, completely abrogated all higher migrating bands (Fig. 4.10 on page 71), which proves that these are not simply generated by independent other kinds of modifications such as ubiquitination or acetylation. It is however possible, that sumoylation attracts and is necessary for subsequent modifications of the Miz1 protein in form of other posttranslational modifications. Still, sumoylation alone could induce this uncommonly big shift, which has been observed similarly for several other proteins [Melchior, 2010b].

Finding sumoylation sites in target proteins is relatively straightforward. Most proteins are sumoylated within the defined tetrapeptide Sumo consensus motif Ψ-K-X-E/D. The Miz1 amino acid sequence contains four lysines surrounded by this motif (Fig. 4.11 on page 72). A fifth one was predicted to possibly be sumoylated using an algorithm which considers all known sumoylation sites. Point mutants that contained a charge-conserving arginine instead of the lysine revealed that Miz1 can get sumoylated at lysine 251. Technically, replacement of this lysine did not completely abrogate all higher migrating bands, but the K251R mutant exhibited a significant downregulation in the shifted Miz1

species. I examined two more possible non-consensus lysines for sumoylation which however did not deliver further insight (data not shown).

The sumoylation site at lysine 251 is additionally surrounded by a stretch of acidic residues, which enhances the efficiency of sumoylation by Ubc9. This kind of acidic cluster is also used to correctly predict novel targets for Sumo modification [Yang et al., 2006]. Point mutations of the valine or glutamic acid at the first and last position of the sumoylation consensus motif around lysine 251 recapitulated the phenotype of the K251R mutant (Fig. 4.12 on page 73). The importance of not only the intact lysine but the motif as a whole once more proves that the higher migrating bands represent sumoylated Miz1 species.

5.2.2. Arf promotes sumoylation of Miz1 by inhibiting Senp3

Several mechanisms were proposed to explain how Arf can induce sumoylation of proteins to which it binds. Rizos et al. [2005] claimed that Arf interacts with the Sumo E2 enzyme Ubc9 to allow direct discharge of Sumo to another Arf binding partner. In the case of nucleophosmin however, another mode of action could be discovered. Arf does not directly induce sumoylation but it inhibits desumoylation of NPM by the Sumo-specific protease Senp3. Mechanistically, Arf promotes phosphorylation of Senp3 which is subsequently ubiquitinated and degraded in the proteasome. The desumoylation of NPM is crucial for its role in rRNA processing and depletion of Senp3 phenocopies the processing defect observed upon depletion of NPM [Haindl et al., 2008; Kuo et al., 2008].

In vivo sumoylation assays revealed that overexpression of Senp3 represses sumoylation of Miz1 while the dominant negative catalytically inactive Senp C352S mutant further induced its sumoylation (Fig. 4.13 on page 74). This leads to the conclusion that Arf induces Sumo modification of Miz1 by the same mechanism as it does for NPM. However, enforced expression of Senp3 could lead to unspecific substrate recognition. RNAi-mediated depletion of Senp3 would verify this proposed mode of action, but successful depletion of Senp3 with shRNA also lead to rapid cell death which made further analysis impossible (data not shown).

5.2.3. Endogenous sumoylation of Miz1 cannot be detected easily

To verify a biological relevance of the Sumo modification of Miz1, I tried to show endogenous sumoylation. However, pulldown of endogenous Miz1 or low levels of infected

Miz1 upon overexpression of His-Sumo constructs did not show the characteristic size shift as seen for the transfected Miz1 protein. Ubc9 or the catalytically inactive Senp3 mutant were expressed to enforce detection of visible sumoylation, this was also performed in different cell lines, without success (data not shown).

The group of Frauke Melchior (ZMBH Heidelberg) performed endogenous large scale IPs with Sumo1 and Sumo2 in HeLa cells followed by mass spectrometry analysis, in unstressed as well as H_2O_2-treated cells. No peptides of Miz1 were found in this analysis [Werner, 2011]. This might be due to a very transient Sumo modification of only a small pool of endogenous Miz1, which is characteristic for the sumoylation of many proteins [Johnson, 2004; Hay, 2005], or because a stimulus triggering *in vivo* sumoylation was missing.

There are several reports about stress factors that increase the overall sumoylation of cellular proteins, such as heat shock, osmotic stress, ethanol stress and high levels of oxidative stress [Saitoh and Hinchey, 2000; Bossis and Melchior, 2006]. Successful identification of a sumoylation inducing-agent for Miz1 could help to detect endogenous sumoylation. Unfortunately, none of the treatments showed any effect on sumoylation of exogenous protein (Fig. 4.14 on page 75).

All in all, an endogenous sumoylation could not be verified. It was thus focused on comparing Miz1 wild type with the Miz1 K251R mutant to possibly expose phenotypic differences between the two.

5.2.4. The non-sumoylatable Miz1 cannot be phenotypically distinguished from Miz1 wild type in cell growth or DNA damage response

I used U2OS cells lentivirally infected with Miz1 and Arf constructs to assess cell growth behavior. Colony assays and growth curve did not display any difference in growth behavior upon expression of Miz1 wild type and the K251R mutant. Both slowed down cell growth, which can be assigned to the expression of cell cycle inhibitors upon Miz1 infection [Staller et al., 2001]. Arf alone also lead to growth retardation with an additive effect of Miz1+Arf expression. Cells did not go into anoikis at this point as seen before upon retroviral infection and selection. The selection stress with two different antibiotics might be needed for the cells to activate the anoikis program, probably because this leads

to elevated Myc levels.

Miz1 plays an active role in DNA damage control by inducing transcription of p21 and thus cell cycle arrest in response to UV stress. It also releases TopBP1 from the chromatin which induces Atr to activate DNA damage response proteins such as Chk1 and p53. Enforced expression of Miz1 by infection in LS174T cells has been shown to enhance and prolong this response [Herold et al., 2008]. As this is one of the best characterized functions of Miz1, it was assessed if Miz1 wild type and the K251R mutant behave differently in this context. However, also in this assay these two proteins could not be distinguished. They both induced an Atr-dependent response visualized as phosphorylation of Chk1 as well as a G1 and S phase arrest in the FACS analysis following UV treatment. The increased subG1 content at later time points for both expression of Miz1 wild type and the non-sumoylatable mutant could be ascribed to additional stress by the very high Miz1 infection levels which were achieved by lentiviral infection in comparison to the retroviral infection in Herold et al. [2008].

5.2.5. Microarray analysis did not reveal different gene expression patterns between Miz1 wild type and the non-sumoylatable mutant

I was unable to show that the known functions of Miz1 in growth arrest and UV response are affected by sumoylation. For a more global approach, I assessed if expression of Miz1 wild type and the K251R mutant induce differential gene expression patterns. The analysis revealed that Arf broadens the spectrum of both Miz1 wild type and K251R to modify genes (Fig. 4.17 on page 80) as has already been observed in [Herkert et al., 2010]. Direct comparison of genes that are either up- or downregulated at least twofold in the Miz1 wild type or K251R conditions, with and without Arf, showed that there always is a highly significant overlap between the two Miz1 conditions. This overlap is even increased if the threshold for regulation is raised to a threefold or fourfold regulation (not shown). This and visualization of the differential regulated genes in a dot plot (not shown) lead to the conclusion, that almost none of the genes that seem to be regulated exclusively by Miz1 wild type or the K251R mutant showed a pronouncedly different regulation. In fact, virtually all these genes clustered around one or the other side of the the chosen cutoff value.

GO term analysis did not point to a particular group of genes which are differentially regulated between the Miz1 wild type and the K251R mutant condition, with or without Arf expression. I could reproduce that genes involved in cell adhesion are regulated by

Miz1+Arf, but also by Miz1 alone and the K251R mutant and K251R+Arf. I however could not find the exact same genes used for validation of the microarray in Herkert et al. [2010] among the regulated targets in this array. Lentiviral infection used for the assays in this work does not immediately induce anoikis, as retroviral infection with subsequent selection did in the previous experiments. This difference could reflect the different targets out of the group of cell adhesion genes that were regulated in this analysis and the previous microarray.

To still be able to identify a difference between Miz1 wild type and the K251R mutant, I picked out four groups of genes that displayed specific patterns of gene regulation. Among these, the group which displayed a downregulation of gene expression only in the Miz1+Arf condition comprised the most members. These genes could possibly experience a downregulation upon overexpression of Arf because of subsequent sumoylation of Miz1, probably via induction of heterochromatinisation as suggested in 5.1.2. To validate the results of the microarray for these genes, I conducted qRT PCR experiments. Even though the downregulation in the Miz1+Arf condition could be reproduced in all but one case, the obtained values did not fit the overall pattern with Miz1+Arf being the exception of downregulation among the other conditions. In contrast to that, randomly picked genes with strong up- or downregulation in any condition could be validated effortlessly (not shown).

It should be noted that for validation of the genes out of the "only Miz1+Arf down" group, I picked out the genes with the most differential regulation for examination by qRT PCR. A closer look on these genes revealed that all of their expression patterns were detected with several probes, either for the exact same nucleic acid sequence or another sequence in the same transcript. Interestingly, almost all of these probes showed an inconsistent regulation for the same gene. Lukas Rycak evaluated this throughout the whole array: about 14 % of genes exhibited a different regulation among probes (threshold=1 for the maximal difference of M-values among the same gene) [Rycak, 2012]. It is thus possible that the microarray analysis fails to be reproducible via qRT PCR because a group of genes that follows the 'only Miz1+Arf down" pattern does not really exist. Picking out genes that follow this pattern may select for genes with dissimilar probe results.

In sum, no genes were found that are regulated in a profoundly different way comparing Miz1 wild type and the non-sumoylatable mutant, either with or without Arf. This might be due to the fact that Miz1 is simply not sumoylated upon mere overexpression of low

levels of Miz1 and Arf, as sumoylation could also not be visualized under these conditions. Probably an additional trigger for attachment of Sumo to Miz1 is needed, or sumoylation occurs only in a certain phase of the cell cycle as has been observed for example for BRCA1 [Vialter et al., 2011]. Expression of Miz1 K251R together with Arf did not relieve repression of cell adhesion genes, which presumably means that sumoylation is not necessary for heterochromatinisation upon formation of the Arf/Myc/Miz1 complex after all. However, as a different set of cell adhesion genes was regulated comparing this microarray and the one from Herkert et al. [2010], it might be that the gene expression profiles differ for example in a temporal way and thus cannot really be compared.

Another explanation could involve varying levels of Myc. Activation of Arf reportedly only occurs in response to an oncogenic trigger such as substantially elevated levels of Myc, and high levels of Myc might be needed for the trimeric Arf/Myc/Miz1 complex to unfold its full potential. Lentiviral infections in U2OS cells did not trigger anoikis compared to the retroviral infection used for the microarray in Herkert et al. [2010], even though expression of Miz1 and Arf was even higher with the lentiviral infection method. It is conceivable that selection stress upon retroviral infection upregulates Myc in U2OS cells which is needed for proper function of the Arf/Myc/Miz1 complex. Future experiments should verify this by inducing oncogenic levels of both Arf and also Myc in an appropriate cell line relevant for the anoikis phenotype such as primary epithelial cells.

5.3. Myc gets sumoylated at many different sites

We discovered that Arf induces a Myc/Miz1 repressive complex and at the same time promotes sumoylation of Miz1. In order to complete the picture, I also tested if Myc could be sumoylated as well.

5.3.1. C-Myc and N-Myc get sumoylated by both Sumo isoforms

I performed *in vivo* sumoylation assays with exogenous protein followed by Western Blot analysis. Both c-Myc as well as N-Myc displayed a whole array of higher migrating bands, starting with a size shift of about 45 kDa and reaching up higher than 170 kDa (Fig. 4.19 on page 86). This pattern phenotypically differed profoundly from the few higher migrating bands observed upon Sumo attachment to Miz1. Arf did not induce sumoylation of Myc, as it did for Miz1 (not shown). Direct Sumo1 and Sumo2 blots of pulldown samples revealed that expression of N-Myc stabilized sumoylated proteins in general. This probably results from the fact that non-attached Sumo protein is highly unstable, and expression of a common sumoylation target may increase overall levels of stable Sumo. The very high turnover of the Sumo modification may consequently allow for other proteins to be increasedly sumoylated as well.

Depletion of Ubc9 as the only E2 enzyme in the sumoylation process severely diminished higher migrating Myc bands in the His-Sumo pulldown (Fig. 4.20 on page 88). These must thus either represent sumoylated species or sumoylation must be necessary for follow-up posttranslational modifications. The ladder of shifted bands cannot be assigned to chain formation, as it also occurs upon modification with Sumo1 as well as the Sumo2 K11R mutant which cannot form chains anymore. Phenotypically, the modification pattern strongly resembles ubiquitination. However, polyubiquitination of the Sumo protein itself when attached to Myc did not occur. Sumoylation of N-Myc did not result in increased ubiquitination and could also not be diminished by treatment with proteasome inhibitors. The only possible interpretation of the particular sumoylation phenotype is thus a multisumoylation at many different lysines in the Myc protein.

5.3.2. Myc is preferredly sumoylated at several C-terminal lysines

Sumoylation often occurs within the defined sumoylation consensus motif Ψ-K-X-E/D, for example in Miz1 (see 5.2.1 on page 109). C-Myc does not contain such a site, and mutation

of the two existing consensus motifs in N-Myc does not abrogate sumoylation. This was already expected from the notion that Myc must get multisumoylated at several different lysines. Mutants of Myc that contained lysines either only in the N-terminal or C-terminal domain did not really help in narrowing down a preferred region for sumoylation (Fig. 4.22 on page 91). Thus, I assessed mutants of Myc containing only single intact lysines one by one for their potential to be sumoylated (Fig. 4.23 on page 93). The analysis revealed that there is a cluster of about seven preferred lysines for modification by Sumo which however are not the only targets, as depletion of these lysines reduced sumoylation but did not completely abolish it (Fig. 4.24 on page 94). Finding the specific sumoylated lysines would have made it possible to compare Myc wild type to a non-sumoylatable mutant. However, as virtually all lysines bear the potential to become sumoylated, one would have to compare the K-less Myc with the wild type version. As lysines in Myc can also be ubiquitinated and acetylated [Kim et al., 2011; Vervoorts et al., 2003], it would be pointless to pursue such an analysis wanting to look for sumoylation-specific effects.

The sumoylation consensus motif recruits Ubc9 directly to the inherent lysine [Bernier-Villamor et al., 2002]. The lack of a sumoylation consensus site in c-Myc already gave a hint to the later observation that no particular lysines in Myc are the sole acceptors of this modification, as had been shown before for other proteins without consensus sites [Yan et al., 2007]. Ubc9 may still interact with a region distant to the sumoylation site, as seen for AP2 or N-CoR [Eloranta and Hurst, 2002; Tiefenbach et al., 2006]. Another possible explanation of how Myc attracts the sumoylation machinery could be that Myc recruits Sumo-loaded Ubc9 via an internal SIM (Sumo interacting motif), which had been shown for USP25 [Mohideen and Lima, 2008] and will be discussed in 5.3.4.

5.3.3. Endogenous sumoylation of Myc could not be detected

I was not able to visualize endogenous sumoylation of Myc in pulldown experiments performed according to previously conducted experiments with Miz1 (see 5.2.3). No peptides of c-Myc or N-Myc were found in the endogenous large scale IPs with Sumo1 and Sumo2 performed in the group of Frauke Melchior from the ZMBH Heidelberg [Werner, 2011]. None of the stress factors known to induce overall sumoylation levels in cells were able to induce sumoylation of exogenous Myc and could thus not be exploited to trigger endogenous sumoylation of the protein (Fig. 4.25 on page 95). It can be concluded that either the steady state sumoylation of Myc is extremely low or modification by Sumo needs an unidentified trigger.

5.3.4. A conserved motif in Myc could not be validated as a Sumo interacting motif

The previously described PEST sequence in c-Myc is one of the most conserved areas among different Myc homologues and paralogues (Fig. 4.26 on page 96). This sequence fulfills all criteria for a reverse Sumo interacting motif (SIMr). While hydrophobic and aromatic amino acids in Sumo are arranged to form a groove, the SIM peptide has an extended shape that can be embedded in this groove to form an intermolecular β-grasp fold [Kerscher, 2007]. SIMs play an important role in the effector proteins that mediate the physiological consequences of sumoylation, but they can also mediate sumoylation of the protein containing the SIM [Rytinki et al., 2009; Mohideen and Lima, 2008]. Both functions could be interesting for the Myc protein: On the one hand several known coactivators of Myc have been shown to be sumoylated upon heat shock and a SIM could thus provide an additional interaction surface for Myc [Golebiowski et al., 2009]. On the other hand sumoylation of Myc itself could be mediated via a SIM motif as c-Myc lacks an internal sumoylation consensus site that recruits Ubc9 to the protein.

To test if the conserved sequence in Myc is a valid Sumo interacting motif, I generated mutants that either lacked the whole conserved SIM area or just the core amino acids. His-Sumo pulldowns revealed that the possible SIM is not needed to induce sumoylation of Myc (Fig. 4.26 on page 96). *In vitro* binding assays showed a weak but consistent binding of c-Myc and N-Myc to Sumo1, which could however also be detected with a mutant lacking the core amino acids of the conserved motif (Fig. 4.27 on page 98). It must thus be concluded that the possible SIM motif in Myc is not necessary for sumoylation of Myc itself and could also not be verified to be an actual Sumo interacting motif in the *in vitro* binding assay.

Bibliography

Adhikary, S. & Eilers, M. (2005). Transcriptional regulation and transformation by Myc proteins. *Nat Rev Mol Cell Biol*, 6(8):635–645.

Adhikary, S., Marinoni, F., Hock, A., Hulleman, E., Popov, N., Beier, R., Bernard, S., Quarto, M., Capra, M., Goettig, S., Kogel, U., Scheffner, M., Helin, K., & Eilers, M. (2005). The ubiquitin ligase HectH9 regulates transcriptional activation by Myc and is essential for tumor cell proliferation. *Cell*, 123(3):409–421.

Adhikary, S., Peukert, K., Karsunky, H., Beuger, V., Lutz, W., Elsässer, H.-P., Möröy, T., & Eilers, M. (2003). Miz1 is required for early embryonic development during gastrulation. *Molecular and Cellular Biology*, 23(21):7648–7657.

Amente, S., Gargano, B., Varrone, F., Ruggiero, L., Dominguez-Sola, D., Lania, L., & Majello, B. (2006). p14ARF directly interacts with Myc through the Myc BoxII domain. *Cancer biology & therapy*, 5(3):287–291.

Apionishev, S., Malhotra, D., Raghavachari, S., Tanda, S., & Rasooly, R. S. (2001). The Drosophila UBC9 homologue lesswright mediates the disjunction of homologues in meiosis I. *Genes Cells*, 6(3):215–224.

Askew, D. S., Ashmun, R. A., Simmons, B. C., & Cleveland, J. L. (1991). Constitutive c-myc expression in an IL-3-dependent myeloid cell line suppresses cell cycle arrest and accelerates apoptosis. *Oncogene*, 6(10):1915–1922.

Badal, V., Menendez, S., Coomber, D., & Lane, D. P. (2008). Regulation of the p14ARF promoter by DNA methylation. *Cell Cycle*, 7(1):112–119.

Bahram, F., von der Lehr, N., Cetinkaya, C., & Larsson, L. G. (2000). c-Myc hot spot mutations in lymphomas result in inefficient ubiquitination and decreased proteasome-mediated turnover. *Blood*, 95(6):2104–2110.

Bayer, P., Arndt, A., Metzger, S., Mahajan, R., Melchior, F., Jaenicke, R., & Becker, J. (1998). Structure determination of the small ubiquitin-related modifier SUMO-1. *J Mol Biol*, 280(2):275–286.

Bentley, D. L. & Groudine, M. (1986). A block to elongation is largely responsible for decreased transcription of c-myc in differentiated HL60 cells. *Nature*, 321(6071):702–706.

Bentley, D. L. & Groudine, M. (1988). Sequence requirements for premature termination of transcription in the human c-myc gene. *Cell*, 53(2):245–256.

Bernier-Villamor, V., Sampson, D. A., Matunis, M. J., & Lima, C. D. (2002). Structural basis for E2-mediated SUMO conjugation revealed by a complex between ubiquitin-conjugating enzyme Ubc9 and RanGAP1. *Cell*, 108(3):345–356.

Bernstein, P. L., Herrick, D. J., Prokipcak, R. D., & Ross, J. (1992). Control of c-myc mRNA half-life in vitro by a protein capable of binding to a coding region stability determinant. *Genes Dev*, 6(4):642–654.

Bertwistle, D., Sugimoto, M., & Sherr, C. J. (2004). Physical and functional interactions of the Arf tumor suppressor protein with nucleophosmin/B23. *Molecular and Cellular Biology*, 24(3):985–996.

Blackwell, T. K., Huang, J., Ma, A., Kretzner, L., Alt, F. W., Eisenman, R. N., & Weintraub, H. (1993). Binding of myc proteins to canonical and noncanonical DNA sequences. *Molecular and Cellular Biology*, 13(9):5216–5224.

Blackwell, T. K., Kretzner, L., Blackwood, E. M., Eisenman, R. N., & Weintraub, H. (1990). Sequence-specific DNA binding by the c-Myc protein. *Science*, 250(4984):1149–1151.

Blackwood, E. M. & Eisenman, R. N. (1991). Max: a helix-loop-helix zipper protein that forms a sequence-specific DNA-binding complex with Myc. *Science*, 251(4998):1211–1217.

Boggio, R., Colombo, R., Hay, R. T., Draetta, G. F., & Chiocca, S. (2004). A mechanism for inhibiting the SUMO pathway. *Mol Cell*, 16(4):549–561.

Bossis, G. & Melchior, F. (2006). Regulation of SUMOylation by reversible oxidation of SUMO conjugating enzymes. *Mol Cell*, 21(3):349–357.

Bouchard, C., Lee, S., Paulus-Hock, V., Loddenkemper, C., Eilers, M., & Schmitt, C. A. (2007). FoxO transcription factors suppress Myc-driven lymphomagenesis via direct activation of Arf. *Genes Dev*, 21(21):2775–2787.

Bouchard, C., Marquardt, J., Brás, A., Medema, R. H., & Eilers, M. (2004). Myc-induced proliferation and transformation require Akt-mediated phosphorylation of FoxO proteins. *EMBO J*, 23(14):2830–2840.

Bradford, M. M. (1976). A rapid and sensitive method for the quantitation of microgram quantities of protein utilizing the principle of protein-dye binding. *Anal Biochem*, 72:248–254.

Brewer, G. & Ross, J. (1988). Poly(A) shortening and degradation of the 3' A+U-rich sequences of human c-myc mRNA in a cell-free system. *Molecular and Cellular Biology*, 8(4):1697–1708.

Cannell, I. G., Kong, Y. W., Johnston, S. J., Chen, M. L., Collins, H. M., Dobbyn, H. C., Elia, A., Kress, T. R., Dickens, M., Clemens, M. J., Heery, D. M., Gaestel, M., Eilers, M., Willis, A. E., & Bushell, M. (2010). p38 MAPK/MK2-mediated induction of miR-34c following DNA damage prevents Myc-dependent DNA replication. *Proceedings of the National Academy of Sciences*, 107(12):5375–5380.

Carter, P. S., Jarquin-Pardo, M., & De Benedetti, A. (1999). Differential expression of Myc1 and Myc2 isoforms in cells transformed by eIF4E: evidence for internal ribosome repositioning in the human c-myc 5'UTR. *Oncogene*, 18(30):4326–4335.

Chan, C.-H., Lee, S.-W., Li, C.-F., Wang, J., Yang, W.-L., Wu, C.-Y., Wu, J., Nakayama, K. I., Kang, H.-Y., Huang, H.-Y., Hung, M.-C., Pandolfi, P. P., & Lin, H.-K. (2010). Deciphering the transcriptional complex critical for RhoA gene expression and cancer metastasis. *Nat Cell Biol*, 12(5):457–467.

Chandramohan, V., Mineva, N. D., Burke, B., Jeay, S., Wu, M., Shen, J., Yang, W., Hann, S. R., & Sonenshein, G. E. (2008). c-Myc represses FOXO3a-mediated transcription of the gene encoding the p27(Kip1) cyclin dependent kinase inhibitor. *Journal of cellular biochemistry*, 104(6):2091–2106.

Chen, C.-R., Kang, Y., Siegel, P. M., & Massagué, J. (2002). E2F4/5 and p107 as Smad cofactors linking the TGFbeta receptor to c-myc repression. *Cell*, 110(1):19–32.

Chen, D., Shan, J., Zhu, W. G., Qin, J., & Gu, W. (2010). Transcription-independent ARF regulation in oncogenic stress-mediated p53 responses. *Nature*, 464(7288):624–627.

Chen, L. & Chen, J. (2003). MDM2-ARF complex regulates p53 sumoylation. *Oncogene*, 22(34):5348–5357.

Cole, M. D. & Cowling, V. H. (2008). Transcription-independent functions of MYC: regulation of translation and DNA replication. *Nat Rev Mol Cell Biol*, 9(10):810–815.

Cole, M. D. & Nikiforov, M. A. (2006). Transcriptional activation by the Myc oncoprotein. *Curr Top Microbiol Immunol*, 302:33–50.

Colombo, E., Bonetti, P., Lazzerini Denchi, E., Martinelli, P., Zamponi, R., Marine, J.-C., Helin, K., Falini, B., & Pelicci, P. G. (2005). Nucleophosmin is required for DNA integrity and p19Arf protein stability. *Molecular and Cellular Biology*, 25(20):8874–8886.

Cowling, V. H., Chandriani, S., Whitfield, M. L., & Cole, M. D. (2006). A conserved Myc protein domain, MBIV, regulates DNA binding, apoptosis, transformation, and G2 arrest. *Molecular and Cellular Biology*, 26(11):4226–4239.

Croce, C. M. (2008). Oncogenes and cancer. *The New England journal of medicine*, 358(5):502–511.

Dalla-Favera, R., Bregni, M., Erikson, J., Patterson, D., Gallo, R. C., & Croce, C. M. (1982). Human c-myc onc gene is located on the region of chromosome 8 that is translocated in Burkitt lymphoma cells. *Proc Natl Acad Sci U S A*, 79(24):7824–7827.

Dani, C., Blanchard, J. M., Piechaczyk, M., El Sabouty, S., Marty, L., & Jeanteur, P. (1984). Extreme instability of myc mRNA in normal and transformed human cells. *Proc Natl Acad Sci U S A*, 81(22):7046–7050.

Datta, A., Nag, A., Pan, W., Hay, N., Gartel, A. L., Colamonici, O., Mori, Y., & Raychaudhuri, P. (2004). Myc-ARF (alternate reading frame) interaction inhibits the functions of Myc. *J Biol Chem*, 279(35):36698–36707.

Davis, A. C., Wims, M., Spotts, G. D., Hann, S. R., & Bradley, A. (1993). A null c-myc mutation causes lethality before 10.5 days of gestation in homozygotes and reduced fertility in heterozygous female mice. *Genes Dev*, 7(4):671–682.

Dedhar, S. (2000). Cell-substrate interactions and signaling through ILK. *Current opinion in cell biology*, 12(2):250–256.

Doyle, G. A., Bourdeau-Heller, J. M., Coulthard, S., Meisner, L. F., & Ross, J. (2000). Amplification in human breast cancer of a gene encoding a c-myc mRNA-binding protein. *Cancer Res*, 60(11):2756–2759.

Eberhardy, S. R. & Farnham, P. J. (2001). c-Myc mediates activation of the cad promoter via a post-RNA polymerase II recruitment mechanism. *J Biol Chem*, 276(51):48562–48571.

Egle, A., Harris, A. W., Bouillet, P., & Cory, S. (2004). Bim is a suppressor of Myc-induced mouse B cell leukemia. *Proc Natl Acad Sci U S A*, 101(16):6164–6169.

Eick, D. & Bornkamm, G. W. (1986). Transcriptional arrest within the first exon is a fast control mechanism in c-myc gene expression. *Nucleic Acids Res*, 14(21):8331–8346.

Eischen, C. M., Packham, G., Nip, J., Fee, B. E., Hiebert, S. W., Zambetti, G. P., & Cleveland, J. L. (2001a). Bcl-2 is an apoptotic target suppressed by both c-Myc and E2F-1. *Oncogene*, 20(48):6983–6993.

Eischen, C. M., Woo, D., Roussel, M. F., & Cleveland, J. L. (2001b). Apoptosis triggered by Myc-induced suppression of Bcl-X(L) or Bcl-2 is bypassed during lymphomagenesis. *Molecular and Cellular Biology*, 21(15):5063–5070.

El-Deiry, W. S., Tokino, T., Velculescu, V. E., Levy, D. B., Parsons, R., Trent, J. M., Lin, D., Mercer, W. E., Kinzler, K. W., & Vogelstein, B. (1993). WAF1, a potential mediator of p53 tumor suppression. *Cell*, 75(4):817–825.

Eloranta, J. J. & Hurst, H. C. (2002). Transcription factor AP-2 interacts with the SUMO-conjugating enzyme UBC9 and is sumolated in vivo. *J Biol Chem*, 277(34):30798–30804.

Evan, G. I., Wyllie, A. H., Gilbert, C. S., Littlewood, T. D., Land, H., Brooks, M., Waters, C. M., Penn, L. Z., & Hancock, D. C. (1992). Induction of apoptosis in fibroblasts by c-myc protein. *Cell*, 69(1):119–128.

Feng, X.-H., Liang, Y.-Y., Liang, M., Zhai, W., & Lin, X. (2002). Direct interaction of c-Myc with Smad2 and Smad3 to inhibit TGF-beta-mediated induction of the CDK inhibitor p15(Ink4B). *Mol Cell*, 9(1):133–143.

Ferlay, J., Shin, H., Bray, F., & Forman, D. (2010). Estimates of worldwide burden of cancer in 2008: GLOBOCAN 2008. *International journal of cancer. Journal international du cancer.*

Fernandez-Pol, J. A., Talkad, V. D., Klos, D. J., & Hamilton, P. D. (1987). Suppression of the EGF-dependent induction of c-myc proto-oncogene expression by transforming growth factor beta in a human breast carcinoma cell line. *Biochem Biophys Res Commun*, 144(3):1197–1205.

Freytag, S. O., Dang, C. V., & Lee, W. M. (1990). Definition of the activities and properties of c-myc required to inhibit cell differentiation. *Cell growth & differentiation : the molecular biology journal of the American Association for Cancer Research*, 1(7):339–343.

Frisch, S. M. & Screaton, R. A. (2001). Anoikis mechanisms. *Current opinion in cell biology*, 13(5):555–562.

Frye, M., Gardner, C., Li, E. R., Arnold, I., & Watt, F. M. (2003). Evidence that Myc activation depletes the epidermal stem cell compartment by modulating adhesive interactions with the local microenvironment. *Development*, 130(12):2793–2808.

Gallant, P., Shiio, Y., Cheng, P. F., Parkhurst, S. M., & Eisenman, R. N. (1996). Myc and Max homologs in Drosophila. *Science*, 274(5292):1523–1527.

Gallant, P. & Steiger, D. (2009). Myc's secret life without Max. *Cell Cycle*, 8(23):3848–3853.

Garcia-Dominguez, M. & Reyes, J. C. (2009). SUMO association with repressor complexes, emerging routes for transcriptional control. *Biochim Biophys Acta*, 1789(6-8):451–459.

Gareau, J. R. & Lima, C. D. (2010). The SUMO pathway: emerging mechanisms that shape specificity, conjugation and recognition. *Nat Rev Mol Cell Biol*, 11(12):861–871.

Gartel, A. L., Ye, X., Goufman, E., Shianov, P., Hay, N., Najmabadi, F., & Tyner, A. L. (2001). Myc represses the p21(WAF1/CIP1) promoter and interacts with Sp1/Sp3. *Proc Natl Acad Sci U S A*, 98(8):4510–4515.

Gebhardt, A., Frye, M., Herold, S., Benitah, S. A., Braun, K., Samans, B., Watt, F. M., Elsässer, H.-P., & Eilers, M. (2006). Myc regulates keratinocyte adhesion and differentiation via complex formation with Miz1. *J Cell Biol*, 172(1):139–149.

Geiss-Friedlander, R. & Melchior, F. (2007). Concepts in sumoylation: a decade on. *Nat Rev Mol Cell Biol*, 8(12):947–956.

Giancotti, F. G. & Ruoslahti, E. (1999). Integrin signaling. *Science*, 285(5430):1028–1032.

Girdwood, D., Bumpass, D., Vaughan, O. A., Thain, A., Anderson, L. A., Snowden, A. W., Garcia-Wilson, E., Perkins, N. D., & Hay, R. T. (2003). P300 transcriptional repression is mediated by SUMO modification. *Mol Cell*, 11(4):1043–1054.

Girdwood, D. W. H., Tatham, M. H., & Hay, R. T. (2004). SUMO and transcriptional regulation. *Seminars in cell & developmental biology*, 15(2):201–210.

Golebiowski, F., Matic, I., Tatham, M. H., Cole, C., Yin, Y., Nakamura, A., Cox, J., Barton, G. J., Mann, M., & Hay, R. T. (2009). System-wide changes to SUMO modifications in response to heat shock. *Sci Signal*, 2(72):ra24.

Gomis, R. R., Alarcón, C., Nadal, C., Van Poznak, C., & Massagué, J. (2006). C/EBPbeta at the core of the TGFbeta cytostatic response and its evasion in metastatic breast cancer cells. *Cancer Cell*, 10(3):203–214.

Gong, L. & Yeh, E. T. (2006). Characterization of a family of nucleolar SUMO-specific proteases with preference for SUMO-2 or SUMO-3. *J Biol Chem*, 281(23):15869–15877.

Goodson, M. L., Hong, Y., Rogers, R., Matunis, M. J., Park-Sarge, O. K., & Sarge, K. D. (2001). Sumo-1 modification regulates the DNA binding activity of heat shock transcription factor 2, a promyelocytic leukemia nuclear body associated transcription factor. *J Biol Chem*, 276(21):18513–18518.

Gregory, M. A. & Hann, S. R. (2000). c-Myc proteolysis by the ubiquitin-proteasome pathway: stabilization of c-Myc in Burkitt's lymphoma cells. *Molecular and Cellular Biology*, 20(7):2423–2435.

Grignani, F., De Matteis, S., Nervi, C., Tomassoni, L., Gelmetti, V., Cioce, M., Fanelli, M., Ruthardt, M., Ferrara, F. F., Zamir, I., Seiser, C., Grignani, F., Lazar, M. A., Minucci, S., & Pelicci, P. G. (1998). Fusion proteins of the retinoic acid receptor-alpha recruit histone deacetylase in promyelocytic leukaemia. *Nature*, 391(6669):815–818.

Haindl, M., Harasim, T., Eick, D., & Muller, S. (2008). The nucleolar SUMO-specific protease SENP3 reverses SUMO modification of nucleophosmin and is required for rRNA processing. *EMBO Rep*, 9(3):273–279.

Hann, S. R. (2006). Role of post-translational modifications in regulating c-Myc proteolysis, transcriptional activity and biological function. *Seminars in cancer biology*, 16(4):288–302.

Hann, S. R. & Eisenman, R. N. (1984). Proteins encoded by the human c-myc oncogene: differential expression in neoplastic cells. *Molecular and Cellular Biology*, 4(11):2486–2497.

Hardeland, U., Steinacher, R., Jiricny, J., & Schär, P. (2002). Modification of the human thymine-DNA glycosylase by ubiquitin-like proteins facilitates enzymatic turnover. *EMBO J*, 21(6):1456–1464.

Hay, R. T. (2005). SUMO: a history of modification. *Mol Cell*, 18(1):1–12.

Hay, R. T. (2007). SUMO-specific proteases: a twist in the tail. *Trends in cell biology*, 17(8):370–376.

Hay, R. T., Vuillard, L., Desterro, J. M., & Rodriguez, M. S. (1999). Control of NF-kappa B transcriptional activation by signal induced proteolysis of I kappa B alpha. *Philosophical transactions of the Royal Society of London. Series B, Biological sciences*, 354(1389):1601–1609.

He, T. C., Sparks, A. B., Rago, C., Hermeking, H., Zawel, L., da Costa, L. T., Morin, P. J., Vogelstein, B., & Kinzler, K. W. (1998). Identification of c-MYC as a target of the APC pathway. *Science*, 281(5382):1509–1512.

Herbst, A., Hemann, M. T., Tworkowski, K. A., Salghetti, S. E., Lowe, S. W., & Tansey, W. P. (2005). A conserved element in Myc that negatively regulates its proapoptotic activity. *EMBO Rep*, 6(2):177–183.

Herkert, B. (2010). Discussion in person.

Herkert, B., Dwertmann, A., Herold, S., Abed, M., Naud, J.-F., Finkernagel, F., Harms, G. S., Orian, A., Wanzel, M., & Eilers, M. (2010). The Arf tumor suppressor protein inhibits Miz1 to suppress cell adhesion and induce apoptosis. *J Cell Biol*, 188(6):905–918.

Herkert, B. & Eilers, M. (2010). Transcriptional repression: the dark side of myc. *Genes & cancer*, 1(6):580–586.

Herold, S., Hock, A., Herkert, B., Berns, K., Mullenders, J., Beijersbergen, R., Bernards, R., & Eilers, M. (2008). Miz1 and HectH9 regulate the stability of the checkpoint protein, TopBP1. *EMBO J*, 27(21):2851–2861.

Herold, S., Wanzel, M., Beuger, V., Frohme, C., Beul, D., Hillukkala, T., Syvaoja, J., Saluz, H.-P., Haenel, F., & Eilers, M. (2002). Negative regulation of the mammalian UV response by Myc through association with Miz-1. *Mol Cell*, 10(3):509–521.

Hiebert, S. W., Lipp, M., & Nevins, J. R. (1989). E1A-dependent trans-activation of the human MYC promoter is mediated by the E2F factor. *Proc Natl Acad Sci U S A*, 86(10):3594–3598.

Hietakangas, V., Anckar, J., Blomster, H. A., Fujimoto, M., Palvimo, J. J., Nakai, A., & Sistonen, L. (2006). PDSM, a motif for phosphorylation-dependent SUMO modification. *Proc Natl Acad Sci U S A*, 103(1):45–50.

Hilgarth, R. S. & Sarge, K. D. (2005). Detection of sumoylated proteins. *Methods Mol Biol*, 301:329–338.

Hochstrasser, M. (2001). SP-RING for SUMO: new functions bloom for a ubiquitin-like protein. *Cell*, 107(1):5–8.

Hong, Y., Rogers, R., Matunis, M. J., Mayhew, C. N., Goodson, M. L., Park-Sarge, O. K., Sarge, K. D., & Goodson, M. (2001). Regulation of heat shock transcription factor 1 by stress-induced SUMO-1 modification. *J Biol Chem*, 276(43):40263–40267.

Hynes, R. O. (2002). Integrins: bidirectional, allosteric signaling machines. *Cell*, 110(6):673–687.

Ikegaki, N., Gotoh, T., Kung, B., Riceberg, J. S., Kim, D. Y., Zhao, H., Rappaport, E. F., Hicks, S. L., Seeger, R. C., & Tang, X. X. (2007). De novo identification of MIZ-1 (ZBTB17) encoding a MYC-interacting zinc-finger protein as a new favorable neuroblastoma gene. *Clinical cancer research : an official journal of the American Association for Cancer Research*, 13(20):6001–6009.

Ioannidis, P., Trangas, T., Dimitriadis, E., Samiotaki, M., Kyriazoglou, I., Tsiapalis, C. M., Kittas, C., Agnantis, N., Nielsen, F. C., Nielsen, J., Christiansen, J., & Pandis, N. (2001). C-MYC and IGF-II mRNA-binding protein (CRD-BP/IMP-1) in benign and malignant mesenchymal tumors. *International journal of cancer. Journal international du cancer*, 94(4):480–484.

Itahana, K., Bhat, K. P., Jin, A., Itahana, Y., Hawke, D., Kobayashi, R., & Zhang, Y. (2003). Tumor suppressor ARF degrades B23, a nucleolar protein involved in ribosome biogenesis and cell proliferation. *Mol Cell*, 12(5):1151–1164.

Izumi, H., Molander, C., Penn, L. Z., Ishisaki, A., Kohno, K., & Funa, K. (2001). Mechanism for the transcriptional repression by c-Myc on PDGF beta-receptor. *J Cell Sci*, 114(Pt 8):1533–1544.

Johnson, E. S. (2004). Protein modification by SUMO. *Annu Rev Biochem*, 73:355–382.

Jones, D., Crowe, E., Stevens, T. A., & Candido, E. P. M. (2002). Functional and phylogenetic analysis of the ubiquitylation system in Caenorhabditis elegans: ubiquitin-conjugating enzymes, ubiquitin-activating enzymes, and ubiquitin-like proteins. *Genome Biol*, 3(1):RESEARCH0002.

Jones, T. R. & Cole, M. D. (1987). Rapid cytoplasmic turnover of c-myc mRNA: requirement of the 3' untranslated sequences. *Molecular and Cellular Biology*, 7(12):4513–4521.

Kahyo, T., Nishida, T., & Yasuda, H. (2001). Involvement of PIAS1 in the sumoylation of tumor suppressor p53. *Mol Cell*, 8(3):713–718.

Kelly, K., Cochran, B. H., Stiles, C. D., & Leder, P. (1983). Cell-specific regulation of the c-myc gene by lymphocyte mitogens and platelet-derived growth factor. *Cell*, 35(3 Pt 2):603–610.

Kerscher, O. (2007). SUMO junction-what's your function? New insights through SUMO-interacting motifs. *EMBO Rep*, 8(6):550–555.

Kerscher, O., Felberbaum, R., & Hochstrasser, M. (2006). Modification of proteins by ubiquitin and ubiquitin-like proteins. *Annu Rev Cell Dev Biol*, 22:159–180.

Kim, J. H. & Baek, S. H. (2009). Emerging roles of desumoylating enzymes. *Biochim Biophys Acta*, 1792(3):155–162.

Kim, S. Y., Herbst, A., Tworkowski, K. A., Salghetti, S. E., & Tansey, W. P. (2003). Skp2 regulates Myc protein stability and activity. *Mol Cell*, 11(5):1177–1188.

Kim, W., Bennett, E. J., Huttlin, E. L., Guo, A., Li, J., Possemato, A., Sowa, M. E., Rad, R., Rush, J., Comb, M. J., Harper, J. W., & Gygi, S. P. (2011). Systematic and quantitative assessment of the ubiquitin-modified proteome. *Mol Cell*, 44(2):325–340.

Kinsella, T. M. & Nolan, G. P. (1996). Episomal vectors rapidly and stably produce high-titer recombinant retrovirus. *Human gene therapy*, 7(12):1405–1413.

Knezevich, S., Ludkovski, O., Salski, C., Lestou, V., Chhanabhai, M., Lam, W., Klasa, R., Connors, J. M., Dyer, M. J. S., Gascoyne, R. D., & Horsman, D. E. (2005). Concurrent translocation of BCL2 and MYC with a single immunoglobulin locus in high-grade B-cell lymphomas. *Leukemia : official journal of the Leukemia Society of America, Leukemia Research Fund, U.K*, 19(4):659–663.

Knoepfler, P. S., Cheng, P. F., & Eisenman, R. N. (2002). N-myc is essential during neurogenesis for the rapid expansion of progenitor cell populations and the inhibition of neuronal differentiation. *Genes Dev*, 16(20):2699–2712.

Korgaonkar, C., Hagen, J., Tompkins, V., Frazier, A. A., Allamargot, C., Quelle, F. W., & Quelle, D. E. (2005). Nucleophosmin (B23) targets ARF to nucleoli and inhibits its function. *Molecular and Cellular Biology*, 25(4):1258–1271.

Kouzarides, T. (2007). Chromatin modifications and their function. *Cell*.

Kress, T. R., Cannell, I. G., Brenkman, A. B., Samans, B., Gaestel, M., Roepman, P., Burgering, B. M., Bushell, M., Rosenwald, A., & Eilers, M. (2011). The MK5/PRAK kinase and Myc form a negative feedback loop that is disrupted during colorectal tumorigenesis. *Mol Cell*, 41(4):445–457.

Krueger, K. E. & Srivastava, S. (2006). Posttranslational protein modifications: current implications for cancer detection, prevention, and therapeutics. *Mol Cell Proteomics*, 5(10):1799–1810.

Kuhnert, A., Schmidt, U., Monajembashi, S., Franke, C., Schlott, B., Grosse, F., Greulich, K. O., Saluz, H.-P., & Hänel, F. (2012). Proteomic identification of PSF and p54(nrb) as TopBP1-interacting proteins. *Journal of cellular biochemistry*, 113(5):1744–1753.

Kuo, M.-L., den Besten, W., Thomas, M. C., & Sherr, C. J. (2008). Arf-induced turnover of the nucleolar nucleophosmin-associated SUMO-2/3 protease Senp3. *Cell Cycle*, 7(21):3378–3387.

Laemmli, U. K., Beguin, F., & Gujer-Kellenberger, G. (1970). A factor preventing the major head protein of bacteriophage T4 from random aggregation. *J Mol Biol*, 47(1):69–85.

Lee, K. K. & Workman, J. L. (2007). Histone acetyltransferase complexes: one size doesn't fit all. *Nat Rev Mol Cell Biol*, 8(4):284–295.

Letai, A., Sorcinelli, M. D., Beard, C., & Korsmeyer, S. J. (2004). Antiapoptotic BCL-2 is required for maintenance of a model leukemia. *Cancer Cell*, 6(3):241–249.

Li, Z., Boone, D., & Hann, S. R. (2008). Nucleophosmin interacts directly with c-Myc and controls c-Myc-induced hyperproliferation and transformation. *Proceedings of the National Academy of Sciences*, 105(48):18794–18799.

Lin, A. W. & Lowe, S. W. (2001). Oncogenic ras activates the ARF-p53 pathway to suppress epithelial cell transformation. *Proc Natl Acad Sci U S A*, 98(9):5025–5030.

Lin, D., Tatham, M. H., Yu, B., Kim, S., Hay, R. T., & Chen, Y. (2002). Identification of a substrate recognition site on Ubc9. *J Biol Chem*, 277(24):21740–21748.

Lin, X., Liang, M., Liang, Y.-Y., Brunicardi, F. C., & Feng, X.-H. (2003). SUMO-1/Ubc9 promotes nuclear accumulation and metabolic stability of tumor suppressor Smad4. *J Biol Chem*, 278(33):31043–31048.

Liu, J., Zhao, Y., Eilers, M., & Lin, A. (2009). Miz1 is a signal- and pathway-specific modulator or regulator (SMOR) that suppresses TNF-alpha-induced JNK1 activation. *Proceedings of the National Academy of Sciences*, 106(43):18279–18284.

Llanos, S., Clark, P., & Rowe, J. (2001). Stabilization of p53 by p14ARF without relocation of MDM2 to the nucleolus. *Nature cell biology*.

Lowe, S. W. & Sherr, C. J. (2003). Tumor suppression by Ink4a-Arf: progress and puzzles. *Curr Opin Genet Dev*, 13(1):77–83.

Luo, Q., Li, J., Cenkci, B., & Kretzner, L. (2004). Autorepression of c-myc requires both initiator and E2F-binding site elements and cooperation with the p107 gene product. *Oncogene*, 23(5):1088–1097.

Lüscher, B. & Vervoorts, J. (2012). Regulation of gene transcription by the oncoprotein MYC. *Gene*, 494(2):145–160.

Lutterbach, B. & Hann, S. R. (1994). Hierarchical phosphorylation at N-terminal transformation-sensitive sites in c-Myc protein is regulated by mitogens and in mitosis. *Molecular and Cellular Biology*, 14(8):5510–5522.

Maggi, L. B., Kuchenruether, M., Dadey, D. Y. A., Schwope, R. M., Grisendi, S., Townsend, R. R., Pandolfi, P. P., & Weber, J. D. (2008). Nucleophosmin serves as a rate-limiting nuclear export chaperone for the Mammalian ribosome. *Mol Cell Biol*, 28(23):7050–7065.

Mahajan, R., Delphin, C., Guan, T., Gerace, L., & Melchior, F. (1997). A small ubiquitin-related polypeptide involved in targeting RanGAP1 to nuclear pore complex protein RanBP2. *Cell*, 88(1):97–107.

Mao, D. Y. L., Watson, J. D., Yan, P. S., Barsyte-Lovejoy, D., Khosravi, F., Wong, W. W.-L., Farnham, P. J., Huang, T. H.-M., & Penn, L. Z. (2003). Analysis of Myc bound loci identified by CpG island arrays shows that Max is essential for Myc-dependent repression. *Current biology : CB*, 13(10):882–886.

Marcu, K. B., Bossone, S. A., & Patel, A. J. (1992). myc function and regulation. *Annu Rev Biochem*, 61:809–860.

Martín-Subero, J. I., Odero, M. D., Hernandez, R., Cigudosa, J. C., Agirre, X., Saez, B., Sanz-García, E., Ardanaz, M. T., Novo, F. J., Gascoyne, R. D., Calasanz, M. J., & Siebert, R. (2005). Amplification of IGH/MYC fusion in clinically aggressive IGH/BCL2-positive germinal center B-cell lymphomas. *Genes, chromosomes & cancer*, 43(4):414–423.

Matunis, M. J., Coutavas, E., & Blobel, G. (1996). A novel ubiquitin-like modification modulates the partitioning of the Ran-GTPase-activating protein RanGAP1 between the cytosol and the nuclear pore complex. *J Cell Biol*, 135(6 Pt 1):1457–1470.

McMahon, S. B., Van Buskirk, H. A., Dugan, K. A., Copeland, T. D., & Cole, M. D. (1998). The novel ATM-related protein TRRAP is an essential cofactor for the c-Myc and E2F oncoproteins. *Cell*, 94(3):363–374.

Melchior, F. (2010a). Discussion in 1rst Thesis Committee.

Melchior, F. (2010b). Discussion in 2nd thesis committee.

Melchior, F. & Hengst, L. (2000). Mdm2-SUMO1: is bigger better? *Nat Cell Biol*, 2(9):E161–E163.

Meyer, N. & Penn, L. Z. (2008). Reflecting on 25 years with MYC. *Nature reviews Cancer*, 8(12):976–990.

Minty, A., Dumont, X., Kaghad, M., & Caput, D. (2000). Covalent modification of p73alpha by SUMO-1. Two-hybrid screening with p73 identifies novel SUMO-1-interacting proteins and a SUMO-1 interaction motif. *J Biol Chem*, 275(46):36316–36323.

Mitchell, K. O., Ricci, M. S., Miyashita, T., Dicker, D. T., Jin, Z., Reed, J. C., & El-Deiry, W. S. (2000). Bax is a transcriptional target and mediator of c-myc-induced apoptosis. *Cancer Res*, 60(22):6318–6325.

Miteva, M., Keusekotten, K., Hofmann, K., Praefcke, G. J. K., & Dohmen, R. J. (2010). Sumoylation as a signal for polyubiquitylation and proteasomal degradation. *Sub-cellular biochemistry*, 54:195–214.

Mohideen, F. & Lima, C. D. (2008). SUMO takes control of a ubiquitin-specific protease. *Mol Cell*, 30(5):539–540.

Mullis, K., Faloona, F., Scharf, S., Saiki, R., Horn, G., & Erlich, H. (1992). *Specific enzymatic amplification of DNA in vitro: the polymerase chain reaction. 1986.*, volume 24.

Murphy, D. J., Junttila, M. R., Pouyet, L., Karnezis, A., Shchors, K., Bui, D. A., Brown-Swigart, L., Johnson, L., & Evan, G. I. (2008). Distinct thresholds govern Myc's biological output in vivo. *Cancer Cell*, 14(6):447–457.

Nacerddine, K., Lehembre, F., Bhaumik, M., Artus, J., Cohen-Tannoudji, M., Babinet, C., Pandolfi, P. P., & Dejean, A. (2005). The SUMO pathway is essential for nuclear integrity and chromosome segregation in mice. *Dev Cell*, 9(6):769–779.

Noubissi, F. K., Elcheva, I., Bhatia, N., Shakoori, A., Ougolkov, A., Liu, J., Minamoto, T., Ross, J., Fuchs, S. Y., & Spiegelman, V. S. (2006). CRD-BP mediates stabilization of betaTrCP1 and c-myc mRNA in response to beta-catenin signalling. *Nature*, 441(7095):898–901.

Owerbach, D., McKay, E. M., Yeh, E. T. H., Gabbay, K. H., & Bohren, K. M. (2005). A proline-90 residue unique to SUMO-4 prevents maturation and sumoylation. *Biochem Biophys Res Commun*, 337(2):517–520.

Palmero, I., Pantoja, C., & Serrano, M. (1998). p19ARF links the tumour suppressor p53 to Ras. *Nature*, 395(6698):125–126.

Park, K., Kwak, K., Kim, J., Lim, S., & Han, S. (2005). c-myc amplification is associated with HER2 amplification and closely linked with cell proliferation in tissue microarray of nonselected breast cancers. *Human pathology*, 36(6):634–639.

Patel, J. H. & McMahon, S. B. (2006). Targeting of Miz-1 is essential for Myc-mediated apoptosis. *J Biol Chem*, 281(6):3283–3289.

Patel, J. H. & McMahon, S. B. (2007). BCL2 is a downstream effector of MIZ-1 essential for blocking c-MYC-induced apoptosis. *J Biol Chem*, 282(1):5–13.

Pelengaris, S., Khan, M., & Evan, G. I. (2002). Suppression of Myc-induced apoptosis in beta cells exposes multiple oncogenic properties of Myc and triggers carcinogenic progression. *Cell*, 109(3):321–334.

Peukert, K., Staller, P., Schneider, A., Carmichael, G., Hänel, F., & Eilers, M. (1997). An alternative pathway for gene regulation by Myc. *EMBO J*, 16(18):5672–5686.

Phan, R. T., Saito, M., Basso, K., Niu, H., & Dalla-Favera, R. (2005). BCL6 interacts with the transcription factor Miz-1 to suppress the cyclin-dependent kinase inhibitor p21 and cell cycle arrest in germinal center B cells. *Nat Immunol*, 6(10):1054–1060.

Popov, N., Schülein, C., Jaenicke, L. A., & Eilers, M. (2010). Ubiquitylation of the amino terminus of Myc by SCF(ß-TrCP) antagonizes SCF(Fbw7)-mediated turnover. *Nat Cell Biol*, 12(10):973–981.

Puthalakath, H., Huang, D. C., O'Reilly, L. A., King, S. M., & Strasser, A. (1999). The proapoptotic activity of the Bcl-2 family member Bim is regulated by interaction with the dynein motor complex. *Mol Cell*, 3(3):287–296.

Puthalakath, H., Villunger, A., & O'Reilly, L. (2001). Bmf: a proapoptotic BH3-only protein regulated by interaction with the myosin V actin motor complex, activated by anoikis. *Science*.

Qi, Y., Gregory, M. A., Li, Z., Brousal, J. P., West, K., & Hann, S. R. (2004). p19ARF directly and differentially controls the functions of c-Myc independently of p53. *Nature*, 431(7009):712–717.

Quelle, D. E., Zindy, F., Ashmun, R. A., & Sherr, C. J. (1995). Alternative reading frames of the INK4a tumor suppressor gene encode two unrelated proteins capable of inducing cell cycle arrest. *Cell*, 83(6):993–1000.

Reginato, M. J., Mills, K. R., Paulus, J. K., Lynch, D. K., Sgroi, D. C., Debnath, J., Muthuswamy, S. K., & Brugge, J. S. (2003). Integrins and EGFR coordinately regulate the pro-apoptotic protein Bim to prevent anoikis. *Nature cell biology*, 5(8):733–740.

Rizos, H., Woodruff, S., & Kefford, R. F. (2005). p14ARF interacts with the SUMO-conjugating enzyme Ubc9 and promotes the sumoylation of its binding partners. *Cell Cycle*, 4(4):597–603.

Rycak, L. (2012). Discussion via Email.

Rytinki, M. M., Kaikkonen, S., Pehkonen, P., Jääskeläinen, T., & Palvimo, J. J. (2009). PIAS proteins: pleiotropic interactors associated with SUMO. *Cellular and molecular life sciences : CMLS*, 66(18):3029–3041.

Sachdeva, M., Zhu, S., Wu, F., Wu, H., Walia, V., Kumar, S., Elble, R., Watabe, K., & Mo, Y.-Y. (2009). p53 represses c-Myc through induction of the tumor suppressor miR-145. *Proceedings of the National Academy of Sciences*, 106(9):3207–3212.

Saitoh, H. & Hinchey, J. (2000). Functional heterogeneity of small ubiquitin-related protein modifiers SUMO-1 versus SUMO-2/3. *J Biol Chem*, 275(9):6252–6258.

Saitoh, H., Pu, R., Cavenagh, M., & Dasso, M. (1997). RanBP2 associates with Ubc9p and a modified form of RanGAP1. *Proc Natl Acad Sci U S A*, 94(8):3736–3741.

Sampson, V. B., Rong, N. H., Han, J., Yang, Q., Aris, V., Soteropoulos, P., Petrelli, N. J., Dunn, S. P., & Krueger, L. J. (2007). MicroRNA let-7a down-regulates MYC and reverts MYC-induced growth in Burkitt lymphoma cells. *Cancer Res*, 67(20):9762–9770.

Sapetschnig, A., Rischitor, G., Braun, H., Doll, A., Schergaut, M., Melchior, F., & Suske, G. (2002). Transcription factor Sp3 is silenced through SUMO modification by PIAS1. *EMBO J*, 21(19):5206–5215.

Savkur, R. S. & Olson, M. O. (1998). Preferential cleavage in pre-ribosomal RNA byprotein B23 endoribonuclease. *Nucleic Acids Res*, 26(19):4508–4515.

Sawai, S., Shimono, A., Wakamatsu, Y., Palmes, C., Hanaoka, K., & Kondoh, H. (1993). Defects of embryonic organogenesis resulting from targeted disruption of the N-myc gene in the mouse. *Development*, 117(4):1445–1455.

Schneider, A., Peukert, K., Eilers, M., & Hänel, F. (1997). Association of Myc with the zinc-finger protein Miz-1 defines a novel pathway for gene regulation by Myc. *Curr Top Microbiol Immunol*, 224:137–146.

Schwinkendorf, D. & Gallant, P. (2009). The conserved Myc box 2 and Myc box 3 regions are important, but not essential, for Myc function in vivo. *Gene*, 436(1-2):90–100.

Sears, R., Nuckolls, F., Haura, E., Taya, Y., Tamai, K., & Nevins, J. R. (2000). Multiple Ras-dependent phosphorylation pathways regulate Myc protein stability. *Genes Dev*, 14(19):2501–2514.

Seoane, J., Le, H.-V., & Massagué, J. (2002). Myc suppression of the p21(Cip1) Cdk inhibitor influences the outcome of the p53 response to DNA damage. *Nature*, 419(6908):729–734.

Seoane, J., Pouponnot, C., Staller, P., Schader, M., Eilers, M., & Massagué, J. (2001). TGFbeta influences Myc, Miz-1 and Smad to control the CDK inhibitor p15INK4b. *Nat Cell Biol*, 3(4):400–408.

Serrano, M., Lin, A. W., McCurrach, M. E., Beach, D., & Lowe, S. W. (1997). Oncogenic ras provokes premature cell senescence associated with accumulation of p53 and p16INK4a. *Cell*, 88(5):593–602.

Shanmugathasan, M. & Jothy, S. (2000). Apoptosis, anoikis and their relevance to the pathobiology of colon cancer. *Pathology international*, 50(4):273–279.

Sheiness, D. & Bishop, J. M. (1979). DNA and RNA from uninfected vertebrate cells contain nucleotide sequences related to the putative transforming gene of avian myelocytomatosis virus. *Journal of virology*, 31(2):514–521.

Sherr, C. J. (2006). Divorcing ARF and p53: an unsettled case. *Nature reviews Cancer*, 6(9):663–673.

Shrivastava, A., Saleque, S., Kalpana, G. V., Artandi, S., Goff, S. P., & Calame, K. (1993). Inhibition of transcriptional regulator Yin-Yang-1 by association with c-Myc. *Science*, 262(5141):1889–1892.

Simpson, C. D., Anyiwe, K., & Schimmer, A. D. (2008). Anoikis resistance and tumor metastasis. *Cancer letters*, 272(2):177–185.

Staller, P., Peukert, K., Kiermaier, A., Seoane, J., Lukas, J., Karsunky, H., Möröy, T., Bartek, J., Massagué, J., Hänel, F., & Eilers, M. (2001). Repression of p15INK4b expression by Myc through association with Miz-1. *Nat Cell Biol*, 3(4):392–399.

Stead, M. A., Trinh, C. H., Garnett, J. A., Carr, S. B., Baron, A. J., Edwards, T. A., & Wright, S. C. (2007). A beta-sheet interaction interface directs the tetramerisation of the Miz-1 POZ domain. *J Mol Biol*, 373(4):820–826.

Stielow, B., Sapetschnig, A., Wink, C., Krüger, I., & Suske, G. (2008). SUMO-modified Sp3 represses transcription by provoking local heterochromatic gene silencing. *EMBO Rep*, 9(9):899–906.

Stone, J., de Lange, T., Ramsay, G., Jakobovits, E., Bishop, J. M., Varmus, H., & Lee, W. (1987). Definition of regions in human c-myc that are involved in transformation and nuclear localization. *Molecular and Cellular Biology*, 7(5):1697–1709.

Strasser, A., Puthalakath, H., & Bouillet, P. (2000). The Role of Bim, a Proapoptotic BH3âOnly Member of the Bclâ2 Family, in CellâDeath Control. *Annals of the New ...*.

Streuli, C. H. & Gilmore, A. P. (1999). Adhesion-mediated signaling in the regulation of mammary epithelial cell survival. *Journal of mammary gland biology and neoplasia*, 4(2):183–191.

Sugiyama, A., Kume, A., Nemoto, K., Lee, S. Y., Asami, Y., Nemoto, F., Nishimura, S., & Kuchino, Y. (1989). Isolation and characterization of s-myc, a member of the rat myc gene family. *Proc Natl Acad Sci U S A*, 86(23):9144–9148.

Suske, G. (1999). The Sp-family of transcription factors. *Gene*, 238(2):291–300.

Tago, K., Chiocca, S., & Sherr, C. J. (2005). Sumoylation induced by the Arf tumor suppressor: a p53-independent function. *Proc Natl Acad Sci U S A*, 102(21):7689–7694.

Tanaka, N. & Fukuzawa, M. (2008). MYCN downregulates integrin alpha1 to promote invasion of human neuroblastoma cells. *International journal of oncology*, 33(4):815–821.

Tatham, M. H., Geoffroy, M.-C., Shen, L., Plechanovova, A., Hattersley, N., Jaffray, E. G., Palvimo, J. J., & Hay, R. T. (2008). RNF4 is a poly-SUMO-specific E3 ubiquitin ligase required for arsenic-induced PML degradation. *Nat Cell Biol*, 10(5):538–546.

Tatham, M. H., Jaffray, E., Vaughan, O. A., Desterro, J. M., Botting, C. H., Naismith, J. H., & Hay, R. T. (2001). Polymeric chains of SUMO-2 and SUMO-3 are conjugated to protein substrates by SAE1/SAE2 and Ubc9. *J Biol Chem*, 276(38):35368–35374.

Thalmeier, K., Synovzik, H., Mertz, R., Winnacker, E. L., & Lipp, M. (1989). Nuclear factor E2F mediates basic transcription and trans-activation by E1a of the human MYC promoter. *Genes Dev*, 3(4):527–536.

Tiefenbach, J., Novac, N., Ducasse, M., Eck, M., Melchior, F., & Heinzel, T. (2006). SUMOylation of the corepressor N-CoR modulates its capacity to repress transcription. *Mol Biol Cell*, 17(4):1643–1651.

Treszl, A., Adány, R., Rákosy, Z., Kardos, L., Bégány, A., Gilde, K., & Balázs, M. (2004). Extra copies of c-myc are more pronounced in nodular melanomas than in superficial spreading melanomas as revealed by fluorescence in situ hybridisation. *Cytometry. Part B, Clinical cytometry*, 60(1):37–46.

van Riggelen, J., Müller, J., Otto, T., Beuger, V., Yetil, A., Choi, P. S., Kosan, C., Möröy, T., Felsher, D. W., & Eilers, M. (2010). The interaction between Myc and Miz1 is required to antagonize TGFbeta-dependent autocrine signaling during lymphoma formation and maintenance. *Genes Dev*, 24(12):1281–1294.

Vennstrom, B., Sheiness, D., Zabielski, J., & Bishop, J. M. (1982). Isolation and characterization of c-myc, a cellular homolog of the oncogene (v-myc) of avian myelocytomatosis virus strain 29. *Journal of virology*, 42(3):773–779.

Vertegaal, A. C. O., Andersen, J. S., Ogg, S. C., Hay, R. T., Mann, M., & Lamond, A. I. (2006). Distinct and overlapping sets of SUMO-1 and SUMO-2 target proteins revealed by quantitative proteomics. *Mol Cell Proteomics*, 5(12):2298–2310.

Vervoorts, J., Lüscher-Firzlaff, J., & Lüscher, B. (2006). The ins and outs of MYC regulation by posttranslational mechanisms. *J Biol Chem*, 281(46):34725–34729.

Vervoorts, J., Lüscher-Firzlaff, J. M., Rottmann, S., Lilischkis, R., Walsemann, G., Dohmann, K., Austen, M., & Lüscher, B. (2003). Stimulation of c-MYC transcriptional activity and acetylation by recruitment of the cofactor CBP. *EMBO Rep*, 4(5):484–490.

Vialter, A., Vincent, A., Demidem, A., & Morvan, D. (2011). Cell cycle-dependent conjugation of endogenous BRCA1 protein with SUMO-2/3. *Biochim Biophys Acta*.

Vita, M. & Henriksson, M. (2006). The Myc oncoprotein as a therapeutic target for human cancer. *Seminars in cancer biology*, 16(4):318–330.

von der Lehr, N., Johansson, S., Wu, S., Bahram, F., Castell, A., Cetinkaya, C., Hydbring, P., Weidung, I., Nakayama, K., Nakayama, K. I., Söderberg, O., Kerppola, T. K., & Larsson, L.-G. (2003). The F-box protein Skp2 participates in c-Myc proteosomal degradation and acts as a cofactor for c-Myc-regulated transcription. *Mol Cell*, 11(5):1189–1200.

Voulgari, A. & Pintzas, A. (2009). Epithelial-mesenchymal transition in cancer metastasis: mechanisms, markers and strategies to overcome drug resistance in the clinic. *Biochim Biophys Acta*, 1796(2):75–90.

Walz, S. & Wolf, E. (2012). Discussion in person about unpublished data.

Wanzel, M. (2010). Discussion via telephone.

Wanzel, M., Russ, A. C., Kleine-Kohlbrecher, D., Colombo, E., Pelicci, P. G., & Eilers, M. (2008). A ribosomal protein L23-nucleophosmin circuit coordinates Miz1 function with cell growth. *Nat Cell Biol*.

Weber, J. D., Jeffers, J. R., Rehg, J. E., Randle, D. H., Lozano, G., Roussel, M. F., Sherr, C. J., & Zambetti, G. P. (2000). p53-independent functions of the p19(ARF) tumor suppressor. *Genes Dev*, 14(18):2358–2365.

Wei, F., Schöler, H. R., & Atchison, M. L. (2007). Sumoylation of Oct4 enhances its stability, DNA binding, and transactivation. *J Biol Chem*, 282(29):21551–21560.

Wei, W., Yang, P., Pang, J., Zhang, S., Wang, Y., Wang, M.-H., Dong, Z., She, J.-X., & Wang, C.-Y. (2008). A stress-dependent SUMO4 sumoylation of its substrate proteins. *Biochem Biophys Res Commun*, 375(3):454–459.

Welcker, M., Orian, A., Grim, J. E., Grim, J. A., Eisenman, R. N., & Clurman, B. E. (2004a). A nucleolar isoform of the Fbw7 ubiquitin ligase regulates c-Myc and cell size. *Current biology : CB*, 14(20):1852–1857.

Welcker, M., Orian, A., Jin, J., Grim, J. E., Grim, J. A., Harper, J. W., Eisenman, R. N., & Clurman, B. E. (2004b). The Fbw7 tumor suppressor regulates glycogen synthase kinase 3 phosphorylation-dependent c-Myc protein degradation. *Proc Natl Acad Sci U S A*, 101(24):9085–9090.

Werner, A. (2011). Discussion via Email.

Wierstra, I. & Alves, J. (2008). The c-myc promoter: still MysterY and challenge. *Advances in cancer research*, 99:113–333.

Wilson, A., Murphy, M. J., Oskarsson, T., Kaloulis, K., Bettess, M. D., Oser, G. M., Pasche, A.-C., Knabenhans, C., Macdonald, H. R., & Trumpp, A. (2004). c-Myc controls the balance between hematopoietic stem cell self-renewal and differentiation. *Genes Dev*, 18(22):2747–2763.

Wimmer, P., Schreiner, S., & Dobner, T. (2012). Human pathogens and the host cell SUMOylation system. *Journal of virology*, 86(2):642–654.

Wolfer, A. & Ramaswamy, S. (2011). MYC and metastasis. *Cancer Res*, 71(6):2034–2037.

Wood, M. A., McMahon, S. B., & Cole, M. D. (2000). An ATPase/helicase complex is an essential cofactor for oncogenic transformation by c-Myc. *Mol Cell*, 5(2):321–330.

Woods, Y. L., Xirodimas, D. P., Prescott, A. R., Sparks, A., Lane, D. P., & Saville, M. K. (2004). p14 Arf promotes small ubiquitin-like modifier conjugation of Werners helicase. *J Biol Chem*, 279(48):50157–50166.

Wu, K. J., Polack, A., & Dalla-Favera, R. (1999). Coordinated regulation of iron-controlling genes, H-ferritin and IRP2, by c-MYC. *Science*, 283(5402):676–679.

Xirodimas, D. P., Chisholm, J., Desterro, J. M. S., Lane, D. P., & Hay, R. T. (2002). P14ARF promotes accumulation of SUMO-1 conjugated (H)Mdm2. *FEBS Lett*, 528(1-3):207–211.

Xirodimas, D. P. & Lane, D. P. (2008). Targeting a nucleolar SUMO protease for degradation: A mechanism by which ARF induces SUMO conjugation. *Cell Cycle*, 7(21).

Xue, Y., Zhou, F., Fu, C., Xu, Y., & Yao, X. (2006). SUMOsp: a web server for sumoylation site prediction. *Nucleic Acids Res*, 34(Web Server issue):W254–7.

Yada, M., Hatakeyama, S., Kamura, T., Nishiyama, M., Tsunematsu, R., Imaki, H., Ishida, N., Okumura, F., Nakayama, K., & Nakayama, K. I. (2004). Phosphorylation-dependent degradation of c-Myc is mediated by the F-box protein Fbw7. *EMBO J*, 23(10):2116–2125.

Yamada, T., Kohno, T., Navarro, J. M., Ohwada, S., Perucho, M., & Yokota, J. (2000). Frequent chromosome 8q gains in human small cell lung carcinoma detected by arbitrarily primed-PCR genomic fingerprinting. *Cancer genetics and cytogenetics*, 120(1):11–17.

Yamaguchi, T., Sharma, P., Athanasiou, M., Kumar, A., Yamada, S., & Kuehn, M. R. (2005). Mutation of SENP1/SuPr-2 reveals an essential role for desumoylation in mouse development. *Molecular and Cellular Biology*, 25(12):5171–5182.

Yan, J., Yang, X.-P., Kim, Y.-S., Joo, J. H., & Jetten, A. M. (2007). RAP80 interacts with the SUMO-conjugating enzyme UBC9 and is a novel target for sumoylation. *Biochem Biophys Res Commun*, 362(1):132–138.

Yang, S.-H., Galanis, A., Witty, J., & Sharrocks, A. D. (2006). An extended consensus motif enhances the specificity of substrate modification by SUMO. *EMBO J*, 25(21):5083–5093.

Yang, S.-H., Jaffray, E., Hay, R. T., & Sharrocks, A. D. (2003). Dynamic interplay of the SUMO and ERK pathways in regulating Elk-1 transcriptional activity. *Mol Cell*, 12(1):63–74.

Yawata, A., Adachi, M., Okuda, H., Naishiro, Y., Takamura, T., Hareyama, M., Takayama, S., Reed, J. C., & Imai, K. (1998). Prolonged cell survival enhances peritoneal dissemination of gastric cancer cells. *Oncogene*, 16(20):2681–2686.

Yu, Y., Maggi, L. B., Brady, S. N., Apicelli, A. J., Dai, M.-S., Lu, H., & Weber, J. D. (2006). Nucleophosmin is essential for ribosomal protein L5 nuclear export. *Molecular and Cellular Biology*, 26(10):3798–3809.

Zhang, F.-P., Mikkonen, L., Toppari, J., Palvimo, J. J., Thesleff, I., & Jänne, O. A. (2008). Sumo-1 function is dispensable in normal mouse development. *Mol Cell Biol*, 28(17):5381–5390.

Zhang, Y., Xiong, Y., & Yarbrough, W. G. (1998). ARF promotes MDM2 degradation and stabilizes p53: ARF-INK4a locus deletion impairs both the Rb and p53 tumor suppression pathways. *Cell*, 92(6):725–734.

Zheng, G. & Yang, Y.-C. (2004). ZNF76, a novel transcriptional repressor targeting TATA-binding protein, is modulated by sumoylation. *J Biol Chem*, 279(41):42410–42421.

Ziegelbauer, J., Shan, B., Yager, D., Larabell, C., Hoffmann, B., & Tjian, R. (2001). Transcription factor MIZ-1 is regulated via microtubule association. *Mol Cell*, 8(2):339–349.

Zinchuk, V., Zinchuk, O., & Okada, T. (2007). Quantitative colocalization analysis of multicolor confocal immunofluorescence microscopy images: pushing pixels to explore biological phenomena. *Acta histochemica et cytochemica*, 40(4):101–111.

Zindy, F., Eischen, C. M., Randle, D. H., Kamijo, T., Cleveland, J. L., Sherr, C. J., & Roussel, M. F. (1998). Myc signaling via the ARF tumor suppressor regulates p53-dependent apoptosis and immortalization. *Genes Dev*, 12(15):2424–2433.

Zindy, F., Williams, R. T., Baudino, T. A., Rehg, J. E., Skapek, S. X., Cleveland, J. L., Roussel, M. F., & Sherr, C. J. (2003). Arf tumor suppressor promoter monitors latent oncogenic signals in vivo. *Proc Natl Acad Sci U S A*, 100(26):15930–15935.

Appendix A.

List of abbreviations

A selection of abbreviations that can be found in this thesis are explained below. Furthermore the abbreviations of the IUPAC (International union of pure und applied Chemistry) and of the SI-System (Système international d'unités) were used.

A.1. Prefixes

abbreviation	prefix	factor
p	Pico-	10^{-12}
n	Nano-	10^{-9}
µ	Mikro-	10^{-6}
m	Milli-	10^{-3}
c	Centi-	10^{-2}
k	Kilo-	10^{3}

Table A.1.: abbreviations for prefixes and multiplication factors

A.2. Units

A ampere

Da dalton

g gram

h hour

J joule

l liter

m meter

min minute

M mol/l

mol mol

OD optical density

s second

U unit

vol. volume

v/v volume per volume

w/v weight per volume

°C degree celsius

A.3. Proteins, protein domains and other biomolecules

A adenine

ATP adenosine-5«-triphosphate

A alanine

aa amino acid

R arginine

bp basepair(s)

BTB broad-complex, tramtrack and bric à brac

C cytosine

cDNA complementary DNA

DNA deoxyribonucleic acid

dNTPs deoxyribonucleoside-5'-triphosphate (dATP, dCTG, dGTP, dTTP)

G guanine

GFP green fluorescent protein

GST glutathione-*S*-transferase

GTP guanosine-5'-triphosphate

HRP horseradish peroxidase

K lysine

nt nucleotide(s)

POZ pox virus and zinc finger

RNA ribonucleic acid

T thymine

TopBP topoisomerase-binding protein

ZBTB4 zinc finger and broad-complex, tramtrack and bric-a-brac (BTB)-domain-containing protein 4

ZF zinc finger

A.4. Chemicals and solutions

APS ammoniumpersulfate

ddH_2O bidestilled water

DMEM Dulbeccos Modified Eagle-Medium

DMSO dimethylsulfoxide

DTT dithiothreitol

EDTA ethylendiamintetraacetate

FCS fetal calf serum

FBS fetal bovine serum

NEM *N*-ethylmaleimide

PBS phosphate-buffered saline

PVDF polyvinylidenfluoride

SDS sodium dodecyl sulfate

TBE Tris-borate-EDTA-buffer

TBS Tris-buffered saline

TBS-T Tris-buffered saline with tween-20

TE Tris-EDTA-buffer

TEMED N,N,N',N'-tetramethylethylendiamine

Tris Tris-(hydroxymethyl)-aminomethan

A.5. Other abbreviations

abs. absolute

approx. approximately

ATCC American Type Culture Collection

ECL enhanced chemoluminescence

E. coli *Escherichia coli*

FPLC fast protein liquid chromatography

Fig. Figure

Inc. Incorporated

IP immunoprecipitation

PAGE polyacrylamide-gelelectrophoresis

PCR polymerase chain reaction

qPCR quantitative PCR

rpm rotations per minute

RT room temperature

o./n. over night; 16-20 h

S1 security level 1

S2 security level 1

wt wild type

Appendix B.

Acknowledgements

"I am still confused, but on a higher level." (Enrico Fermi)

I would like to thank my supervisor, Prof. Martin Eilers, for the guidance, encouragement and advice he constantly provided throughout my time as his student. I have been lucky to have had a supervisor who despite his many obligations always found a sympathetic ear for me.

I also thank Prof. Dr. Manfred Schartl, Prof. Dr. Stefan Gaubatz and Prof. Dr. Frauke Melchior for their support as my thesis committee.

I would like to thank all the members of the Eilers, Murphy, Popov and Gallant group who stood by me with technical help and countless discussions. I especially thank all the people that corrected my thesis: Steffi, Christina, Lisa, Susanne and Stefanie. Thanks for also providing moral support throughout the years - I wouldn't have made it without you! I especially thank Christina for almost 10 years of friendship in science - I am so glad we had each other.

I want to express my gratitude towards the Graduate School of Life Sciences for providing valuable experiences outside the research-related work of my PhD. I also like to thank the German National Academic Foundation for providing the funding which allowed me to undertake this research.

And finally, but not least, thanks goes to Peter and my whole family for their continued support and encouragement, and for enduring all the ups and downs of my research. You have been an indispensable source of spiritual support.

Appendix D.

Affidavit

I hereby confirm that my thesis entitled "Impact of the Tumor Suppressor Arf on Miz1 and Sumoylation of Myc and Miz1" is the result of my own work. I did not receive any help or support from commercial consultants. All sources and/or materials applied are listed and specified in the thesis.

Furthermore, I confirm that this thesis has not yet been submitted as part of another examination process neither in identical nor in similar form.

Würzburg, July 3, 2012